REMARKS

Consideration and continuing examination of the above-identified application is respectfully requested in view of the amendments above and the discussion that follows.

Claims 21, 54 and 56 have been amended. Claims 21-26, 28-29 and 52-57 are in the case and are before the Examiner.

A. The Amendments

Claims 21, 54 and 56 were amended to more clearly recite the claimed invention by clarifying that the recited enzymes "are utilized in a single reaction mixture" as was recited in the claims of the issued parental patent.

It is thus seen that no new matter has been added.

B. Responses to the "Attachment to Advisory Action"

Although maintaining the previous rejections, the Examiner was kind enough to provide extensive comments to further underscore his views in making those rejections. This paper is provided to respond to those comments and provide requested answers to several questions.

In the second paragraph of the Attachment, it is noted that it was unclear how Schachter's separation of the fucose kinase from the pyrophosphorylase could teach away from claims 21, 23, 26, 52-54 and 56. It is first noted that the enumerated claims were grouped together with claim 25 in the original rejection. It is next noted that counsel's claims 23 and 25 recite the presence of a kinase.

The Attachment notes in the next paragraph that there is "nothing in Schachter suggesting that the enzymes must be separated in order to be active." It is submitted that the suggestion here is from the observation that Schachter did in fact separate the two activities from the same preparation before he used them. If he thought they were compatible, he would have done the reaction using a single preparation and saved himself a great deal of time and difficulty in the laboratory. It is further submitted that those separation activities and the self-subjection to further work are akin to the non-assertive conduct exception to the hearsay rule of evidence such as where a ship's captain inspects his ship prior to setting sail being evidence that he thought the ship to be in safe condition prior to leaving port.

This portion of the Attachment continued with the comment that the fact that both enzymes were active at the same pH value was suggestive of their being coupled in an *in vitro* synthesis system in accordance with the reaction scheme shown on page 285 of Schachter. One major problem with that line of reasoning is that the text above that scheme talks of separated enzymes, which again is non-assertive conduct relating to the enzymes needing to be used separately.

That paragraph continued with the assertion that because applicant provided no factual evidence of a requirement for separating the enzymes such as a statement by Schachter to that effect, the argument for separation is based on conjecture and lacks support. Actually, it is submitted that the only fact present here is that the relied-on art taught the separation of both enzymes and their separate use, and that those actions speak louder than the requested words. As such, the contrary conclusion expressed in the Attachment is itself unsupported

supposition that should be supported by art or a evidence under 37 C.F.R. §1.104(d)(2).

In discussing Dr. Paulson's expert testimony, the Attachment complains that no literature citations were provided in its support. It is submitted that Dr. Paulson's expert testimony should be more than enough to refute an unsupported Examiner's assertion. However, as will be seen from the following, the literature supports Dr. Paulson's position. To reiterate, that position was as follows:

> 12) That the enzymes involved in the claims do not naturally occur together in the same compartment in eukaryotic cells, rather,
>
> a) the fucosyltransferase is inside the Golgi apparatus, and the GDP-fucose and GDP-mannose forming enzymes are in the cytoplasm,
>
> b) the enzymes are thus separated by a membrane; and
>
> c) the finished GDP-fucose is transported into the Golgi apparatus, and the GDP product is exported back into the cytoplasm.

The Examiner's attention is invited to attached Exhibit 1 that is a true copy of Capasso and Hirschberg, *Proc. Natl. Acad. Sci, USA* **81**:7051-7055(Nov. 1984), hereinafter Capasso, and

particularly to Fig. 3 on page 7055. That figure and the discussion immediately therebelow illustrates the art-recognized flow of GDP-fucose fucose from the cytosol through the Golgi membrane and into the inside of the Golgi where it is used to fucosylate an appropriate substrate using an internal fucosyltransferase.

The Examiner's attention is also invited t Fig. 2 of Pauslon et al. *J. Biol. Chem.* **264(30):**17615-17618 (1989) at page 17616 that is attached as Exhibit 2. That figure provides a schematic drawing showing the structure of a glycosyltransferase such as one of the fucosyltransferases noted in Table 1 on that same page. The exemplified fucosyltransferase has a cytoplasmic N-terminal tail, a signal-anchor region embedded in the Golgi membrane and a catalytic domain within the Golgi. Enclosed Exhibit 3, Larsen et al., *Proc. Natl. Acad. Sci., USA* **87**:6674-6678 (1990), discloses a nucleotide sequence encoding a fucosyltransferase and the discussion on ;the right-hand side of page 6676 notes the structural features and presumed Golgi location for the enzyme. These three papers are noted on enclosed Form PTO 1449.

The Golgi location for a fucosyltransferase is thus believed to be established.

The Action asserted that applicant or Dr. Paulson had claimed that the enzymes involved here had different pH maxima. Actually, Dr. Paulson's statements at paragraph 13 were:

> 13) That the two cellular two compartments [Golgi and cytoplasm] are documented to be quite different from each other in pH, reducing environment, and the like;

Attached Exhibit 4 [Cosson et al., *J. Cell Biol.*, **108**:377-387 (1989)] illustrates that the pH value for the cytoplasm is usually between 7.0 and 7.2, whereas the Golgi pH value is in the 6's. Attached Exhibit 5 [http://mcb.berkeley.edu/courses/mcb137/exercises/Lesson9%20-%20pH%20Regulation.pdf] is a more recent compilation that provides pH values for several intracellular compartments.

In regard to the possible interactions recited previously, it was known in the art that the similar system containing the enzyme that forms CDP from CMP (nucleoside monophosphokinase), pyruvate kinase and CMPNeu5Ac synthase were incompatible because the synthase is inhibited by CMP. See, for example, David and Auge', *Pure & Appl. Chem.*, **59(11)**:1501-1508 (1987) that is attached as Exhibit 6, and page 215 of document A29 of the IDS that is re-provided in more complete form here as Exhibit 7. The application, beginning at midway down page 24 and continuing over the next several pages provides ample citations and data such as at least the data of application Fig. 3 showing inhibition of a fucosyltransferase by GDP in the presence of GDP-fucose for the skilled worker to appreciate the similarity of the feed-back product inhibition that these enzymes undergo. Thus, similar pH optima notwithstanding, there was ample art-recognized evidence for believing there could be an adverse interaction in the present system.

The Advisory notes that the Schachter enzyme was present in a sufficient quantity to catalyze the there desired reaction and therefore used a catalytic amount. It is respectfully submitted that workers of ordinary skill in this art are well aware of the meaning of "catalytic amount" and in view of the interaction between the enzymes, the reactants and

the reaction products discussed above and in the specification would understand the necessity for use of catalytic amounts, which Schachter did not need because he separated the reactions. That use of catalytic amounts is still nowhere to be found in the relied-on teachings and should not be tossed off as if it were of no consequence.

In regard to the use of pyruvate kinase, it is agreed that it can be used to make ATP. However, ATP is used in only some reactions for the preparation of unclaimed materials. Here, pyruvate kinase is linked with GDP to form GTP that is used to make the activated fucosylating entity, GDP-fucose. It is submitted that ATP will not substitute here. It is further submitted that the paragraph bridging pages 7 and 8 of the Advisory should be reviewed for their use of ADP and ATP, and the disclosures of Scheme 1 at page 13 should be compared in regard to the claimed subject matter with the disclosures of Schemes 12 and 13.

In regard to the Yamamoto teaching, the Action continues to in not owning up to its mis-citation of the Yamamoto disclosure, while counsel will agree that Yamamoto was relied-on for a teaching but not actually quoted. What was quoted was the wrong page number. More pertinently however, the Yamamoto teaching is submitted to be no better than the Schachter teaching. There is nothing in that paper nor in Bergh nor in Schachter that suggests putting everything together. That suggestion is the message of this application. To simply provide a cookbook list of all of the ingredients and say here they are it is obvious to put them together is to minimize Dr. Wong's contribution with hindsight.

The Advisory asserts that the applicant has provided not evidence of a long felt need that has been alleviated by the

claimed combination. It is submitted that such evidence is of record in the Borman C&EN article of December 7, 1992 that was made of record herein as Document A37 of the IDS. Here, four pages of a weekly chemical science news magazine were devoted almost exclusively to Dr. Wong and his cyclic reactions such as the present fucosylation and the ability that Cytel Corporation had through its licenses with Dr. Wong "to make sialyl Lewis^X enzymatically on a large scale." (Page 27, left column, last lines.) It was noted on page 26, bottom left to middle column, that in 1991 the cost of xxx was $3 billion per kg that was reduced to $2 billion per kg in 1992. This invention thus did help to answer a long felt need and that evidence has been of record for some time.

It is again submitted that these bases for rejection should be withdrawn.

C. Summary

Claims 21, 54 and 56 have been amended. Each of the bases for rejection has been dealt with and overcome or otherwise made moot.

It is therefore believed that this application is in condition for allowance of all of the pending claims. An early notice to that effect is earnestly solicited.

A Petition for an Extension of Time and its required fee are enclosed. No further fee or petition is believed to be necessary. However, should any further fee be needed, please charge our Deposit Account No. 23-0920, and deem this paper to be the required petition.

The Examiner is requested to phone the undersigned should any questions arise that can be dealt with over the phone to expedite this prosecution.

Respectfully submitted,

By _____
Edward P. Gamson, Reg. No. 29,381

WELSH & KATZ, LTD.
120 South Riverside Plaza, 22nd Floor
Chicago, Illinois 60606
Phone (312) 655-1500
Fax No. (312) 655-1501

Enclosures
- Petition and fee
- Exhibits 1-7
- RCE and fee
- Fee Sheet

CERTIFICATE OF MAILING

I hereby certify that this Amendment and Reply, Exhibits, a One-Month Extension of Time and it fee, an RCE, Fee Sheet and Fee are being deposited with the United States Postal Service with sufficient postage as First Class Mail in an envelope addressed to: Mail Stop Amendments, Commissioner for Patents, P.O. Box 1450, Alexandria, VA 22313-1450, on February 8, 2005.

By _____
Edward P. Gamson

EXHIBIT 1

Proc. Natl. Acad. Sci. USA
Vol. 81, pp. 7051–7055, November 1984
Biochemistry

Mechanisms of glycosylation and sulfation in the Golgi apparatus: Evidence for nucleotide sugar/nucleoside monophosphate and nucleotide sulfate/nucleoside monophosphate antiports in the Golgi apparatus membrane

JUAN M. CAPASSO* AND CARLOS B. HIRSCHBERG

E. A. Doisy Department of Biochemistry, St. Louis University School of Medicine, St. Louis, MO 63104

Communicated by Phillips W. Robbins, July 25, 1984

ABSTRACT **The mechanism of translocation *in vitro* of sugar nucleotides and adenosine 3'-phosphate 5'-phosphosulfate (PAPS) into the lumen of rat liver Golgi apparatus vesicles has been studied. It has been previously shown that the Golgi apparatus membrane has specific carrier proteins for PAPS and sugar nucleotides. We now report that translocation of the above nucleotide derivatives across Golgi membranes occurs via a coupled equimolar exchange with the corresponding nucleoside monophosphates. An initial incubation of Golgi vesicles with GDP-fucose radiolabeled in the guanidine ring resulted in accumulation within the lumen of radiolabeled GMP. Exit of GMP from these vesicles was specifically dependent on the entry of (additional) GDP-fucose into the vesicles (GDP-mannose and other sugar nucleotides had no effect). GDP-fucose-stimulated exit of GMP was temperature dependent, was blocked by inhibitors of GDP-fucose transport, such as 4,4'-diisothiocyanostilbene-2,2'-disulfonic acid, and appeared to be equimolar with GDP-fucose entry. Preliminary evidence for specific, equimolar exchange of CMP-*N*-acetylneuraminic acid with CMP, PAPS with 3'-AMP, and UDP-galactose and UDP-*N*-acetylglucosamine with UMP was also obtained. These results strongly suggest the existence of different antiport proteins within the Golgi membrane that mediate the 1:1 exchange of sugar nucleotides or PAPS with the corresponding nucleoside monophosphate. Such proteins may have a regulatory role in glycosylation and sulfation reactions within the Golgi apparatus.**

Recent studies from this laboratory have shown that rat liver Golgi-derived vesicles can translocate *in vitro* CMP-*N*-acetylneuraminic acid (AcNeu), GDP-fucose, UDP-*N*-acetylglucosamine (GlcNAc), and adenosine 3'-phosphate 5'-phosphosulfate (PAPS) from an external compartment into a lumenal one (1–5). These reactions were found to be (*i*) saturable at high concentrations of sugar nucleotides and PAPS, (*ii*) temperature dependent, (*iii*) inhibited by treatment of the Golgi vesicles with proteases under conditions where lumenal marker enzymes were not inhibited, and (*iv*) inhibited competitively by the corresponding nucleoside mono-, di-, and triphosphate (6). Since the above sugar nucleotides and PAPS did not inhibit translocation of each other, it was hypothesized that there were different translocator proteins in the membrane of the Golgi apparatus and that portions of these proteins face the cytoplasmic side of the Golgi apparatus membranes. Evidence for translocation of UDP-galactose (Gal) into Golgi vesicles from mammary gland and rat liver (7, 8), CMP-AcNeu into rat liver Golgi (9) and hen oviduct microsomes (10) has also been obtained in other laboratories.

The aim of the present study was to understand the energy mechanism by which the above sugar nucleotides and PAPS are translocated across the Golgi vesicle membranes. We now present evidence suggesting that such a mechanism involves exchange with the corresponding nucleoside monophosphate via an antiport protein.

MATERIALS AND METHODS

Radioactive Substrates. The following radioactive compounds were used: GDP-L-[1-^{14}C]fucose (264 Ci/mol; 1 Ci = 37 GBq), New England Nuclear; [*guanidine*-8-^{3}H]GDP-fucose (667 Ci/mol) synthesized as described (1); [*guanidine*-8-^{3}H]GMP (22 Ci/mmol) synthesized as described (1); [*adenine*-8-^{3}H]PAPS (870 Ci/mol) synthesized as described (4); [U-^{14}C]CMP (375 Ci/mol), Amersham; [U-^{14}C]UMP (484 Ci/mol), Amersham; CMP-[^{14}C]AcNeu (1.6 Ci/mol), New England Nuclear; [^{35}S]PAPS (1.3 Ci/mmol), New England Nuclear;

Isolation, Integrity, and Topography of Golgi Vesicles. Golgi vesicles were isolated from rat liver according to the procedure described by Leelavathi *et al.* (11). The vesicles were enriched, on average, ≈40-fold in sialyltransferase activity (compared to crude homogenate) (1, 4). At least 90% were sealed and of the same topographical orientation as *in vivo* (12).

Translocation Assay. The theoretical basis for the assays of translocation of the different nucleotide derivatives into Golgi vesicles has been described in detail (1, 2, 4). Briefly, it consists of (*i*) determining the total radioactive solutes associated with the Golgi pellet (S_t) after incubation with radiolabeled substrates and centrifugation of the Golgi vesicles (see below), and (*ii*) subtracting from this amount the total radioactive solutes trapped between the vesicles in the Golgi pellet (S_o). This latter value is obtained by multiplying the volume outside the vesicles in the Golgi pellet (V_o) by the concentration of radioactive solutes in the incubation medium ([S_m]). The volume outside (trapped) vesicles in the pellet was measured with a standard nonpenetrator such as [^{3}H]methoxyinulin.

RESULTS

In previous studies we had shown that sugar nucleotides and PAPS were translocated into Golgi vesicles *in vitro* (1, 5). This was done using sugar nucleotides and PAPS labeled with different radioisotopes in the nucleotide and sugar or sulfate. It was also shown that subsequent to translocation into the Golgi vesicle lumen, the sugars and sulfate were transferred to macromolecules facing the lumen of the vesi-

The publication costs of this article were defrayed in part by page charge payment. This article must therefore be hereby marked "*advertisement*" in accordance with 18 U.S.C. §1734 solely to indicate this fact.

Abbreviations: PAPS, adenosine 3'-phosphate 5'-phosphosulfate; DIDS, 4,4'-diisothiocyanostilbene-2,2'-disulfonic acid; GlcNAc, *N*-acetylglucosamine; AcNeu, *N*-acetylneuraminic acid; Gal, galactose.

*Permanent address: Facultad de Ciencias Exactas y Naturales, Universidad de Buenos Aires, Buenos Aires, Argentina.

cles, while nucleotides accumulated within the vesicles (relative to their concentration in the incubation medium) (1, 5). That these nucleotides were also leaving the Golgi lumen was suggested from experiments in which translocation of PAPS radiolabeled in the nucleotide and sulfate was measured (4).

Entry of GDP-Fucose into Golgi Vesicles Appears to Be Concomitant with Exit of GMP. The above studies led us to design an experiment to determine whether translocation of sugar nucleotides into the lumen of Golgi vesicles was coupled with exit of nucleotides from the Golgi lumen. For this purpose, Golgi vesicles were incubated with GDP-fucose ^{3}H-labeled in the guanidine ring; the total amount of radioactive solutes within the vesicles was determined after different incubation times. As can be seen in Fig. 1, there was a time-dependent accumulation of radiolabeled solutes within the Golgi vesicles that became constant after 10 min. No acid-insoluble radioactivity was detected (not shown).

In parallel experiments, GDP-[^{14}C]fucose was added (for 0.5–2 min) to Golgi vesicle suspensions that had been previously incubated with [^{3}H]GDP-fucose (for 1, 5, and 10 min). Fig. 1 shows that addition of GDP-[^{14}C]fucose resulted in (*i*) a concomitant decrease of the tritiated solutes within the vesicles (shown below to be [^{3}H]GMP) and (*ii*) a parallel increase in ^{14}C-containing species within the vesicles. This latter radioactivity was found to be, as previously determined, the sum of ^{14}C-containing solutes within vesicles and ^{14}C-containing radioactivity covalently bound to macromolecules facing the lumen of the vesicles (1). For example, when vesicles that had been incubated with [^{3}H]GDP-fucose for 10 min were then incubated with GDP-[^{14}C]fucose for 2 min, 50% of the [^{14}C]fucose within vesicles was acid-insoluble (not shown).

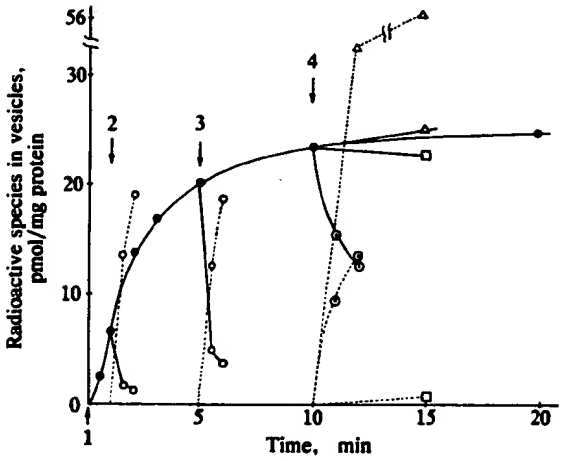

FIG. 1. Translocation of [^{3}H]GDP-fucose into Golgi vesicles and subsequent exchange of radiolabeled solutes from within the vesicles. Ultracentrifuge tubes, each containing Golgi vesicles (0.4 mg of protein), were incubated for different times at 25°C with [*guanidine*-8-^{3}H]GDP-L-fucose (0.27 μCi; final concentration, 0.4 μM; arrow 1) in 1.0 ml of buffer containing 10 mM Tris·HCl/0.25 M sucrose/1 mM $MgCl_2$/10 mM NaF/0.5 mM 2,3-dimercaptopropanol, final pH 7.5 (●). To samples that had been incubated for 1 (arrow 2) and 5 min (arrow 3), GDP-[^{14}C]fucose (5 μl, 0.12 μCi; 2 μM, final concentration) was added and the incubation was continued for 0.5 and 1 min (○). To samples that had been incubated for 10 min (arrow 4) with [*guanidine*-8-^{3}H]GDP-fucose, GDP-[^{14}C]fucose (5 μl; 0.12 μCi; final concentration, 0.45 μM was added and the mixture was incubated for 1 and 2 min (◎). To another set of samples that had been incubated for 10 min (arrow 4) with [*guanidine*-8-^{3}H]GDP-fucose, [^{35}S]PAPS (5 μl; 0.44 μCi; final concentration, 2 μM) was added and the mixture was incubated for 2 and 5 min (△). To another group of samples incubated with [*guanidine*-8-^{3}H]GDP-fucose for 10 min (arrow 4), GDP-[^{14}C]mannose (5 μl; 0.31 μCi; final concentration, 1 μM) was added for 5 min (□). All reactions were stopped by placing tubes in a mixture of ice containing NaCl. Samples were then centrifuged, followed by determination of soluble (——; ^{3}H species) and total (soluble and insoluble) (——; ^{14}C or ^{35}S species) radioactivity within the Golgi pellet as described (1, 4).

The radioactive species within Golgi vesicles, after a 10-min incubation with [^{3}H]GDP-fucose were [^{3}H]GMP (65%–90%) and [^{3}H]guanosine (10%–35%). This result is in agreement with our previous studies (1). The soluble ^{14}C radioactive species within vesicles, after a 2-min incubation of the Golgi vesicle suspension described above with GDP-[^{14}C]fucose was mostly fucose, while the acid insoluble radioactivity was in fucoproteins. This result is also in agreement with our previous observations (1).

Exit of GMP from Golgi Vesicles Is Specifically Dependent on Entry of GDP-Fucose. Two types of experiment were done to determine that exit of GMP from Golgi vesicles was specifically dependent on entry of GDP-fucose into the vesicles: (*i*) Virtually no exit of ^{3}H-labeled solutes was observed from vesicles that had been incubated first with [^{3}H]GDP-fucose for 10 min and then with GDP-[^{14}C]mannose for 5 min (Fig. 1). We have obtained no evidence for entry of this latter sugar nucleotide into the Golgi lumen. These results strongly suggest that exit of [^{3}H]GMP of the previous experiment was dependent on entry of GDP-fucose into the vesicles. (*ii*) When [^{35}S]PAPS was added to vesicles that had been previously incubated with [^{3}H]GDP-fucose (for 10 min) there was no exit of [^{3}H]GMP from the vesicles (Fig. 1); however, the vesicles accumulated both soluble and acid-insoluble radioactive sulfur-containing species within their lumen (Fig. 1). We have recently shown that translocation of PAPS into Golgi vesicles is followed by transfer of sulfate into macromolecules facing the lumen of the vesicles (4, 5). The above experiment, therefore, strongly suggests that after a 10-min incubation with [^{3}H]GDP-fucose, the Golgi vesicles continue to be active in their ability to translocate other nucleotide derivatives and that exit of [^{3}H]GMP was specifically dependent on entry of GDP-fucose.

Additional evidence for the specificity of stimulation of exit of [^{3}H]GMP from Golgi vesicles is shown in Table 1. It can be seen that addition of 1–10 μM GDP-fucose to vesicles preloaded with [^{3}H]GDP-fucose resulted in exit of 68%–89% of [^{3}H]GMP from the vesicles. Considerably less exit was observed with UDP-Gal and with UDP-GlcNAc, both sugar nucleotides that are known to enter Golgi vesicles (3). Table

Table 1. Effect of sugar nucleotides, temperature, and inhibitors of anion transport on exit of [^{3}H]GMP from Golgi vesicles preincubated with [^{3}H]GDP-fucose for 10 min

Incubation		Exit
Substrate	Time, min	% [^{3}H]GMP remaining in vesicles
GDP-fucose (1 μM)	10	32
GDP-fucose (10 μM)	10	11
GDP-fucose/DIDS (1 μM)	10	68
GDP-fucose (2 μM) 4°C	10	80
UDP-GlcNAc (3 μM)	2	100
	5	100
UDP-Gal (25 μM)	10	89
PAPS (2 μM)	2	100
	5	100

Experimental conditions were the same as those described in the legend of Fig. 1. DIDS (5 μl; 100 μM, final concentration) was added after the preincubation; after 5 min, 1 μM GDP-fucose was added to the suspension. For studies on temperature dependence, the reaction was cooled to 4°C after the preincubation and continued thereafter at that temperature.

1 also shows that exit of [^{3}H]GMP was dependent on temperature. Addition of 4,4'-diisothiocyanostilbene-2,2'-disulfonic acid (DIDS), a known inhibitor of GDP-fucose translocation (5), to preloaded vesicles resulted in inhibition of GDP-fucose-stimulated exit of [^{3}H]GMP from the vesicles (Table 1). This experiment provides additional evidence that exit of GMP from the vesicles is dependent on entry of GDP-fucose.

Stoichiometry Between Entry of GDP-Fucose to and Exit of GMP from Golgi Vesicles. An important assumption has to be made to measure the stoichiometry of entry of GDP-fucose into, and exit of GMP from, Golgi vesicles. The specific radioactivity of each radioactive species within Golgi vesicles cannot be accurately determined, because the size of the endogenous nonradioactive pool of GMP within the vesicles is not known. We have therefore made the assumption, for subsequent calculations, that the specific radioactivity of GMP within vesicles, after a 10-min incubation of vesicles with [^{3}H]GDP-fucose, is the same as that of the radioactive sugar nucleotide at the beginning of the incubation. This appears reasonable from the results seen in Fig. 1. These show that the amount of ^{3}H-labeled solutes within vesicles appeared to be constant after a 10-min incubation with [^{3}H]GDP-fucose; this suggests that equilibration between the external and internal pool of nucleotides has occurred at this time.

Table 2 shows that there was apparent stoichiometric exit of [^{3}H]GMP from the vesicles relative to entry of GDP-[^{14}C]fucose after 1 and 2 min. We hypothesize that the apparent somewhat lower amount of GMP that had exited in comparison to the amount of GDP-fucose that had entered is the result of assuming that the specific radioactivity of [^{3}H]GMP within vesicles is equal to that of the original [^{3}H]GDP-fucose of the incubation medium; the true former value is always less, with the highest value approaching that of the original [^{3}H]GDP-fucose, when both external and internal pools are fully equilibrated. This is almost achieved after a 10-min incubation with [^{3}H]GDP-fucose, (Fig. 1). This assumption predicts that at times prior to reaching equilibrium between the nucleotide pools, differences between exit and entry of nucleotides would be magnified if one used calculations of specific radioactivity values as those outlined above. That this is indeed the case can be seen when entry and exit of solutes are calculated after incubation of vesicles with [^{3}H]GDP-fucose for 1 min. As seen in Table 2, addition of GDP-[^{14}C]fucose for 1 min to such vesicles leads to an apparent larger entry of GDP-fucose than exit of GMP. After a 5-min incubation with [^{3}H]GDP-fucose, a time where the nucleotide pools are closer to reaching equilibrium (Fig. 1), the apparent difference between entry of sugar nucleotide and exit of GMP is similar to that observed at 10 min (Table 2).

Exit of GMP from Golgi Vesicles Preloaded with GMP Is Specific. The experiments described in the previous sections strongly suggest that entry of GDP-fucose into Golgi vesicles is coupled with a 1:1 stoichiometric exit of GMP from the vesicles. We had observed, in a preliminary experiment that Golgi vesicles transported GMP *in vitro* from an external compartment into a lumenal one. It was therefore of interest to determine whether one could measure GDP-fucose-dependent exit of GMP from Golgi vesicles that had been preloaded with GMP. For this, vesicles were incubated with [^{3}H]GMP for 20 min; at this time GDP-[^{14}C]fucose was added to the vesicle suspension and the amount of ^{3}H-labeled solutes that remained in the vesicles and the amount of ^{14}C radioactive species accumulating within the vesicles was measured at different times (up to 10 min). Fig. 2 shows that upon addition of GDP-[^{14}C]fucose to the Golgi vesicle suspension there was (*i*) a rapid decrease of ^{3}H-labeled solutes from the vesicles and (*ii*) a rapid increase of ^{14}C radioactive species within vesicles. Incubation of GDP-[^{14}C]fucose for 0.5 min resulted in exit of 2.6 pmol of [^{3}H]GMP and entry of 2.9 pmol of ^{14}C-containing radioactive species. This result suggests, similarly to those shown in Fig. 1 and Table 2, an equimolar exchange between GMP and GDP-fucose. Examination of Fig. 2 for the stoichiometry of exchange at times longer than 0.5 min suggests that more sugar nucleotides enter vesicles than those that exit (Table 2). The reason for this discrepancy is more apparent than real, because at these longer incubation times with GDP-[^{14}C]fucose, the initial assumption of the specific radioactivities of species within vesicles being equal to the specific radioactivity of the nucleotide derivatives of the incubation medium is no longer valid because nonradioactive GMP, derived from entry of GDP-[^{14}C]fucose, causes a decrease in the specific radioactivity of the [^{3}H]GMP pool within the Golgi vesicles.

Fig. 2 also shows that exit of GMP from Golgi vesicles was specific. Upon addition to the vesicles of CMP-AcNeu, no exit of radiolabeled GMP was detected, even though CMP-AcNeu is known to enter vesicles rather efficiently (1). Analyses by HPLC of the solutes within vesicles prelabeled with [^{3}H]GMP showed no exit of [^{3}H]guanosine after exchange with GDP-[^{14}C]fucose (not shown).

It was also of interest to determine whether addition of GTP or GDP to vesicles first incubated with [^{3}H]GMP resulted in exit of this latter nucleotide from the vesicles. Table 3 shows that both nucleotides stimulate exit of [^{3}H]GMP, although the effect was less than for the corresponding concentration of GMP. This suggests that the nucleoside tri- and diphosphates were first converted to the monophosphates (presumably by Golgi surface phosphatases) prior to entry of the monophosphate into the vesicles; however, the possibility that the translocator selectivity may not be absolute cannot be ruled out.

Table 2. Stoichiometry of entry and exit of guanidine nucleosides in Golgi vesicles

Preincubation		Incubation				
Substrate	Time, min	Substrate	Time, min	Exit of ^{3}H solutes, pmol	Entry of ^{14}C solutes, pmol	Entry/exit
[^{3}H]GDP-fucose	1	GDP-[^{14}C]fucose (2 μM)	1	4.8	19.0	4.0
	5		1	16.0	19.1	1.2
	10	GDP-[^{14}C]fucose (0.45 μM)	1	8.2	9.5	1.2
	10		2	10.8	13.3	1.2
[^{3}H]GMP	20	GDP-[^{14}C]fucose (2 μM)	0.5	2.6	2.9	1.1
	20		1	10.7	25.4	2.4
	20		10	14.9	47.1	3.2

Golgi vesicles were first incubated with [^{3}H]GDP-fucose or [^{3}H]GMP as described in the experiments shown in Figs. 1 and 2. At different times, GDP-[^{14}C]fucose was then added to the vesicle suspension for 0.5–10 min. Determination of amount of solutes entering and leaving the vesicles was done as described in the legend of Fig. 1.

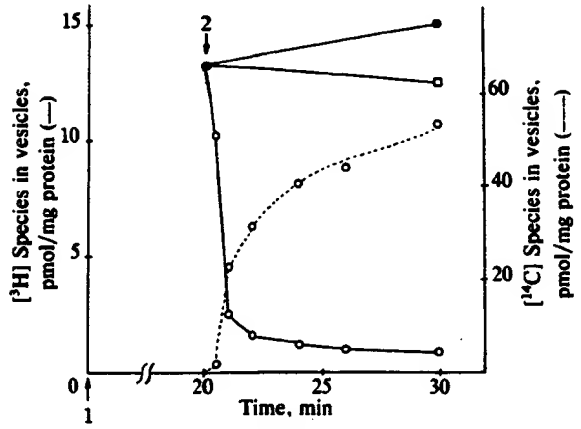

FIG. 2. Translocation of [³H]GMP into Golgi vesicles and subsequent exchange of radioactive solutes from within the vesicles. Ultracentrifuge tubes, each containing Golgi vesicles as described in the legend of Fig. 1, were incubated for 20 min with [*guanidine*-8-³H]GMP (0.3 μCi; final concentration, 0.3 μM; arrow 1, ●). At that time (arrow 2) GDP-[¹⁴C]fucose (5 μl; 0.13 μCi; final concentration, 2 μM) was added to a group of tubes and the incubations were continued for 0.5, 1, 2, 4, 6, and 10 min (○). To another group of tubes that had been incubated for 20 min (arrow 2) with [*guanidine*-8-³H]-GMP, CMP-AcNeu (5 μl; final concentration, 10 μM) was added and the mixtures were incubated for 10 min (□). Samples were then processed as described in the legend of Fig. 1 and *Materials and Methods*.

Preliminary Evidence for Other Coupled Sugar Nucleotide/Nucleoside Monophosphate and Nucleotide Sulfate/Nucleoside Monophosphate Exchange Reactions in the Golgi Apparatus Membrane. The above results strongly suggest that nucleotide sugars enter Golgi vesicles via a coupled equimolar exchange with nucleoside monophosphates. Previous studies from our and other laboratories have shown that Golgi vesicles can also translocate CMP-AcNeu, PAPS, UDP-GlcNAc, and UDP-Gal. We therefore hypothesized that these four nucleotide derivatives enter Golgi vesicles via a coupled exchange with the corresponding nucleoside monophosphate. To obtain preliminary evidence for such a mechanism, Golgi vesicles were first incubated for 20 min with [¹⁴C]CMP, [³H]UDP-GlcNAc, or [³H]PAPS. Table 3 shows that exit of the nucleoside monophosphates from the vesicles was specifically stimulated by the corresponding nucleotide sugar and nucleotide sulfate. Quantitation of solutes entering and leaving the vesicles showed these to be occurring in ratios of close to 1. We know that part of the deviation from 1 is the result of assumptions on specific activity of solutes as previously discussed in detail for GDP-fucose/GMP exchange. Exact quantification of the intralumenal pools of nucleotide derivatives cannot be made; it is also possible that the equilibration time for uridine and cytidine pools is somewhat different from the guanidine pools. These results therefore suggest, in a preliminary manner, that the mechanism of exchange described in detail for GDP-fucose does also occur for other nucleotide sugars and PAPS.

Absence of Effect of Other Potential Perturbants on Translocation of Sugar Nucleotides and PAPS into Golgi Vesicles. The following compounds, when added to the incubation medium, had no effect on translocation *in vitro* of CMP-AcNeu into Golgi vesicles: ATP (200 μM), valinomycin (20 μg/ml), insulin (1 unit/ml), carbonyl cyanide *p*-trifluoromethoxy phenylhydrazone (1–10 μM), cytochalasin B (2 μg/ml), nigericin (1–10 μg/ml), and monensin (1–20 μM). These same compounds as well as phospho*enol*pyruvate (100 μM) and oligomycin (10 μg/ml) had no effect on the translocation *in vitro* of PAPS. Together, these results therefore support our hypothesis that translocation of sugar nucleotides and PAPS into Golgi vesicles occurs via an antiport mechanism with the corresponding nucleoside monophosphates.

DISCUSSION

Evidence *in vitro* has been obtained showing that entry of GDP-fucose into the lumen of Golgi vesicles appears to be coupled with equimolar exit of GMP from the vesicles' lumen (Fig. 1). This phenomenon appears to be temperature dependent (Table 1), inhibited by DIDS, an inhibitor of GDP-fucose translocation, and specific for the type of sugar nucleotide. Thus, GDP-mannose, which does not enter Golgi vesicles, cannot stimulate exit of GMP (Fig. 1).

The Golgi vesicles used in this study have the same topographical orientation as *in vivo* (12). This, together with the fact that GDP-fucose appears to be synthesized in the cytosol (13) and previous evidence suggesting translocation of intact GDP-fucose into such vesicles (1), leads us to hypothesize that this translocation assay *in vitro* is of significance *in vivo* (1). We now postulate that translocation of GDP-fucose *in vivo* occurs via an antiport system such as shown in Fig. 3.

Table 3. Effect of nucleotide derivatives on exit of nucleoside monophosphates from Golgi vesicles preincubated with nucleoside monophosphates or sugar nucleotides

Preincubation (20 min)	Incubation					
			Exit			
Substrate	Substrate	Time, min	% radioactive solutes remaining in vesicles	pmol	Entry pmol	Entry/exit
[³H]GMP (0.4 μM)	GTP (1 μM)	1	60			
	GDP (1 μM)		46			
	GMP (1 μM)		22			
	GDP-[¹⁴C]fucose (1 μM)		29	19.3	22.9	1.2
	GDP-mannose (1 μM)		93			
[¹⁴C]CMP (0.48 μM)	CMP-[³H]AcNeu (1 μM)		43	70.7	124.8	1.8
	CMP (1 μM)		33			
	UDP-GlcNAc (1 μM)	5	85			
[³H]PAPS (0.5 μM)	[³⁵S]PAPS (1 μM)	1	59	25.3	29.2	1.2
	GDP-fucose (1 μM)	5	96			
[³H]UDP-GlcNAc (0.39 μM)	UDP-[¹⁴C]GlcNAc (2.1 μM)	1	46	121.5	248.7	2.0
	[¹⁴C]UMP (2 μM)	1	50	109.3	262.4	2.4

Golgi vesicles were first incubated for 20 min with [³H]GMP, [¹⁴C]CMP, [³H]PAPS, and [³H]UDP-GlcNAc. At that time, different radioactive and nonradioactive nucleotide derivatives were added to the vesicle suspension for 1–5 min. Determination of radioactive solutes entering and leaving the vesicle was done as described in the legend of Fig. 1.

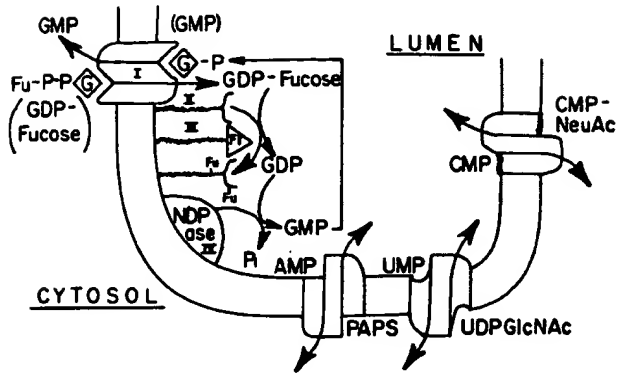

FIG. 3. Proposed mechanism of translocation of sugar nucleotides and PAPS across Golgi vesicle membranes. GDP-fucose binds through the guanidine to a specific antiport protein with a domain on the cytosolic side of the Golgi membrane (I). The sugar nucleotide is then translocated intact across the Golgi membrane into the lumen. Inside the Golgi lumen, GDP-fucose is a substrate, together with endogenous glycoproteins and glycolipids (II) for fucosylation reactions catalyzed by fucosyltransferases (III). GDP can then react with NDPase (IV) to yield GMP, which then binds the antiport protein through its lumenal domain. The nucleoside monophosphate can then exchange with cytosolic GDP-fucose in an equimolar stoichiometry. Similar specific antiport proteins are postulated to occur for PAPS, CMP-AcNeu, and UDP-GlcNAc (UDP-Gal).

Several lines of evidence support the scheme shown in Fig. 3: GDP-fucose is synthesized in the cytosol (13) and is translocated intact across Golgi vesicles via a carrier protein (1) now postulated to be an antiport protein. The sugar nucleotide appears to bind to the antiport protein through the nucleotide moiety (6). Once inside the Golgi lumen, the sugar nucleotide serves as substrate, together with endogenous acceptors (glycoproteins and glycolipids), for fucosylation reactions catalyzed by fucosyltransferases. These enzymes are known to occur in the Golgi (14, 15) and evidence consistent with their lumenal orientation as well as that of fucosylated products has also been obtained (1).

GDP is further degraded to GMP by nucleoside diphosphatase. This enzyme, which appears to be the same as thiamine pyrophosphatase (16), has been shown biochemically and cytochemically to have the active site toward the lumen of the Golgi (17–21). GMP has been detected in the lumen of Golgi vesicles (1, 22) and would then exit the vesicles via a coupled equimolar exchange with additional GDP-fucose.

Preliminary evidence has also been obtained suggesting that other sugar nucleotides and PAPS enter Golgi vesicles via specific antiports. It was shown that exit of radiolabeled nucleoside monophosphates (which had been allowed to enter vesicles during an initial incubation) could only occur if the corresponding nucleotide sugar entered the vesicles (Table 3). This coupled exchange also appeared to be equimolar, although more definitive studies on this have to be made. Coupled specific equimolar exchange was also observed with vesicles preloaded with UDP-GlcNAc or PAPS radiolabeled in the nucleotide. Previous studies from our and other laboratories (4, 8) strongly suggest that the radioactive species leaving the vesicles were UMP and 3'-AMP, respectively.

Kuhn and White (7) and Brandan and Fleischer (8) had previously shown that UMP (derived from UDP-galactose) was exiting the lumen of Golgi vesicles from mammary gland and rat liver. This was postulated as a mechanism for decreasing lumenal accumulation of UMP. Our results are in agreement with these observations and further suggest that both entry of sugar nucleotides and exit of nucleotide monophosphates are coupled in an equimolar stoichiometry. Isolation and characterization of these different antiport proteins should lead to a better understanding of their mechanism of action, including a possible role in regulation of glycosylation and sulfation reactions in the Golgi apparatus.

We thank Mary Perez for a generous gift of [^{3}H]UDP-GlcNAc, Drs. R. Cockrell and M. Snider for helpful discussions, and Ms. Janet Kaufhold for typing. This work was supported by National Institutes of Health Grant GM 30365.

1. Sommers, L. W. & Hirschberg, C. B. (1982) *J. Biol. Chem.* **257**, 10811–10817.
2. Carey, D. J., Sommers, L. W. & Hirschberg, C. B. (1980) *Cell* **19**, 597–605.
3. Perez, M. & Hirschberg, C. B. (1984) *Fed. Proc. Fed. Am. Soc. Exp. Biol.* **43**, 1715 (abstr.).
4. Schwarz, J. K., Capasso, J. M. & Hirschberg, C. B. (1984) *J. Biol. Chem.* **259**, 3554–3559.
5. Capasso, J. M. & Hirschberg, C. B. (1984) *J. Biol. Chem.* **259**, 4263–4266.
6. Capasso, J. M. & Hirschberg, C. B., *Biochim. Biophys. Acta*, in press.
7. Kuhn, N. J. & White, A. (1977) *Biochem. J.* **168**, 423–433.
8. Brandan, E. & Fleischer, B. (1982) *Biochemistry* **21**, 4640–4645.
9. Creek, K. & Morre, D. J. (1981) *Biochim. Biophys. Acta* **643**, 292–305.
10. Hanover, J. A. & Lennarz, W. J. (1982) *J. Biol. Chem.* **257**, 2787–2794.
11. Leelavathi, D. E., Estes, L. W., Feingold, D. S. & Lombardi, B. (1970) *Biochim. Biophys. Acta* **211**, 124–138.
12. Carey, D. J. & Hirschberg, C. B. (1981) *J. Biol. Chem.* **256**, 939–993.
13. Coates, S. W., Gurney, T., Sommers, L. W., Yeh, M. & Hirschberg, C. B. (1981) *J. Biol. Chem.* **255**, 9225–9229.
14. Schachter, H. (1974) *Biochem. Soc. Symp.* **40**, 50–71.
15. Haddad, A., Smith, M. D., Herscovics, A., Nadler, N. J. & Leblond, C. P. (1971) *J. Cell Biol.* **49**, 856–882.
16. Ohkubo, I., Ishibashi, T., Tanigushi, N. & Makita, A. (1980) *Eur. J. Biochem.* **112**, 111–118.
17. Farquhar, M. G., Bergeron, J. J. M. & Palade, G. E. (1974) *J. Cell Biol.* **60**, 8–25.
18. Little, J. S. & Widnell, C. C. (1975) *Proc. Natl. Acad. Sci. USA* **72**, 4013–4017.
19. Novikoff, A. B. & Goldfischer, S. (1961) *Proc. Natl. Acad. Sci. USA* **47**, 802–810.
20. Goldfischer, S., Essner, E. & Schiller, B. (1971) *J. Histochem. Cytochem.* **19**, 349–360.
21. Kuriyama, Y. (1972) *J. Biol. Chem.* **247**, 2979–2988.
22. Fleischer, B. (1981) *Arch. Biochem. Biophys.* **212**, 602–610.

THE JOURNAL OF BIOLOGICAL CHEMISTRY
Vol. 264, No. 30, Issue of October 25, pp. 17615–17618, 1989

Minireview

Glycosyltransferases

STRUCTURE, LOCALIZATION, AND CONTROL OF CELL TYPE-SPECIFIC GLYCOSYLATION

James C. Paulson and Karen J. Colley‡

From the Department of Biological Chemistry and the Molecular Biology Institute, UCLA School of Medicine, Los Angeles, California 90024-1737

Glycosyltransferases involved in the biosynthesis of glycoprotein and glycolipid sugar chains are resident membrane proteins of the endoplasmic reticulum and the Golgi apparatus. Although the glycosylation pathways in which they participate have been extensively studied and reviewed (1–3), major questions remain concerning the molecular basis for the subcellular organization of the glycosylation machinery and how cells are able to regulate the expression of specific carbohydrate sequences. This latter subject is of current interest in view of increasing evidence that cell surface carbohydrate groups mediate a variety of cellular interactions during development, differentiation, and oncogenic transformation (4–8). This review examines insights into these areas afforded by recent successes in the cloning and expression of several glycosyltransferases involved in the synthesis of terminal sequences of glycoproteins and glycolipids.

Terminal Glycosyltransferases in the Synthesis of Glycoproteins and Glycolipids

Glycosyltransferases transfer sugar residues from an activated donor substrate, usually a nucleotide sugar, to a growing carbohydrate group. The specificity of the enzymes for their donor and acceptor substrates constitutes the primary basis for determining the structures of the sugar chains produced by a cell. It is estimated that 100 or more glycosyltransferases are required for the synthesis of known carbohydrate structures on glycoproteins and glycolipids, and most of these are involved in elaborating the highly diverse terminal sequences (2, 9). These enzymes are typically grouped into families based on the type of sugar they transfer (galactosyltransferases, sialyltransferases, etc.).

Listed in Table I are six glycosyltransferases for which cDNAs have been obtained (10–18).[1,2] Each enzyme elaborates common terminal glycosylation sequences which have been reported to occur on *N*- and *O*-linked sugar chains of glycoproteins and on sugar chains of glycolipids (2, 4–8, 20). It is likely that common terminal sequences of glycoprotein and glycolipid sugar chains are synthesized by the same glycosyltransferases. Indeed, each of the cloned glycosyltransferases represented in Table I has been purified to homogeneity from one or more mammalian sources (2, 9, 21–24), and several have been shown to utilize both glycolipids and glycoproteins as acceptor substrates *in vitro*.

‡ Supported by United States Public Health Service Grant GM-11557.

[1] J. Lowe, L. Ernst, J. Kukowska-Lattallo, and R. Larson, personal communication.

[2] F. Yamamoto, J. Marken, T. Tsuji, T. White, H. Clausen, and S. Hakomori, *J. Biol. Chem.*, submitted for publication.

Domain Structure of Glycosyltransferases

Glycosyltransferases Share a Common Domain Structure—Comparison of the deduced amino acid sequences of the cDNA clones encoding the glycosyltransferases listed in Table I (10–18)[1,2] reveals that these enzymes have virtually no sequence homology. However, as depicted in Fig. 1, they all have a short NH_2-terminal cytoplasmic tail, a 16–20-amino acid signal-anchor domain, and an extended stem region which is followed by the large COOH-terminal catalytic domain (26). Signal-anchor domains (25) act as both uncleavable signal peptides and as membrane-spanning regions and orient the catalytic domains of these glycosyltransferases within the lumen of the Golgi apparatus, as illustrated in Fig. 2.

Relationship between the Stem Region and Occurrence of Soluble Glycosyltransferases—The stem region depicted in Fig. 2 should serve as a flexible tether, allowing the catalytic domain to glycosylate carbohydrate groups of membrane-bound and soluble proteins of the secretory pathway enroute through the Golgi apparatus. Direct evidence for a "stem" or spacer region has been obtained for the Gal α2,6-ST and the GlcNAc β1,4-GT[3] (13, 18). Results from NH_2-terminal sequence analysis of soluble forms of these enzymes suggest a luminal stem region of at least 35 and 62 residues for the two enzymes, respectively, which separates the catalytic domain from the transmembrane domain and is exposed to proteases.

Soluble forms of glycosyltransferases have been demonstrated and purified from milk, serum, and other body fluids (2, 9), and increased serum levels have been noted in disease states (28) and inflammation (29). The origin of these enzymes has long been thought to result from proteolytic release from the membrane-bound forms of the enzymes (reviewed in Refs. 2, 9, 26, 27). Recently results of Jamieson and colleagues suggest that the Gal α2,6-ST is released from rat liver Golgi membranes in response to induced inflammation as a result of cleavage by a cathepsin D-like protease within the acidic *trans* Golgi compartment (29). These observations suggest that soluble glycosyltransferases could result from the release of membrane-bound enzymes by endogenous proteases, presumably by cleavage between the catalytic domain and the transmembrane domain (26, 29).

Lack of Sequence Homology within Glycosyltransferase Families—Common amino acid sequences would be expected within families of glycosyltransferases which share similar acceptor or donor substrates; however, surprisingly few regions of homology have been found within the catalytic domains of glycosyltransferases, and no significant sequence homology is found with any other protein in GenBank (10–18).[1,2] This is especially surprising for the Gal α1,3-GT and GlcNAc β1,4-GT, two galactosyltransferases. However, while these galactosyltransferases exhibit no overall homology, Jo-

[3] The abbreviations used are: GlcNAc β1,4-GT, β-*N*-acetylglucosaminide β1,4-galactosyltransferase; GlcNAc α1,3/4-FT, *N*-acetylglucosaminide α1,3/4-fucosyltransferase; Gal α1,3-GT, β-galactoside α1,3-galactosyltransferase; Gal α2,6-ST, Galβ1,4GlcNAc α2,6-sialyltransferase; Gal α1,2-FT, β-galactoside α1,2-fucosyltransferase; Gal α1,3-GalNAcT,β-(Fucα1,2)Gal α1,3-*N*-acetylgalactosaminyltransferase; SSEA, stage-specific embryonic antigen; ER, endoplasmic reticulum; TPA, tetradecanoylphorbol acetate; G_{D3}, NeuAcα2,8NeuAcα2,3Galβ1,4Glc-ceramide; sialoparagloboside, NeuAcα2,3Galβ1,4GlcNAcβ1,3Galβ1,4Glc-ceramide; G_{M3}, NeuAcα2,3Galβ1,4Glc-ceramide.

TABLE I

Cloned glycosyltransferases involved in the synthesis of terminal sequences in sugar chains of glycoproteins and glycolipids

Abbreviated names combine the acceptor sugar, the linkage formed, and the glycosyltransferase family (GT, galactosyltransferase; ST, sialyltransferase; FT, fucosyltransferase; GalNAcT, *N*-acetylgalactosaminyltransferase). For the *sequence formed*, the sugar transferred is highlighted in boldface, and the acceptor sequence is shown in lightface. R represents the remainder of the glycoprotein or glycolipid sugar chain.

GLYCOSYL-TRANSFERASE	DONOR SUBSTRATE	SEQUENCE FORMED
Galactosyltransferases		
GlcNAc β1,4-GT (10-15) (E.C. 2.4.1.38)	UDP-Gal	**Galβ1,4**GlcNAc-R
Gal α1,3-GT (16,17) (E.C. 2.4.1.151)	UDP-Gal	**Galα1,3Galβ1,4**GlcNAc-R
Sialyltransferase		
Gal α2,6-ST (18) (E.C. 2.4.99.1)	CMP-NeuAc	**NeuAcα2,6Galβ1,4**GlcNAc-R
Fucosyltransferases		
GlcNAc α1,3-FT [1] (E.C. 2.4.1.65)	GDP-Fuc	**Fucα1,3** Galβ1,4 GlcNAc-R **Fucα1,4** Galβ1,3 GlcNAc-R
Gal α1,2-FT [1] (E.C. 2.4.1.69)	GDP-Fuc	**Fucα1,2Galβ1,4**GlcNAc-R **Fucα1,2Galβ1,3**GalNAc-R
N-Acetylgalactosaminyltransferase		
Gal α1,3-GalNAcT [2] (Blood group A transferase)	UDP-GalNAc	**GalNAcα1,3** Gal-R **Fucα1,2**

ziasse *et al.* (16) have pointed out a common hexapeptide KDKKND for the Gal α1,3-GT (bovine, 304–309 (16); and RDKKNE for the GlcNAc β1,4-GT (bovine, human, murine amino acids 346–351 (10–15)). Although the significance of this homology is unknown, a possible role in UDP-Gal binding has been suggested (16).

More extensive amino acid sequence homologies may be found for some enzymes that are yet to be cloned. For example, both blood group A Gal α1,3-GalNAc transferase and blood group B Gal α1,3-GT share the same acceptor substrate, Fuc α1,2-Gal-R, and have been shown to have similar amino acid compositions, cross-react with one another's antibodies, and share the same genetic locus (reviewed in Refs. 2 and 24), suggesting that they have similar nucleotide and amino acid sequences with subtle alterations to accommodate their different donor substrates.[2]

Species Variations in Glycosyltransferase Sequence—The overall amino acid sequence homology for a glycosyltransferase cloned from different species is quite high (80% or greater), with the least homology found in the stem regions (10–18).[2] The bovine (16) and murine (17) Gal α1,3-GTs differ in the predicted lengths of their cytoplasmic tails with the murine enzyme containing an extra 35 amino acids at the NH_2 terminus. However, inspection of the sequence surrounding the ATG start site of the murine Gal α1,3-GT suggests a weak translation start site (TTCATGA (30)), allowing the possibility that the internal ATG may be used, resulting in the same length NH_2-terminal cytoplasmic tails for both species. Two mRNAs that differ in length by 200 base pairs

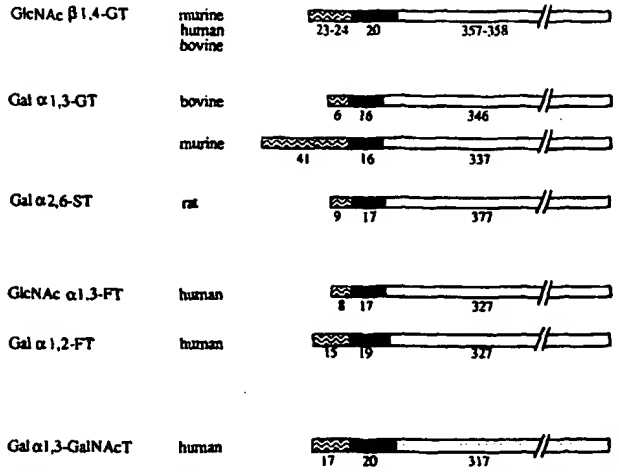

FIG. 1. **Amino acid sequences of cloned terminal glycosyltransferases predict NH_2-terminal signal-anchor domains.** Compared are the predicted domain structures of six glycosyltransferases listed in Table I. The number of amino acids in each domain is listed beneath it. ▨, cytoplasmic domain; ■, signal-anchor domain; □, luminal domain.

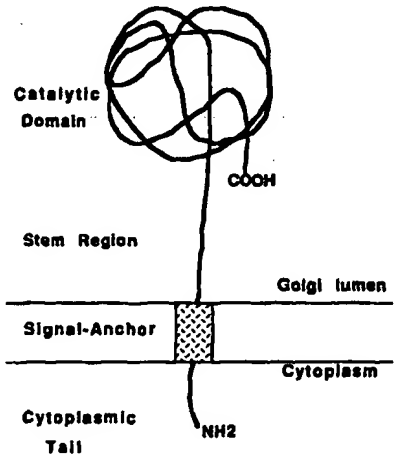

FIG. 2. **Common topology of cloned terminal glycosyltransferases.** Deduced amino acid sequences of the terminal glycosyltransferases cloned to date predict that these enzymes have a characteristic topology in the Golgi apparatus consisting of a short NH_2-terminal cytoplasmic tail, a signal-anchor domain which spans the membrane, an extended stem region, and a large COOH-terminal catalytic domain oriented within the lumen of the Golgi cisternae.

at the 5′ end have also been reported for the murine GlcNAc β1,4-GT which code for enzymes that differ only by 13 amino acids at the NH_2 terminus (10).

Subcellular Localization of Glycosyltransferases

The subcellular localization of the enzymes involved in *N*- and *O*-linked glycosylation has been extensively studied, with terminal glycosyltransferases being found in the Golgi apparatus (1, 31–33). Subcompartmentation within the Golgi apparatus is also well documented, with *N*-acetylglucosaminyltransferase I localized to the *medial* cisternae and the GlcNAc β1,4-GT, Gal α2, 6-ST, and the Gal α1,3-GalNAcT localized to the *trans* cisternae and *trans* Golgi network (33–36). However, recent studies of the localization of Gal α2,6-ST and the Gal α1,3-GalNAcT and the localization of various sialylglycoproteins have suggested that terminal glycosyltransferases may have diffuse distributions throughout the Golgi stack in some cells (33, 37–39).

Although the basis for the localization of glycosyltransferases in the Golgi apparatus has not been elucidated, it is widely believed that membrane proteins of the Golgi apparatus possess specific retention signals that are absent in plasma membrane proteins and proteins that are secreted from the cell (reviewed in Ref. 40). The demonstration of a KDEL sequence that mediates the retention and return of soluble ER proteins provides ample precedence for this concept (41). Evidence cited above for secretion of soluble glycosyltransferases following proteolytic release from the NH_2-terminal signal-anchor implies that the retention signal is not associated with the catalytic domain. Colley *et al.* (42) have tested this hypothesis by replacing the first 57 amino acids of the Gal α2,6-ST, including the cytoplasmic tail, signal-anchor, and stem regions, with the cleavable signal peptide of γ-interferon. This fusion protein when expressed in Chinese hamster ovary cells results in the secretion of a catalytically active, soluble enzyme. A similar result was obtained by Larsen *et al.* (17) when they expressed in Cos-1 cells a fusion protein containing a secretable form of protein A fused to the putative stem and catalytic domains of the Gal α1,3-GT (amino acids 63–394) and found galactosyltransferase activity secreted into the cell media. These data demonstrate that the Golgi apparatus retention signal of these glycosyltransferases must reside in the NH_2-terminal portion of the enzymes, which includes the cytoplasmic tail, signal-anchor, and stem regions.

Regulation of Terminal Glycosylation

Differential Expression of Glycosyltransferases—There is abundant evidence that terminal glycosylation sequences are differentially expressed in cells and are subject to change during development, differentiation, and oncogenic transformation (reviewed in Refs. 4, 5, and 7). The concept that the cellular glycosylation machinery largely determines the structures of glycoprotein sugar chains stems from observed differences in the carbohydrate structures elaborated on viral glycoproteins and recombinant glycoproteins produced in various cultured cell lines (43, 44) and from the sugar structures of glycoproteins naturally expressed in different tissues (reviewed in Ref. 5). Although protein structure places secondary constraints of accessibility on the glycosylation machinery (1) and in the extreme provides recognition determinants for glycosyltransferases that act on sugar chains of one protein or class of proteins (1, 45–47), the terminal glycosylation sequences produced by a cell are presumed to reflect the expression of the corresponding glycosyltransferases which synthesize them.

Strong support for this idea comes from recent examples of altering the cellular glycosylation machinery by transfection of cells with DNA fragments or expression vectors containing cDNAs coding for glycosyltransferases which synthesize terminal glycosylation sequences (17, 37, 48–50). For example, although wild type Chinese hamster ovary cells produce *N*-linked carbohydrate groups with the NeuAcα2,3Gal linkage, Lee *et al.* (37) demonstrated that stably transfected Chinese hamster ovary cells expressing the Gal α2,6-ST (Table I) produce both the NeuAcα2,6Gal and NeuAcα2,3Gal linkages. Similarly, Larsen *et al.* (17) showed that Cos-1 cells transfected with the cDNA for the Gal α1,3-GT (Table I) produce the Galα1,3Gal-R sequence on cell surface carbohydrate groups, a structure not expressed on wild type cells. Lowe and co-workers (17, 49, 50)[1] have exploited such observations in developing strategies for the functional cloning of glycosyltransferases, successfully cloning three of the six glycosyltransferases listed in Table I.

Glycosyltransferase expression is most likely regulated at the level of transcription. In support of this suggestion, the level of Gal α2,6-ST mRNA varies 50–100-fold in various rat tissues, correlating with the activity of the enzyme (51). The level of the Gal α2,6-ST has also been demonstrated to increase 4–5-fold in the liver after induction of inflammation, presumably to provide for the increased production of liver glycoproteins such as α_1 acid glycoprotein and α_1 antitrypsin during the acute phase response (28, 29). Wang *et al.* (53) have recently demonstrated an equivalent induction of sialyltransferase and sialyltransferase mRNA in primary hepatocyte cultures treated with dexamethasone, suggesting that the increased expression following inflammation is controlled by plasma levels of glucocorticoids (53, 54). In contrast to the sialyltransferase, the ubiquitous GlcNAc β1,4-GT is expressed rather uniformly in most murine tissues. However, during spermatogenesis, novel mRNA species are produced which exhibit developmental regulation (52).

Several reports have demonstrated that the changes in glycolipid or glycoprotein glycosylation in transformed cells correspond to quantitative or qualitative changes in the expression of the relevant glycosyltransferases (55–58). The *de novo* expression of a terminal glycosylation sequence is especially interesting with respect to the regulation of glycosylation, because it implies the expression of a glycosyltransferase not expressed in the normal tissue.

Exposure of cells to differentiation agents such as butyrate (19), phorbol esters (59), or retinoic acid (60–62) has also been reported to produce qualitative changes in levels of cell surface terminal glycosylation sequences as well as the specific glycosyltransferases that produce them. Such results are particularly intriguing in view of evidence that terminal glycosylation sequences may play an important role in differentiation pathways, as will be discussed further below.

Biological Implications of Regulated Expression of Terminal Glycosylation Sequences—All the observations cited above suggest that cell type-specific glycosylation sequences can result from regulated expression of glycosyltransferase genes. While not all glycoprotein or glycolipid carbohydrate structures produced by a cell have functional significance (6), it is increasingly apparent that specific sequences in the proper context play important roles in biological recognition.

Developmentally regulated expression of specific glycosylation sequences has been implicated in a variety of cell-cell interactions. Polysialic acid addition onto the neural cell adhesion molecule occurs only in early development and is thought to regulate the adhesive properties of the homotypic neural cell adhesion molecule interactions (47). The embryonic antigen SSEA-1, the product of the GlcNAc α1,3/4-FT (Table I), is expressed at the 16 cell stage of mouse embryo, coincident with the process of compaction (4). Because analogs of the SSEA-1 structure can inhibit compaction, its expression has been suggested to mediate the compaction process (63, 64) and to occur directly through a carbohydrate-carbohydrate interaction rather than a carbohydrate-protein interaction (65). Developmentally regulated glycosylation events have also been implicated in the induction of ureter bud growth into the undifferentiated mesenchyme of the embryonic kidney (66) and in the maturation of thymocytes (67).

Specific gangliosides (sialic acid-containing glycosphingolipids) have been implicated in cell differentiation and cell cycle control (59, 68–73). Retinoic acid-induced differentiation of the hematopoetic precursor cell line HL-60 to granulocytes and TPA-induced differentiation of the same cells to monocytes have been associated with qualitative changes in the expression of sialic acid-containing glycolipids (59, 69,

70). Indeed, TPA-induced monocyte differentiation increased synthesis of ganglioside G_{M3} and the sialyltransferase, G_{M3} synthetase (59). A direct role of ganglioside G_{M3} is suggested by the fact that differentiation to monocytes can be induced without TPA by adding exogenous G_{M3} to the culture media (69). Although the mechanism by which gangliosides might participate in differentiation pathways is not clear at present, specific gangliosides have been implicated in the modulation of growth factor receptor protein kinase activities (72, 73) and in the control of the cell cycle (71).

Glycoprotein and glycolipid sugar chains have been implicated in many other examples of protein targeting and cell-cell interactions too numerous to mention here (4–6, 8, 45, 46, 74, 75). Such observations mark the elucidation of the biological roles of glycoprotein and glycolipid sugar chains as an emerging fronteir. In the future, understanding the regulation of the cellular glycosylation machinery, which produces the specific sugar sequences required for recognition events, will take on increasing importance.

Summary and Future Prospects

It is striking that the glycosyltransferases cloned to date have similar domain structure but little sequence homology. As additional glycosyltransferase cDNAs are cloned and sequenced, it will be of interest to establish the degree to which this diverse group of enzymes might have evolved from common ancestral genes. The availability of a variety of glycosyltransferase cDNAs should allow production of these enzymes through standard expression technology, allowing their use as enzymatic reagents in glycoconjugate research and in the large scale synthesis of oligosaccharides (76). Through gene transfer technologies, glycosyltransferase cDNAs can also be expected to be used in various strategies to explore the biological roles of glycoprotein and glycolipid sugar chains (17, 37).

Acknowledgments—We are grateful to the many investigators who generously shared ideas, unpublished results, and manuscripts prior to publication: Dr. Giacomo D'Agostaro, Dr. Brad Bediak, Dr. Senitiroh Hakomori, Dr. James Jamieson, Dr. David Joziasse, Dr. John Lowe, Drs. Nancy and Joel Shaper, and Dr. Fumi-ichiro Yamamoto.

REFERENCES

1. Kornfeld, R., and Kornfeld, S. (1985) *Annu. Rev. Biochem.* **54**, 631–664
2. Sadler, J. E. (1984) *Biology of Carbohydrates* (Ginsburg, V., and Robbins, P. W., eds) Vol. 2, pp. 87–131, John Wiley and Sons, New York
3. Basu, S., and Basu, M. (1982) in *Glycoconjugates* (Horowitz, M., ed) Vol. 3, pp. 265–285, Academic Press, New York
4. Feizi, T. (1985) *Nature* **314**, 53–57
5. Rademacher, T. W., Parekh, R. B., and Dwek, R. A. (1988) *Annu. Rev. Biochem.* **57**, 785–838
6. Paulson, J. C. (1989) *Trends Biochem. Sci.* **14**, 272–276
7. Hakomori, S. (1984) *Annu. Rev. Immunol.* **2**, 103–126
8. Alhadef, J. (1989) *CRC Crit. Rev. Oncol. Hematol.* **9**, 37–107
9. Beyer, T. A., Sadler, J. E., Rearick, J. I., Paulson, J. C., and Hill, R. L. (1981) *Adv. Enzymol. Relat. Areas Mol. Biol.* **52**, 23–175
10. Shaper, N. L., Hollis, G. F., Douglas, J. G., Kirsch, I. R., and Shaper, J. H. (1988) *J. Biol. Chem.* **263**, 10420–10428
11. Nakazawa, K., Ando, T., Kimura, T., and Narimatsu, H. (1988) *J. Biochem. (Tokyo)* **104**, 165–168
12. Masri, K. A., Appert, H. E., and Fukuda, M. N. (1988) *Biochem. Biophys. Res. Commun.* **157**, 657–663
13. D'Agostaro, G., Bendiak, B., and Tropak, M. (1989) *Eur. J. Biochem.* **183**, 211–217
14. Shaper, N. L., Shaper, J. H., Meuth, J. L., Fox, J. L., Chang, H., Kirsch, I. R., and Hollis, G. F. (1986) *Proc. Natl. Acad. Sci. U. S. A.* **83**, 1573–1577
15. Narimatsu, H., Sinha, S., Brew, K., Okayama, H., and Quasba, P. K. (1986) *Proc. Natl. Acad. Sci. U. S. A.* **83**, 4720–4724
16. Joziasse, D. H., Shaper, J. H., Van den Eijnden, D. H., Van Tunen, A. J., and Shaper, N. L. (1989) *J. Biol. Chem.* **264**, 14290–14297
17. Larsen, R. D., Rajan, V. P., Ruff, M. M., Kukowska-Latello, J., Cummings, R. D., and Lowe, J. B. (1989) *Proc. Natl. Acad. Sci. U. S. A.*, in press
18. Weinstein, J., Lee, E. U., McEntee, K., Lai, P.-H., and Paulson, J. C. (1987) *J. Biol. Chem.* **263**, 17735–17743
19. Fishman, P. H., Bradley, R. M., and Henneberry, R. C. (1976) *Arch. Biochem. Biophys.* **172**, 618–626
20. Galili, U., Shohet, S. B., Kobrin, E., Stults, C. L. M., and Macher, B. A. (1988) *J. Biol. Chem.* **263**, 17755–17762
21. Blanken, W. M., and Van den Eijnden, D. H. (1985) *J. Biol. Chem.* **260**, 12927–12934
22. Elices, M. J., Blake, D. A., and Goldstein, I. J. (1986) *J. Biol. Chem.* **261**, 6064–6072
23. Prieels, J.-P., Monnom, D., Dolmans, M., Beyer, T. A., and Hill, R. L. (1981) *J. Biol. Chem.* **256**, 10456–10463
24. Watkins, W. M. (1980) *Adv. Hum. Genet.* **10**, 1–136
25. Wickner, W. T., and Lodish, H. F. (1985) *Science* **230**, 400–407
26. Paulson, J. C., Weinstein, J., Ujita, E. L., Riggs, K. J., and Lai, P.-H. (1987) *Biochem. Soc. Trans.* **15**, 618–620
27. Strous, G. J. A. M., and Berger, E. G. (1982) *J. Biol. Chem.* **257**, 7623–7628
28. Kim, Y. S., Perdomo, J., Whitehead, J. S., and Curtis, K. J. (1972) *J. Clin. Invest.* **51**, 2033–2039
29. Lammers, G., and Jamieson, J. C. (1989) *Biochem. J.* **261**, 389–393
30. Kozak, M. (1987) *Nucleic Acids Res.* **15**, 8125–8148
31. Roth, J. (1984) *J. Cell Biol.* **98**, 399–406
32. Tooze, S. A., Tooze, J., and Warren, G. (1988) *J. Cell Biol.* **106**, 1475–1487
33. Roth, J. (1987) *Biochim. Biophys. Acta* **906**, 405–436
34. Berger, E. G., and Hesford, F. J. (1985) *Proc. Natl. Acad. Sci. U. S. A.* **82**, 4736–4739
35. Bergeron, J. J. M., Paiement, J., Khan, M. N., and Smith, C. E. (1985) *Biochim. Biophys. Acta* **821**, 393–403
36. Duncan, J. R., and Kornfeld, S. (1988) *J. Cell Biol.* **106**, 617–628
37. Lee, E. U., Roth, J., and Paulson, J. C. (1989) *J. Biol. Chem.* **264**, 13848–13855
38. Yuan, L., Barriocanal, J. G., Bonifacino, J. S., and Sandoval, I. V. (1987) *J. Cell Biol.* **105**, 215–227
39. Gonatas, J. O., Mezitis, S. G. E., Stieber, A., Fleischer, B., and Gonatas, N. K. (1989) *J. Biol. Chem.* **264**, 646–653
40. Rose, J. K., and Doms, R. W. (1988) *Annu. Rev. Cell Biol.* **4**, 257–288
41. Pelham, H. R. B. (1988) *EMBO J.* **7**, 913–918
42. Colley, K. J., Lee, E. U., Adler, B., Browne, J. K., and Paulson, J. C. (1989) *J. Biol. Chem.* **264**, 17619–17622
43. Hsieh, P., Rosner, M. R., and Robbins, P. W. (1983) *J. Biol. Chem.* **258**, 2548–2554
44. Takeuchi, M., Takasaki, S., Miyazaki, H., Kato, T., Hoshi, S., Kochibe, N., and Kobata, A. (1988) *J. Biol. Chem.* **263**, 3657–3663
45. Kornfeld, S. (1987) *FASEB J.* **1**, 462–468
46. Smith, P. L., and Baenziger, J. U. (1988) *Science* **242**, 930–932
47. Rutishauser, U., Acheson, A., Hall, A. K., Mann, D. M., and Sunshine, J. (1988) *Science* **240**, 53–57
48. Kojima, H., Tsuchiya, S., Sekiguchi, K., Gelinas, R., and Hakomori, S. (1987) *Biochem. Biophys. Res. Commun.* **143**, 716–722
49. Ernst, L. K., Rajan, V. P., Larsen, R. D., Ruff, M. M., and Lowe, J. B. (1989) *J. Biol. Chem.* **264**, 3436–3447
50. Rajan, V. P., Larsen, R. D., Ajmera, S., Ernst, L. K., and Lowe, J. B. (1989) *J. Biol. Chem.* **264**, 11158–11167
51. Paulson, J. C., Weinstein, J., and Schauer, A. (1989) *J. Biol. Chem.* **264**, 931–934
52. Shaper, N. L., Wright, W. W., and Shaper, J. H. (1989) *Proc. Natl. Acad. Sci. U. S. A.*, in press
53. Wang, X., O'Hanlon, T. P., and Lau, J. T. Y. (1989) *J. Biol. Chem.* **264**, 1854–1859
54. van Dijk, W., Boers, W., Sala, M., Lasthuis, A.-M., and Mookerjea, S. (1986) *Biochem. Cell Biol.* **64**, 79–84
55. Coleman, P. L., Fishman, P. H., Brady, R. O., and Todaro, G. J. (1975) *J. Biol. Chem.* **250**, 55–60
56. Nakaishi, H., Sanai, Y., Shiroki, K., and Nagai, Y. (1988) *Biochem. Biophys. Res. Commun.* **150**, 760–765
57. Nakaishi, H., Sanai, Y., Shibuya, M., and Nagai, Y. (1988) *Biochem. Biophys. Res. Commun.* **150**, 768–774
58. Matsuura, H., Greene, T., and Hakomori, S. (1989) *J. Biol. Chem.* **264**, 10472–10476
59. Momoi, T., Shinmoto, M., Kasuya, J., Senoo, H., and Suzuki, Y. (1986) *J. Biol. Chem.* **261**, 16270–16273
60. Deutch, V., and Lotan, R. (1983) *Exp. Cell Res.* **149**, 237–245
61. Cummings, R. D., and Mattox, S. A. (1988) *J. Biol. Chem.* **263**, 511–519
62. Chen, C., Fenderson, B. A., Andrews, P. W., and Hakomori, S. (1989) *Biochemistry* **28**, 2229–2238
63. Fenderson, B. A., Zehavi, U., and Hakomori, S. (1984) *J. Exp. Med.* **160**, 1591–1596
64. Bird, J. M., and Kimber, S. J. (1984) *Dev. Biol.* **104**, 449–460
65. Eggens, I., Fenderson, B., Toyokuni, T., Dean, B., Stroud, M., and Hakomori, S. (1989) *J. Biol. Chem.* **264**, 9476–9484
66. Sariola, H., Aufderheide, E., Bernhard, H., Henke-Fahle, S., Dippold, W., and Ekblom, P. (1988) *Cell* **54**, 235–245
67. Francois, L. (1987) *J. Immunol.* **139**, 2220–2229
68. Tsuji, S., Arita, M., and Nagai, Y. (1989) *J. Biochem. (Tokyo)* **94**, 303–306
69. Norjiri, H., Takaku, R., Terui, Y., Miura, Y., and Saito, M. (1986) *Proc. Natl. Acad. Sci. U. S. A.* **83**, 782–786
70. Nojiri, H., Kitagawa, S., Nakamura, M., Kirito, K., Enomoto, Y., and Saito, M. (1988) *J. Biol. Chem.* **263**, 7443–7449
71. Usuki, S., Hoops, P., and Sweeley, C. C. (1988) *J. Biol. Chem.* **263**, 10595–10599
72. Hanai, N., Nores, G. A., MacLeod, C., Torres-Mendez, C.-R., and Hakomori, S. (1988) *J. Biol. Chem.* **263**, 10915–10921
73. Chan, K-F. (1988) *J. Biol. Chem.* **263**, 568–574
74. Drickamer, K. (1988) *J. Biol. Chem.* **263**, 9557–9560
75. Wasserman, P. M. (1987) *Annu. Rev. Cell Biol.* **3**, 109–142
76. Toone, E. J., Simon, E. S., Bednarski, M. D., and Whitesides, G. M. (1989) *Tetrahedron Rep.*, in press

Proc. Natl. Acad. Sci. USA
Vol. 87, pp. 6674–6678, September 1990
Biochemistry

EXHIBIT 3

Molecular cloning, sequence, and expression of a human GDP-L-fucose:β-D-galactoside 2-α-L-fucosyltransferase cDNA that can form the H blood group antigen

(oligosaccharide biosynthesis/glycosyltransferase/surface antigen/chromosome 19)

ROBERT D. LARSEN*, LINDA K. ERNST*, RAJAN P. NAIR*, AND JOHN B. LOWE*†‡

*Howard Hughes Medical Institute and †Department of Pathology, University of Michigan Medical School, Ann Arbor, MI 48109-0650

Communicated by Stuart Kornfeld, June 4, 1990

ABSTRACT **We have previously used a gene-transfer scheme to isolate a human genomic DNA fragment that determines expression of a GDP-L-fucose:β-D-galactoside 2-α-L-fucosyltransferase [α(1,2)FT; EC 2.4.1.69]. Although this fragment determined expression of an α(1,2)FT whose kinetic properties mirror those of the human H blood group α(1,2)FT, their precise nature remained undefined. We describe here the molecular cloning, sequence, and expression of a human cDNA corresponding to these human genomic sequences. When expressed in COS-1 cells, this cDNA directs expression of cell surface H structures and a cognate α(1,2)FT activity with properties analogous to the human H blood group α(1,2)FT. The cDNA sequence predicts a 365-amino acid polypeptide characteristic of a type II transmembrane glycoprotein with a domain structure analogous to that of other glycosyltransferases but without significant primary sequence similarity to these or other known proteins. To directly demonstrate that the cDNA encodes an α(1,2)FT, the COOH-terminal domain predicted to be Golgi-resident was expressed in COS-1 cells as a catalytically active, secreted, and soluble protein A fusion peptide. Southern blot analysis showed that this cDNA identifies DNA sequences syntenic to the human *H* locus on chromosome 19. These results strongly suggest that this cloned α(1,2)FT cDNA represents the product of the human H blood group locus.**

The antigens of the human ABO blood group system are carbohydrate molecules constructed by the sequential action of a series of distinct glycosyltransferases (1, 2). The terminal step in this pathway, catalyzed by the allelic glycosyltransferase products of the ABO locus, requires the expression of a precursor molecule called the H antigen. The blood group H antigen is an oligosaccharide molecule whose expression is normally restricted to the surfaces of human erythrocytes and a variety of epithelial cells, including those that line the gastrointestinal, urinary, and respiratory tracts (1, 3). The H antigen is a fucosylated structure of the form Fucα1-2Galβ-, whose expression is determined by GDP-L-fucose:β-D-galactoside 2-α-L-fucosyltransferases [α(1,2)FTs; EC 2.4.1.69]. These enzymes catalyze a transglycosylation reaction between their sugar nucleotide substrate GDP-L-fucose and oligosaccharide acceptor substrates with terminal type I (Galβ1-3GlcNAc-) or type II (Galβ1-4GlcNAc-) moieties (1).

Surface-expressed H determinants exhibit precise temporal and spatial changes in their expression patterns during human and murine development (4, 5). The functional significance of these changes is as yet unknown, although evidence suggests that other fucosylated molecules participate in adhesive events during development (6–8). Cloned gene segments that determine H antigen expression represent tools to address this question by genetic approaches that perturb H antigen expression during development. We, therefore, established a gene-transfer approach to isolate human DNA segments that determine expression of cell surface H molecules and their corresponding α(1,2)FTs (9, 10). These experiments yielded a cloned human DNA segment that determines expression of an α(1,2)FT acfivity when transfected into a mammalian cell line deficient in this enzyme activity. This enzyme activity was kinetically similar to the human H blood group α(1,2)FT but distinct from the human secretor (SE) α(1,2)FT. Although these data were consistent with the hypothesis that this segment represented part or all of the structural gene encoding the H α(1,2)FT, they were consistent also with the possibility that the DNA sequences trans-determined enzyme expression by interaction with an endogenous gene, transcript, or protein. We report here our analysis of a cloned cDNA representing the product of this human genomic DNA segment.§ These data indicate that this segment encodes the human H blood group α(1,2)FT.

MATERIALS AND METHODS

Cell Lines and DNA Samples. DNA from the cell line UV5HL9-5 (11) and from the Chinese hamster ovary hybrid parent were provided by H. Mohrenweiser and K. Tynan (Lawrence Livermore National Laboratory, Livermore, CA). The origins of all other cell lines and conditions for cell culture are as described (9, 10, 12, 13). Genomic DNA samples from a panel of Chinese hamster ovary × human somatic cell hybrids informative for human chromosomes were purchased from BIOS (New Haven, CT).

Isolation of Human α(1,2)FT cDNA Clones. Approximately 1.8×10^6 recombinant clones from an A431 cell cDNA mammalian expression library (13) were screened by colony hybridization using a ^{32}P-labeled (14) 1.2-kilobase (kb) *Hin*fI fragment of pH3.4 (10) as a probe. Filters were hybridized for 18 hr at 42°C in a hybridization solution as described (9, 10), washed, and subjected to autoradiography. Two hybridization-positive colonies were obtained and isolated by two additional rounds of hybridization and colony purification. Preliminary sequence analysis of the inserts in both hybridization-positive cDNA clones indicated that they each were in the anti-sense orientation with respect to the pCDM7 expression vector (15, 16) promoter sequences. The largest insert was, therefore, recloned into pCDM7 in the sense

The publication costs of this article were defrayed in part by page charge payment. This article must therefore be hereby marked "*advertisement*" in accordance with 18 U.S.C. §1734 solely to indicate this fact.

Abbreviation: α(1,2)FT, GDP-L-fucose:β-D-galactoside 2-α-L-fucosyltransferase.

‡To whom reprint requests should be addressed at: Howard Hughes Medical Institute, Medical Science Research Building I, Room 3510, 1150 West Medical Center Drive, Ann Arbor, MI 48109-0650.

§The sequence reported in this paper has been deposited in the GenBank data base (accession no. M35531).

orientation for expression studies, and the resulting plasmid was designated pCDM7-α(1,2)FT.

Flow Cytometry Analysis. COS-1 cells were transfected with plasmid DNAs by using a DEAE-dextran procedure (17) as described (16). Transfected cells were harvested after a 72-hr expression period and stained either with a mouse IgM anti-H monoclonal antibody (10 μg/ml; Chembiomed, Edmonton, AB, Canada) or with a mouse IgM anti-Lewis^a monoclonal antibody (10 μg/ml; Chembiomed). Cells were then stained with fluorescein-conjugated goat anti-mouse IgM antibody (40 μg/ml; Sigma) and subjected to analysis by flow cytometry (9, 13, 16).

Northern and Southern Blot Analysis. A431 poly(A)$^+$ RNA (10 μg per lane) was subjected to Northern blot analysis as described (16). Genomic DNA (10 μg per lane) was subjected to Southern blot analysis as described (9). Blots were probed with a ^{32}P-labeled (14) 1.2-kb *Hin*fI fragment of pH3.4.

DNA Sequence Analysis. The insert in pCDM7-α(1,2)FT was sequenced by the method of Sanger *et al.* (18) using T7 DNA polymerase (Pharmacia) and 20-mer oligonucleotide primers synthesized according to the sequence of the cDNA insert. Sequence analyses and data base searches were performed using the Microgenie package (Beckman) and the Sequence Analysis software package of the University of Wisconsin Genetics Computer Group (19).

Assay of α(1,2)FT Activity. Cell extracts, conditioned medium from transfected COS-1 cells, and IgG-Sepharose-bound enzyme were prepared and assayed for α(1,2)FT activity by methods described (10, 13). One unit of α(1,2)FT activity is defined as 1 pmol of product formed per hr. The apparent Michaelis constant for the acceptor phenyl β-D-galactoside (20) was determined exactly as described (10).

Construction and Analysis of a Protein A–α(1,2)FT Fusion Vector. A 3196-base-pair *Stu* I–*Xho* I segment of the cDNA insert representing the putative catalytic domain and 3′-untranslated sequences was isolated from pCDM7-α(1,2)FT. This fragment was blunt-ended using the Klenow fragment of DNA polymerase I and ligated to phosphorylated (17) and annealed oligonucleotides (CGGAATTCCCCACATGGCC-TAGG and CCTAGGCCATGTGGGGAATTCCG) designed to reconstruct the coding sequence between the putative transmembrane segment proximal to the *Stu* I site. The ligated fragment was gel-purified, digested with *Eco*RI, and gel-purified again. This *Eco*RI-"linkered" fragment was ligated into the unique *Eco*RI site of pPROTA (21). One plasmid, designated pPROTA-α(1,2)FT$_c$, containing a single insert in the correct orientation, was analyzed by DNA sequencing to confirm the sequence across the vector, linker, and insert junctions. Plasmids pPROTA-α(1,2)FT$_c$, pPROTA, pCDM7-α(1,2)FT, or pCDM7 were transfected into COS-1 cells. After a 72-hr expression period, α(1,2)FT activities in the medium and associated with cells were quantitated as described (10, 13, 16). Affinity chromatography of conditioned medium was performed exactly as described (13, 16).

RESULTS

We have isolated (9, 10) a cloned human genomic DNA restriction fragment whose presence correlates with *de novo* expression of an α(1,2)FT in a set of stably transfected mouse L cells. This fragment determines α(1,2)FT expression in COS-1 cells transfected with a plasmid vector containing these sequences (plasmid pH3.4, ref. 10). The results of these analyses are consistent with the hypothesis that this segment represents a structural gene that encodes the H blood group α(1,2)FT. Nonetheless, these observations are also consistent with the possibility that this segment trans-determines enzyme expression by interaction with an endogenous gene, transcript, or protein. To discriminate between these possibilities and to characterize the nature of the genomic sequences, we first isolated various restriction fragments from the insert in plasmid pH3.4 and tested these for their ability to identify transcripts in the H-expressing stable transfectants and in a human cell line (A431) that also expresses H determinants and a cognate α(1,2)FT (9, 10). We found that a 1.2-kb *Hin*fI restriction fragment identifies a single relatively nonabundant 3.6-kb transcript in A431 cells (Fig. 1). This probe also detects transcripts in the H-expressing mouse L cell transfectants but not in the nontransfected parental L cells (R.D.L. and J.B.L., unpublished data).

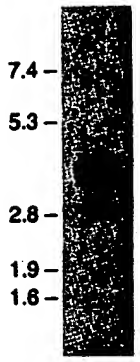

FIG. 1. Northern blot analysis. Poly(A)$^+$ RNA (10 μg) isolated from A431 cells was subjected to Northern blot analysis. The blot was probed with the ^{32}P-labeled 1.2-kb *Hin*fI fragment of pH3.4 (10). The mobilities of RNA molecular size standards, in kb, are indicated at left.

A Cloned cDNA That Directs Expression of Cell Surface H Structures and an α(1,2)FT. We used the 1.2-kb *Hin*fI fragment and colony hybridization to isolate two hybridization-positive cDNA clones from an A431 cell cDNA library (13). To test the cloned cDNAs for their ability to determine expression of surface-localized H antigen and a cognate α(1,2)FT activity, a plasmid was constructed [pCDM7-α(1,2)FT] that consisted of the largest cDNA insert cloned into the mammalian expression vector pCDM7 (15, 16) in the sense orientation with respect to the vector enhancer-promoter sequences. Flow cytometry analysis of COS-1 cells transfected with pCDM7-α(1,2)FT indicates that this cDNA determines expression of cell surface H molecules (Fig. 2). Moreover, COS-1 cells transfected with pCDM7-α(1,2)FT, but not cells transfected with pCDM7, express substantial

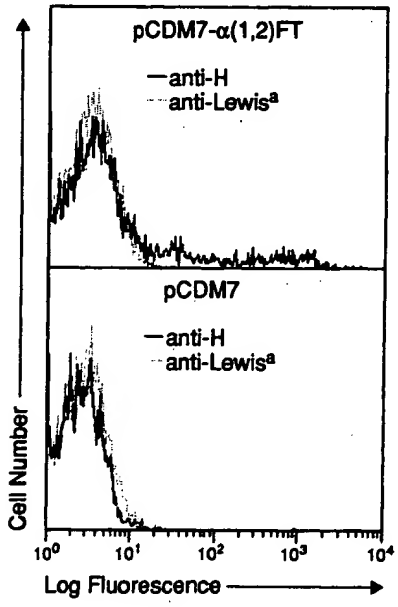

FIG. 2. Flow cytometry analysis of transfected COS-1 cells. COS-1 cells were transfected with plasmid pCDM7-α(1,2)FT (*Upper*) or with the control vector plasmid pCDM7 (*Lower*) and then stained with murine monoclonal IgM antibodies specific for the H antigen (solid lines) or for a negative control antigen (Lewis^a, dotted lines). The cells were then stained with a fluorescein-conjugated goat anti-mouse IgM antibody and subjected to flow cytometry analysis.

quantities of an α(1,2)FT activity. We determined the apparent Michaelis constant exhibited by this α(1,2)FT for an artificial acceptor, phenyl β-D-galactoside, that is specific for this enzyme (20) and that can discriminate between the human H and SE α(1,2)FTs (10, 22). This apparent K_m (2.4 mM) is nearly identical to the apparent K_m we (3.1 mM, ref. 10) and others (4.6 mM and 6.4 mM, ref. 22; 1.4 mM, ref. 23) have determined for the blood group H α(1,2)FT. Moreover, this apparent K_m is also very similar to the one exhibited by the α(1,2)FT in extracts prepared from COS-1 cells transfected with pH3.4 (4.4 mM, ref. 10). This apparent K_m is distinct from the one exhibited by an α(1,2)FT found in human milk (15.1 mM, ref. 10) that is thought to represent the α(1,2)FT encoded by the *SE* locus (22). These data demonstrate that the cDNA in plasmid pCDM7-α(1,2)FT determines expression of an α(1,2)FT whose kinetic properties reflect those exhibited by the human H blood group α(1,2)FT.

The cDNA Sequence Predicts a Type II Transmembrane Glycoprotein. The cDNA insert in pCDM7-α(1,2)FT is 3373 base pairs long (Fig. 3). Its corresponding transcript is 3.6 kb long (Fig. 1), suggesting that this cDNA is virtually full-length. Two potential initiator codons are found within its first 175 nucleotides. Only the second of these, however, is embedded within a sequence context associated with mammalian translation initiation (24). This methionine codon initiates a long open reading frame that predicts a protein of 365 amino acids, with a calculated M_r of 41,249. Hydropathy analysis (25) of the predicted protein sequence indicates that it is a type II transmembrane protein (26), as noted for several other cloned glycosyltransferases (for review, see ref. 27). This topology predicts an 8-residue NH_2-terminal cytosolic domain, a 17-residue hydrophobic transmembrane domain flanked by basic amino acids, and a 340-amino acid COOH-terminal domain that is presumably Golgi-resident and catalytically functional (27). Two potential N-glycosylation sites are found in this latter domain (Fig. 3), suggesting that this sequence, like other glycosyltransferases, may exist as a glycoprotein. No significant similarities were found between this sequence and other sequences in protein or DNA data bases (Protein Identification Resource, release 21.0, and GenBank, release 60.0), with the exception of a 642-base-pair sequence within the 3'-untranslated segment of the cDNA (Fig. 3) that is similar to the human *Alu* consensus sequence (28). Moreover, we identified no significant sequence similarities between this cDNA sequence or its predicted protein sequence and those of other cloned glycosyltransferase cDNAs (13, 16, 29–32).

```
-103 GCCTGGCGTTCCAGGGGCGGCCGGATGTGGCCTGCCTTTGCGGAGGGTGCGCTCCGGCCACGAAAAGCGGACTGTGGATCTGCCACCTGCAAGCAGCTCGGCC

  1  M  W  L  R  S  H  R  Q  L  C  L  A  F  L  L  V  C  V  L  S  V  I  F  F  L  H  I  H  Q  D  S  F  P  H  G  L  G  L  S  I
  1 ATGTGGCTCCGGAGCCATCGTCAGCTCTGCCTGGCCTTCCTGCTAGTCTGTGTCCTCTCTGTAATCTTCTTCCTCCATATCCATCAAGACAGCTTTCCACATGGCCTAGGCCTGTCGATC

 41  L  C  P  D  R  R  L  V  T  P  P  V  A  I  F  C  L  P  G  T  A  M  G  P  Ⓝ  A  S  S  S  C  P  Q  H  P  A  S  L  S  G  T
121 CTGTGTCCAGACCGCCGCCTGGTGACACCCCCAGTGGCCATCTTCTGCCTGCCGGGTACTGCGATGGGCCCCAACGCCTCCTCTTCCTGTCCCCAGCACCCTGCTTCCCTCTCCGGCACC

 81  W  T  V  Y  P  N  G  R  F  G  N  Q  M  G  Q  Y  A  T  L  L  A  L  A  Q  L  N  G  R  R  A  F  I  L  P  A  M  H  A  A  L
241 TGGACTGTCTACCCCAATGGCCGGTTTGGTAATCAGATGGGACAGTATGCCACGCTGCTGGCTCTGGCCCAGCTCAACGGCCGCCGGGCCTTTATCCTGCCTGCCATGCATGCCGCCCTG

121  A  P  V  F  R  I  T  L  P  V  L  A  P  E  V  D  S  R  T  P  W  R  E  L  Q  L  H  D  W  M  S  E  E  Y  A  D  L  R  D  P
361 GCCCCGGTATTCCGCATCACCCTGCCCGTGCTGGCCCCAGAAGTGGACAGCCGCACGCCGTGGCGGGAGCTGCAGCTTCACGACTGGATGTCGGAGGAGTACGCGGACTTGAGAGATCCT

161  F  L  K  L  S  G  F  P  C  S  W  T  F  F  H  H  L  R  E  Q  I  R  R  E  F  T  L  H  D  H  L  R  E  E  A  Q  S  V  L  G
481 TTCCTGAAGCTCTCTGGCTTCCCCTGCTCTTGGACTTTCTTCCACCATCTCCGGGAACAGATCCGCAGAGAGTTCACCCTGCACGACCACCTTCGGGAAGAGGCGCAGAGTGTGCTGGGT

201  Q  L  R  L  G  R  T  G  D  R  P  R  T  F  V  G  V  H  V  R  R  G  D  Y  L  Q  V  M  P  Q  R  W  K  G  V  V  G  D  S  A
601 CAGCTCCGCCTGGGCCGCACAGGGGACCGCCCCGCGCACCTTTGTCGGCGTCCACGTGCGCCGTGGGGACTATCTGCAGGTTATGCCTCAGCGCTGGAAGGGTGTGGTGGGCGACAGCGCC

241  Y  L  R  Q  A  M  D  W  F  R  A  R  H  E  A  P  V  F  V  V  T  S  N  G  M  E  W  C  K  E  N  I  D  T  S  Q  G  D  V  T
721 TACCTCCGGCAGGCCATGGACTGGTTCCGGGCACGGCACGAAGCCCCCGTTTCGTGGTCACCAGCAACGGCATGGAGTGGTGTAAAGAAAACATCGACACCTCCCAGGGCGATGTGACG

281  F  A  G  D  G  Q  E  A  T  P  W  K  D  F  A  L  L  T  Q  C  N  H  T  I  M  T  I  G  T  F  G  F  W  A  A  Y  L  A  G  G
841 TTTGCTGGCGATGGACAGGAGGCTACACCGTGGAAAGACTTTGCCCTGCTCACACAGTGCAACCACACCATTATGACCATTGGCACCTTCGGCTTCTGGGCTGCCTACCTGGCTGGCGGA

321  D  T  V  Y  L  A  Ⓝ  F  T  L  P  D  S  E  F  L  K  I  F  K  P  E  A  A  F  L  P  E  W  V  G  I  N  A  D  L  S  P  L  W
961 GACACTGTCTACCTGGCCAACTTCACCCTGCCAGACTCTGAGTTCCTGAAGATCTTTAAGCCGGAGGCGGCCTTCCTGCCCGAGTGGGTGGGCATTAATGCAGACTTGTCTCCACTCTGG

361  T  L  A  K  P  *
1081 ACATTGGCTAAGCCTTGAGAGCCAGGGAGACTTTCTGAAGTAGCCTGATCTTTCTAGAGCCAGCAGTACGTGGCTTCAGAGGCCTGGCATCTTCTGGAGAAGCTTGTGGTGTTCCTGAAG

1201 CAAATGGGTGCCCGTATCCAGAGTGATTCTAGTTGGGAGAGTTGGAGAGAAGGGGGACGTTTCTGGAACTGTCTGAATATTCTAGAACTAGCAAAACATCTTTTCCTGATGGCTGGCAGG
1321 CAGTTCTAGAAGCCACAGTGCCCACCTGCTCTTCCCAGCCCATATCTACAGTACTTCCAGATGGCTGCCCCCAGGAATGGGGAACTCTCCCTCTGGTCTACTCTAGAAGAGGGGTTACTT
1441 CTCCCCTGGGTCCTCCAAAGACTGAAGGAGCATATGATTGCTCCAGAGCAAGCATTCACCAAGTCCCCTTCTGTGTTTCTGGAGTGATTCTAGAGGGAGACTTGTTCTAGAGAGGACCAG
1561 GTTTGATGCCTGTGAAGAACCCTGCAGGGCCCTTATGGACAGGATGGGGTTCTGGAAATCCAGATAACTAAGGTGAAGAATCTTTTTAGTTTTTTTTTTTTTTTTTGGAGACAGGGTCT
1681 CGCTCTGTTGCCCAGGCTGGAGTGCAGTGGCGTGATCTTGGCTCACTGCAACTTCCGCCTCCTGTGTTCAAGCGATTCTCCTGTCTCAGCCTCCTGAGTAGATGGGACTACAGGCACAGG
1801 CCATTATGCCTGGCTAATTTTTGTATTTTTAGTAGAGACAGGGTTTCACCATGTTGGCCGGGATGGTCTCGATCTCCTGACCTTGTCATCCACCTGTCTTGGCCTCCCAAAGTGCTGGGA
1921 TTACTGGCATGAGCCACTGTGCCCAGCCCGGATATTTTTTTTTAATTATTTATTTATTTATTTATTGAGACGGAGTCTTGCTCTGTAGCCCAGGCCAGAGTGCAGTGGCGCGATCT
2041 CAGCTCACTGCAAGCTCTGCCTCCCGGGTTCATGCCATTCTCCTGCCTCAGCCTCCTGAGTAGCTGGGACTACAGGCGCCCGCCACCACGCCCGGCTAATTTTTTTGTATTTTTAGTAGAGA
2161 CGGGGTTTCATCGTGTTAACCAGGATGGTCTCGATCTCCTGACCTGGTGATCTGCCCACCTCGGCCTCCCACAGTGCTGGGATTACCGGCGTGAGCCACCATGCCTGGCCCGGATAATTT
2281 TTTTTAATTTTTGTAGAGACGAGGTCTTGTGATATTGCCCAGGCTGTTCTTCAACTCCTGGGCTCAAGCAGTCCTCCCACCTTGGCCTCCCAGAATGCTGGGTTTATAGATGTGAGCCAG
2401 CACACCGGGCCAAGTGAAGAATCTAATGAATGTGCAACCTAATTGTAGCATCTAATGAATGTTCCACCATTGCTGGAAAAATTGAGATGGAAAACAAACCATCTCTAGTTGGCCAGCGTC
2521 TTGCTCTGTTCACAGTCTCTGGAAAAGCTGGGGTAGTTGGTGAGCAGAGCGGGACTCTGTCCAACAAGCCCCACAGCCCCTCAAAGACTTTTTTTTGTTTGTTTTGAGCAGACAGGCTAA
2641 AATGTGAACGTGGGGTGAGGGATCACTGCCAAAATGGTACAGCTTCTGGAGCAGAACTTTCCAGGGATCCAGGGACACTTTTTTTTAAAGCTCATAAACTGCCAAGAGCTCCATATATTG
2761 GGTGTGAGTTCAGGTTGCCTCTCACAATGAAGGAAGTTGGTCTTTGTCTGCAGGTGGGCTGCTGAGGGTCTGGGATCTGTTTTCTGGAAGTGTGCAGGTATAAACACACCCTCTGTGCTT
2881 GTGACAAACTGGCAGGTACCGTGCTCATTGCTAACCACTGTCTGTCCCTGAACTCCCAGAACCACTACATCTGGCTTTGGGCAGGTCTGAGATAAAACGATCTAAAGGTAGGCAGACCCT
3001 GGACCCAGCCTCAGATCCAGGCAGGAGCACGAGGTCTGGCCAAGGTGGACGGGGTTGTCGAGATCTCAGGAGCCCCTTGCTGTTTTTTGGAGGGTGAAAGAAGAAACCTTAAACATAGTC
3121 AGCTCTGATCACATCCCCTGTCTACTCATCCAGACCCCATGCCTGTAGGCTTATCAGGGAGTTACAGTTACAATTGTTACAGTACTGTTCCCAACTCAGCTGCCACGGGTGAGAGAGCAG
3241 GAGGTATGAATTAAAAGTCTACAGCACTAA
```

FIG. 3. DNA and derived polypeptide sequence of the cDNA insert in pCDM7-(1,2)FT. The amino acid sequence is shown in single-letter code. The hydrophobic segment representing the putative transmembrane domain is double underlined. Asparagine residues that represent potential N-glycosylation sites are circled. The two copies of a sequence homologous to the human *Alu* consensus sequence are underlined. Not shown are 16 additional deoxyadenine residues found at the 3' end of the insert that represent a portion of the transcript's poly(A) tail.

The Protein Encoded by the cDNA Is an α(1,2)FT. The results of the expression experiments presented above, when considered together with the domain structure predicted by the cDNA sequence, are consistent with the presumption that it encodes an α(1,2)FT. Nonetheless, we wished to directly confirm this and thus exclude the possibility that it instead encodes a molecule that trans-determines this enzyme activity. We, therefore, fused the putative catalytic domain of the predicted protein to a secreted form of the IgG-binding domain of *Staphylococcus aureus* protein A in the mammalian expression vector pPROTA (21), to yield the vector pPROTA-α(1,2)FT$_c$ (Fig. 4). By analogy to similar constructs we have prepared with other cloned glycosyltransferases (13, 16), we expected that, if the cDNA sequence actually encodes an α(1,2)FT, then plasmid pPROTA-α(1,2)FT$_c$ would generate a secreted, soluble, and affinity-purifiable α(1,2)FT. Indeed, conditioned medium prepared from a plate of COS-1 cells transfected with pPROTA-α(1,2)FT$_c$ contained a total of 5790 units of α(1,2)FT activity, whereas a total of 1485 units were found to be cell-associated. Moreover, virtually 100% of the released α(1,2)FT activity was specifically retained by IgG-Sepharose, and most could be recovered after exhaustive washing of this matrix (Table 1). By contrast, we found that most of the activity in COS-1 cells transfected with pCDM7-α(1,2)FT was cell-associated (3450 units), with only trace amounts of activity in the conditioned medium prepared from these cells (≈80 units). Virtually none of this latter activity bound to either matrix (Table 1). Extracts prepared from COS-1 cells transfected with vector pCDM7 or vector pPROTA did not contain any detectable cell-associated or released α(1,2)FT activity. These data demonstrate that the cDNA insert in pCDM7-α(1,2)FT encodes an α(1,2)FT and that information sufficient to generate a catalytically active α(1,2)FT is encompassed within the 333 amino acids distal to the putative transmembrane segment.

The cDNA Corresponds to Genomic Sequences Syntenic to the H Locus on Human Chromosome 19. Genetic evidence indicates that expression of the human H α(1,2)FT is determined by a locus on chromosome 19 (33, 34). By using the 1.2-kb *Hin*fI probe, we identified a cross-hybridizing 6.5-kb *Eco*RI restriction fragment in the genome of the Chinese hamster ovary × human somatic cell hybrid line UV5HL9-5 (Fig. 5, lane 1) that contains human chromosome 19 as its only detectable human DNA (11). This fragment comigrates with a 6.5-kb *Eco*RI restriction fragment detectable in human

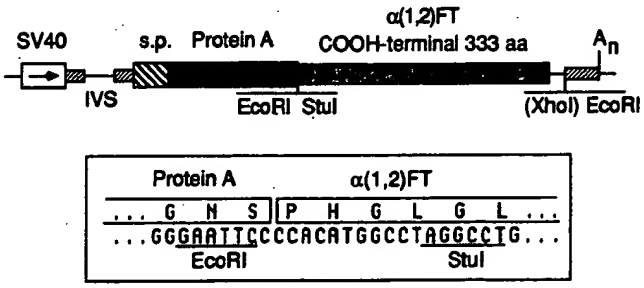

FIG. 4. Protein A–α(1,2)FT fusion vector. The vector pPROTA-α(1,2)FT$_c$ contains amino acids 33–365, representing the putative α(1,2)FT catalytic domain encoded by pCDM7-α(1,2)FT, fused in-frame with the IgG binding domain of *S. aureus* protein A. SV40, simian virus 40 early gene promoter sequences. Sequences denoted by ▨ indicate segments of the vector derived from rabbit β-globin sequences including an intervening sequence (IVS) and a polyadenylylation signal (An). s.p., Transin signal peptide. The *Xho* I (destroyed during the construction, in parentheses) and *Stu* I restriction sites used to isolate the catalytic domain from pCDM7-α(1,2)FT are depicted below the vector cartoon. The DNA sequence and the derived amino acid sequence across the protein A–α(1,2)FT junction are shown in the inset. The *Eco*RI and *Stu* I sites derived from the synthetic linker are underlined.

Table 1. Affinity chromatography of α(1,2)FT activity released from transfected COS-1 cells

	α(1,2)FT activity, units					
	IgG-Sepharose			Sepharose		
Vector	Applied	Spn	Bound	Applied	Spn	Bound
pCDM7-α(1,2)FT	≈30	≈50	<1	≈30	≈80	<1
pPROTA-α(1,2)FT$_c$	2316	<1	1464	2316	2136	<1

Conditioned medium from COS-1 cells transfected with pCDM7-α(1,2)FT or with pPROTA-α(1,2)FT$_c$ was chromatographed on IgG-Sepharose or Sepharose. Unbound (Spn) and matrix-retained materials (Bound) were assayed for α(1,2)FT activity (10, 13, 16).

genomic DNA (Fig. 5, lane 3) but absent from the hybrid parent Chinese hamster ovary cell line (Fig. 5, lane 2). The assignment of these sequences to human chromosome 19 was independently confirmed by Southern blot analysis of a pair of karyotypically stable (35) mouse 3T3 × human somatic cell hybrids (KLEJ-47 and KLEJ-47/P1, ref. 12) that differ only in their human chromosome 19 complement (data not shown). These results were also confirmed by Southern blot analysis of a commercial panel of Chinese hamster ovary × human somatic cell hybrid DNAs (BIOS) (data not shown). These observations support the results of the transfection experiments indicating that the cloned cDNA encodes the human H blood group α(1,2)FT.

Our previous observations indicated that the 3.4-kb *Eco*RI fragment in the plasmid pH3.4 (10) and detected in the genomes of H-expressing mouse L cell transfectants (9) was responsible for determining α(1,2)FT expression. Sequence analysis of this fragment and of the 6.5-kb *Eco*RI fragment identified in these Southern blot experiments indicates that the 3.4-kb segment is encompassed within the 6.5-kb human *Eco*RI fragment, which was apparently truncated at a position on the 3′ side of the coding sequences during the transfection process (R.D.L., L.K.E., and J.B.L., unpublished data).

DISCUSSION

Genetic and biochemical evidence indicates that the human genome encodes at least two discrete α(1,2)FT activities thought to represent the products of two distinct loci (*H* and *SE*) closely linked on human chromosome 19 (33, 34). A third distinct α(1,2)FT activity may also be expressed by human cells (36). Isolation of cloned genes or cDNAs encoding these molecules has not been possible because these enzymes are found in small amounts and are difficult to purify. The isolation of the α(1,2)FT cDNA described here was made possible by a gene-transfer approach (9, 10) designed to isolate genes that determine α(1,2)FT expression without the need to first purify the enzyme. Although it remains to be demonstrated by formal linkage analysis that this cDNA represents the human H blood group locus, we nonetheless

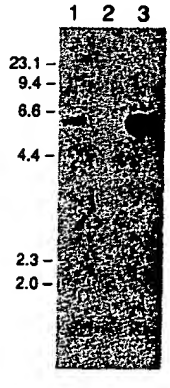

FIG. 5. Southern blot analysis of somatic cell hybrids. Genomic DNA samples prepared from various cell lines were digested with *Eco*RI and subjected to Southern blot analysis. The blot was probed with the ^{32}P-labeled 1.2-kb *Hin*fI fragment of pH3.4 (10). Mobilities of DNA molecular size standards, in kb, are indicated at left. Lanes: 1, somatic cell hybrid line UV5HL9-5; 2, Chinese hamster ovary cell parent of UV5HL9-5 hybrid; 3, human peripheral blood leukocytes.

believe the kinetic analyses reported here and elsewhere (10) plus the chromosomal localization studies provide very strong support for this assignment. Structural and functional analyses of null alleles isolated from rare H-negative individuals (Bombay and para-Bombay phenotypes, ref. 1) should also contribute to our understanding of this gene.

It appears that, in general, glycosyltransferases exist as Golgi-resident membrane-anchored molecules as well as secreted, soluble, and catalytically active forms thought to be derived from the membrane-bound precursors by intracellular proteolytic cleavage (27, 29). Our transfection studies using the cloned α(1,2)FT cDNA indicate, however, that only trace amounts of α(1,2)FT activity are released from COS-1 cells. This observation differs from our results with two other cloned glycosyltransferase cDNAs (13, 16) that determine significant quantities of released soluble enzyme activities when transfected into COS-1 cells. Apparent lack of α(1,2)FT release by transfected COS-1 cells is also at odds with the observation that the H blood group α(1,2)FT can generally be detected in human serum (10, 22, 23). Resolution of these apparent discrepancies will await biosynthetic studies designed to establish the structure(s) of polypeptides (catalytically active or not) encoded by transfected glycosyltransferase cDNAs and subsequently retained or released from the transfected cells.

The cDNA sequence predicts a type II transmembrane glycoprotein whose domain structure appears to be topologically and functionally identical to other cloned glycosyltransferases (13, 16, 27). However, we found no significant primary sequence similarities between this fucosyltransferase and other glycosyltransferase sequences, including those that utilize identical oligosaccharide acceptor molecules [α(1,3)galactosyltransferase, refs. 16 and 32; α(2,6)-sialyltransferase, ref. 29] or sugar nucleotide substrates [human α(1,3/1,4)FT, ref. 13]. These observations are in keeping with other glycosyltransferase sequence comparisons (29–32) as well as our analyses (13, 16) and suggest that the structural basis for substrate recognition by glycosyltransferases is not necessarily predicated upon generic protein domains with specificity for distinct oligosaccharide acceptors or nucleotide sugar substrates. Indeed, we have noted (37) substantial primary sequence similarity between a murine α(1,3)galactosyltransferase (16) and a human α(1,3)*N*-acetylgalactosaminyltransferase (31) that exhibit distinct nucleotide sugar and oligosaccharide acceptor substrate requirements. Nevertheless, low-stringency Southern blot analyses using the α(1,2)FT cDNA described here and other cloned glycosyltransferase sequences (J.B.L., unpublished data) suggest that structural similarities may exist within distinct classes of glycosyltransferases. The outcome of cloning experiments designed to determine the structures and test the function(s) of such cross-hybridizing sequences should determine whether this is indeed the case.

We thank Jeff Leiden for his review of this manuscript, Craig Thompson for helpful comments, and Brian Seed for the gift of the plasmid pCDM7. This work was supported by the Howard Hughes Medical Institute. Dr. Lowe is an Assistant Investigator of the Howard Hughes Medical Institute.

1. Watkins, W. M. (1980) *Adv. Hum. Genet.* **10**, 1–116.
2. Sadler, J. E. (1984) in *Biology of Carbohydrates*, eds. Ginsburg, V. & Robbins, P. W. (Wiley, New York), Vol. 2, pp. 199–213.
3. Szulman, A. E. (1962) *J. Exp. Med.* **115**, 977–996.
4. Szulman, A. E. (1964) *J. Exp. Med.* **119**, 503–523.
5. Fenderson, B. A., Holmes, E. H., Fukushi, Y. & Hakomori, S.-I. (1986) *Dev. Biol.* **114**, 12–21.
6. Fenderson, B. A., Zehavi, U. & Hakomori, S.-I. (1984) *J. Exp. Med.* **160**, 1591–1596.
7. Bird, J. M. & Kimber, S. J. (1984) *Dev. Biol.* **104**, 449–460.
8. Eggens, I., Fenderson, B., Toyokuni, T., Dean, B., Stroud, M. & Hakomori, S.-I. (1989) *J. Biol. Chem.* **264**, 9476–9484.
9. Ernst, L. K., Rajan, V. P., Larsen, R. D., Ruff, M. M. & Lowe, J. B. (1989) *J. Biol. Chem.* **264**, 3436–3447.
10. Rajan, V. P., Larsen, R. D., Ajmera, S., Ernst, L. K. & Lowe, J. B. (1989) *J. Biol. Chem.* **264**, 11158–11167.
11. Thompson, L. H., Bachinski, L. L., Stallings, R. L., Dolf, G., Weber, C. A., Westerveld, A. & Siciliano, M. J. (1989) *Genomics* **5**, 670–679.
12. Miller, D. A., Miller, O. J., Dev, V. G., Hashmi, S., Tantravahi, R., Medrano, L. & Green, H. (1974) *Cell* **1**, 167–173.
13. Kukowska-Latallo, J. F., Larsen, R. D., Nair, R. P. & Lowe, J. B. (1990) *Genes Dev.*, in press.
14. Feinberg, A. P. & Vogelstein, B. (1983) *Anal. Biochem.* **132**, 6–13.
15. Seed, B. (1987) *Nature (London)* **329**, 840–842.
16. Larsen, R. D., Rajan, V. P., Ruff, M. M., Kukowska-Latallo, J., Cummings, R. D. & Lowe, J. B. (1989) *Proc. Natl. Acad. Sci. USA* **86**, 8227–8231.
17. Davis, L. G., Dibner, M. D. & Battey, J. F. (1986) *Methods in Molecular Biology* (Elsevier, New York).
18. Sanger, F., Nicklen, S. & Coulson, A. R. (1977) *Proc. Natl. Acad. Sci. USA* **74**, 5463–5467.
19. Devereux, J., Haeberli, P. & Smithies, O. (1984) *Nucleic Acids Res.* **12**, 387–395.
20. Chester, M. A., Yates, A. D. & Watkins, W. M. (1976) *Eur. J. Biochem.* **69**, 583–593.
21. Sanchez-Lopez, R., Nicholson, R., Gesnel, M.-C., Matrison, L. M. & Breathnach, R. (1988) *J. Biol. Chem.* **263**, 11892–11899.
22. Kumazaki, T. & Yoshida, A. (1984) *Proc. Natl. Acad. Sci. USA* **81**, 4193–4197.
23. Le Pendu, J., Cartron, J. P., Lemieux, R. U. & Oriol, R. (1985) *Am. J. Hum. Genet.* **37**, 749–760.
24. Kozak, M. (1989) *J. Cell Biol.* **108**, 229–241.
25. Kyte, J. & Doolittle, R. F. (1982) *J. Mol. Biol.* **157**, 105–132.
26. Wickner, W. T. & Lodish, H. F. (1985) *Science* **230**, 400–407.
27. Paulson, J. C. & Colley, K. J. (1989) *J. Biol. Chem.* **264**, 17615–17618.
28. Kariya, Y., Kato, K., Hayashizaki, Y., Himeno, S., Tarui, S. & Matsubara, K. (1987) *Gene* **53**, 1–10.
29. Weinstein, J., Lee, E. U., McEntee, K., Lai, P.-H. & Paulson, J. C. (1987) *J. Biol. Chem.* **262**, 17735–17743.
30. Shaper, N. L., Hollis, G. F., Douglas, J. G., Kirsch, I. R. & Shaper, J. H. (1988) *J. Biol. Chem.* **263**, 10420–10428.
31. Yamamoto, F.-I., Marken, J., Tsuji, T., White, T., Clausen, H. & Hakomori, S.-I. (1990) *J. Biol. Chem.* **264**, 1146–1151.
32. Joziasse, D. H., Shaper, J. H., Van den Eijunden, D. H., Van Tunen, A. J. & Shaper, N. L. (1989) *J. Biol. Chem.* **264**, 14290–14297.
33. Oriol, R., Danilovs, J. & Hawkins, B. R. (1981) *Am. J. Hum. Genet.* **33**, 421–431.
34. Le Beau, M. M., Ryan, D., Jr., & Pericak-Vance, M. A. (1989) *Cytogenet. Cell Genet.* **51**, 338–357.
35. Medrano, L. & Green, H. (1973) *Virology* **54**, 515–524.
36. Blaszczyk-Thurin, M., Sarnesto, A., Thurin, J., Hindsgaul, O. & Koprowski, H. (1988) *Biochem. Biophys. Res. Commun.* **151**, 100–108.
37. Larsen, R. D., Rivera-Marrero, C. A., Ernst, L. K., Cummings, R. D. & Lowe, J. B. (1990) *J. Biol. Chem.* **265**, 7055–7061.

EXHIBIT 4

Low Cytoplasmic pH Inhibits Endocytosis and Transport from the *Trans*-Golgi Network to the Cell Surface

Pierre Cosson, Ivan de Curtis, Jacques Pouysségur,* Gareth Griffiths, and Jean Davoust

European Molecular Biology Laboratory, D-6900 Heidelberg, Federal Republic of Germany; and
*Centre de Biochimie CNRS, Université de Nice, Parc de Valrose, 06034 Nice, France

Abstract. A fibroblast mutant cell line lacking the Na^+/H^+ antiporter was used to study the influence of low cytoplasmic pH on membrane transport in the endocytic and exocytic pathways. After being loaded with protons, the mutant cells were acidified at pH 6.2 to 6.8 for 20 min while the parent cells regulated their pH within 1 min. Cytoplasmic acidification did not affect the level of intracellular ATP or the number of clathrin-coated pits at the cell surface. However, cytosolic acidification below pH 6.8 blocked the uptake of two fluid phase markers, Lucifer Yellow and horseradish peroxidase, as well as the internalization and the recycling of transferrin. When the cytoplasmic pH was reversed to physiological values, both fluid phase endocytosis and receptor-mediated endocytosis resumed with identical kinetics. Low cytoplasmic pH also inhibited the rate of intracellular transport from the Golgi complex to the plasma membrane. This was shown in cells infected by the temperature-sensitive mutant ts 045 of the vesicular stomatitis virus (VSV) using as a marker of transport the mutated viral membrane glycoprotein (VSV-G protein). The VSV-G protein was accumulated in the *trans*-Golgi network (TGN) by an incubation at 19.5°C and was transported to the cell surface upon shifting the temperature to 31°C. This transport was arrested in acidified cells maintained at low cytosolic pH and resumed during the recovery phase of the cytosolic pH. Electron microscopy performed on epon and cryo-sections of mutant cells acidified below pH 6.8 showed that the VSV-G protein was present in the TGN. These results indicate that acidification of the cytosol to a pH < 6.8 inhibits reversibly membrane transport in both endocytic and exocytic pathways. In all likelihood, the clathrin and nonclathrin coated vesicles that are involved in endo- and exocytosis cannot pinch off from the cell surface or from the TGN below this critical value of internal pH.

ANIMAL cells maintain a very precise cytoplasmic pH usually between pH 7.0 and 7.2 (reviewed in Roos and Boron, 1981). Growth factors, neurotransmitters, or direct cell–cell interactions can modify the regulation of the intracellular pH in receptive cells (reviewed in Rozengurt, 1986), but little is known about the effect of these variations on membrane traffic. In the case of the endocytic pathway, we showed that the concomitant decrease of the extracellular and intracellular pH inhibits the endocytosis of plasma membrane proteins and fluid phase markers in baby hamster kidney (BHK) cells (Davoust et al., 1987). Clathrin-coated pits, which concentrate receptors and ligands to be internalized, were still present at the cell surface of the acidified cells without apparently being able to pinch off from the cell surface. As a possible interpretation of these data we proposed that clathrin present on coated pits and coated vesicles was unable to depolymerize because of the acidic pH. Another group reported that cytoplasmic acidification inhibits specifically the endocytosis of different receptors located in coated pits, but that the internalization of fluid phase or of ricin which binds to terminal galactose residues was unaffected (Sandvig et al., 1987, 1988). This led to the proposal that an alternative pathway of internalization independent of clathrin-coated pits was responsible for the uptake of ricin or of fluid phase in the acidified cells. In the exocytic direction, a recent report indicated that cytoplasmic acidification can trigger the insertion of proton translocating ATPase in the apical plasma membrane of acid-secreting cells in turtle bladder epithelium (van Adelsberg and Al-Awqati, 1986). These are specialized cells and in the present report, we used fibroblasts to determine whether cytoplasmic acidification could be used to affect differentially the endocytic and exocytic pathways.

To look at several pathways of membrane transport, we assayed simultaneously the internalization and the recycling of ligands, the uptake of two fluid phase markers, and the exocytic transport of a membrane protein from the trans-Golgi

Pierre Cosson's and Jean Davoust's present address is Centre d'Immunologie INSERM-CNRS de Marseille-Luminy, Case 906 13 288 Marseille Cedex 9, France. Ivan de Curtis' present address is Department of Physiology and Howard Hughes Medical Institute, University of California, San Francisco, San Francisco, California 94143-0724.

network (TGN)[1] to the cell surface. We used a mutated cell line, PS120, derived from the hamster lung fibroblast CCL39 cells, which lacks the Na^+/H^+ exchange activity (Pouysségur et al., 1984). These cells could be acidified for 20–30 min using a pulse of NH_4Cl in bicarbonate-free medium followed by a washout. Under the same conditions, the parent cells regulate their cytoplasmic pH because of the activity of the Na^+/H^+ antiport. The mutant cells allowed us to manipulate the intracellular pH without the need of external buffers or substitution of ions, and the parent cells were used to control our experimental conditions. The results indicate that cytoplasmic acidification has an inhibitory effect on the internalization of ligands and markers of the fluid phase, as well as on the export of a membrane protein from the TGN to the cell surface.

Materials and Methods

Materials

FCS, Hepes, horseradish peroxidase (HRP), BSA, transferrin, Lucifer Yellow (LY) CH, and pronase were purchased from Sigma Chemical Co. (St. Louis, MO). Dulbecco's modified essential medium with bicarbonate (DME) or without bicarbonate (DMEb) and Glasgow modified essential medium with bicarbonate (GME) was obtained from Gibco Laboratories (Grand Island, NY). ^{14}C ring-labeled benzoic acid was from Amersham International (Amsersham, UK).

To prepare ^{125}I-labeled transferrin, 0.5 mg of iron-loaded transferrin was diluted in 200 μl PBS (Dulbecco's formulation) and incubated 10 min on ice in the presence of 500 μCi $Na^{125}I$ (Amersham Buchler GmbH, Braunshweig, FRG) in a 20 × 150-mm test tube plated with Iodo-Gen (Pierce Chemical Co., Rockford, IL). The reaction was stopped by removing the sample from the tube and the nonincorporated iodine was removed by chromatography on a Sephadex G50 10 × 0.5-cm column (Pharmacia Fine Chemicals, Piscataway, NJ) equilibrated with PBS supplemented with 0.2% BSA (PBS/BSA). The labeled transferrin (900 cpm/ng) was stored at 4°C and used within 1 month. ^{55}Fe-loaded transferrin (93 cpm/ng) was a generous gift from S. Fuller (EMBL, Heidelberg, FRG).

Cell Cultures and Viruses

CCL39 cell line (American Type Culture Collection, Rockville, MD) and CCL39-derived mutant cell line PS120 lacking functional Na^+/H^+ antiport (Pouysségur et al., 1984) were maintained in DME supplemented with 20 mM Hepes, 4.5 g/liter D-glucose, and 10% FCS (DME/FCS) in a 5% CO_2 incubator. Unless otherwise specified experiments were carried out with 3-d-old confluent cells grown on 5-cm-diam plastic Falcon dishes (~10^7 cells/dish). BHK cells were grown in GME containing 5% FCS, 10% tryptose phosphate broth from Gibco Laboratories, and 10 mM Hepes, pH 7.4 (GME/FCS). 90% confluent monolayers of BHK cells were used after ~2 d of culture. A stock of the clone ts O45–6 of VSV (Griffiths et al., 1985) with a titer of 5.1×10^{11} plaque-forming units (pfu) per ml at 32°C and $< 3 \times 10^5$ pfu per ml at 39.5°C was prepared as described (de Curtis et al., 1988).

Acidification Protocol and Determination of Intracellular pH

To provide an acidification, parent and mutant cells were rinsed with 3 ml DMEb, supplemented with 20 mM Hepes, 4.5 g/liter glucose, and 10% FCS, pH 7.4 (DMEb/FCS), and preincubated at 37°C for 30 min in 3 ml of the same medium containing 20 mM NH_4Cl. The cells were then quickly rinsed twice with DMEb/FCS and incubated in the same medium. The pulse with NH_4Cl was omitted for control experiments.

The measurement of intracellular pH was based on the partition of trace amounts of ^{14}C-labeled benzoic acid between the cytoplasm and the extracellular medium. We used a protocol modified from a previous report (L'Allemain et al., 1984). Briefly, the cells grown in 3.5-cm-diam dishes were incubated for 1 min in 2 ml DMEb/FCS containing 1 μCi [^{14}C]benzoic acid. The dishes were immediately transferred to ice temperature and the cells rinsed four times with PBS within 10 s. After the last wash the cells were extracted for 30 min at 0°C in lysis buffer (10 mM Tris, pH 7.4, 0.05% Triton X-100). The cells were then scraped and homogenized by repeated pipetting through a 1-ml Eppendorf tip. The homogenate was assayed for ^{14}C radioactivity and protein using a Biorad assay (Bradford et al., 1976). The intracellular pH was calculated as previously described (L'Allemain et al., 1984).

Fluid Phase Uptake

LY uptake was tested on cells grown on glass coverslips. LY was used after inactivation of its reactive hydrazine group to reduce the nonspecific background on the cell support. For that, LY was first dissolved in methanol/acetone, 2:1, aliquoted, and dried in defined quantities in 10-ml test tubes. LY was presented to acidified or control cells at 37°C at a concentration of 1 mg/ml. The incubation was stopped at the desired time by chilling the cells which were then rinsed five times with PBS/BSA at 0°C, and photographed in a fluorescence Zeiss photomicroscope equipped with a 63× water immersion lens.

For HRP uptake, parent and mutant cells were incubated in the presence of 1 mg/ml HRP for 5–60 min, then chilled on ice, and washed at 0°C for 5 × 5 min with 20 ml of PBS/BSA and 5 × 5 min with 20 ml of PBS. The amount of internalized HRP was determined as described in a previous report (Davoust et al., 1987).

Transferrin Binding, Uptake, and Recycling

For all the studies using transferrin, 0.2% BSA was substituted for 10% FCS in all the media. The cells were depleted of endogenous transferrin by two washes with 10 ml of DME/BSA followed by three incubations in 10 ml of DME/BSA for 40 min at 37°C in the presence of 5% CO_2 as described (Fuller and Simons, 1986).

To monitor ^{55}Fe uptake, the cells were incubated for 5–60 min in 3 ml DMEb/BSA containing 75 nM of ^{55}Fe-loaded transferrin. They were then cooled on ice and submitted to five cycles of acid and alkaline washes at 0°C: 15 min with 10 ml PBS supplemented with 10% FCS pH 5.0, and 15 min with 10 ml PBS supplemented with 10% FCS pH 8.0 as described (Fuller and Simons, 1986). The cells were then rinsed five times with PBS, extracted at 0°C for 30 min in 500 μl of lysis buffer, scraped, and homogenized. Cellular proteins and radioactivity corresponding to internalized ^{55}Fe were assayed in the lysate.

To monitor the internalization of transferrin at different times after the acidification, the cells were incubated for 5 min at 37°C in 2 ml DMEb/BSA containing 50 nM ^{125}I-labeled transferrin. The cells were cooled on ice to stop the internalization, washed at 0°C 3 × 5 min with 10 ml PBS/BSA and 3 × 5 min with 10 ml PBS, and then treated for 1 h at 4°C with 2 ml pronase solution (DMEb supplemented with 2.5 mg/ml pronase and 20 mM Hepes pH 7.4) to remove ^{125}I-transferrin bound to the cell surface as described (Dautry-Varsat et al., 1983; Ciechanover et al., 1983). The detached cells were resuspended by gentle pipetting through a 1-ml Eppendorf tip, pelleted at 4°C in an Eppendorf microfuge for 5 min, and radioactivity of the total pellet, corresponding to internalized transferrin, was counted. Cellular proteins assayed on separate dishes varied by <10% during the time course of the experiment. Nonspecific internalization was determined in the presence of a 400-fold excess unlabeled transferrin.

To assay the transferrin binding sites on the cell surface, ^{125}I-transferrin was allowed to bind to the cell surface receptors for 90 min using a saturating concentration of 50 nM ^{125}I-transferrin in DMEb/BSA. Unbound transferrin was removed by washing the cells 5 × 5 min with 10 ml PBS/BSA, and 5 × 5 min with 10 ml PBS. The cells were then extracted in 500 μl of lysis buffer, scraped, homogenized, and aliquoted. Cellular proteins and radioactivity were determined. Nonspecific binding was determined in the presence of a 400-fold excess unlabeled transferrin.

To monitor the recycling of transferrin from the endosomes to the cell surface the cells were allowed to internalize ^{125}I-transferrin at a concentration of 50 nM during the pulse with 20 mM NH_4Cl. At time zero the cells were rinsed two times with DMEb/BSA and chased in the same medium for 5–30 min to allow the recycling of ^{125}I-transferrin accumulated in the cells. The dishes were then transferred on ice and the cell medium was collected and replaced with 3 ml of ice-cold PBS/BSA. The cells were then successively washed and treated with pronase, as described for ^{125}I-

1. *Abbreviations used in this paper*: DMEb, Dulbecco's modified essential medium without bicarbonate; GME, Glasgow modified essential medium with bicarbonate; HRP, horseradish peroxidase; LY, Lucifer Yellow; MEMb, minimal essential medium without bicarbonate; TGN, *trans*-Golgi network; VSV-G, vesicular stomatitis virus G protein.

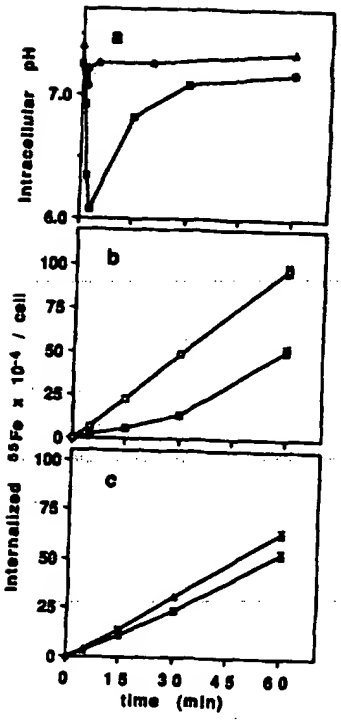

Figure 1. Effect of cytoplasmic acidification on transferrin-mediated ^{55}Fe uptake. Mutant cells lacking the Na^+/H^+ antiport and parent cells were incubated for 30 min at 37°C in the presence of 20 mM NH_4Cl and rinsed twice with a NH_4Cl-free medium. (*a*) Intracellular pH was deduced from the partition of [^{14}C]benzoic acid between the cytoplasm and the extracellular medium at the indicated times after acidification in the mutant cells (■) or the parent cells (▲). (*b*) Uptake of ^{55}Fe in mutant cells incubated in the presence of 75 nM ^{55}Fe-loaded transferrin for the indicated time after acidification (■) or without acidification (□). (*c*) Uptake of ^{55}Fe in parent cells determined as in *b*, after acidification (▲) or without acidification (△). Nonspecific uptake (10%) was determined in the presence of a 400-fold excess of unlabeled transferrin and subtracted from the total counts. The experiments were performed in duplicate and the results expressed as the mean ± SD.

transferrin uptake (Dautry-Varsat et al., 1983; Ciechanover et al., 1983). The total radioactivity of the pellet (pronase resistant counts), of the supernatant (pronase sensitive counts), and of the cell medium was assayed.

Immunofluorescence and Surface Immunoassay of ts O45–infected Cells

Parent and mutant cells were grown on 10 × 10 glass coverslips to ~75% confluency for immunofluorescence or on plastic Petri dishes for the quantitative surface immunoassay. Monolayers were infected with VSV ts O45 at a concentration of 5×10^7 pfu/ml of minimal essential medium without bicarbonate (MEMb) containing 1% FCS and 10 mM Hepes, pH 7.4, for 1 h at 31°C. The virus was discarded and the cells were incubated for 3.5 h at 39°C in DME/FCS. After one wash with DMEb/FCS containing 40 μg/ml of cycloheximide the infected cells were incubated for 105 min in a waterbath at 19.5°C. To acidify the cells, they were rinsed after 75 min at 19.5°C with DMEb/FCS containing cycloheximide and 50 mM NH_4Cl, and incubated in the same medium for another 30 min at 19.5°C. At the end of the 19.5°C incubation, all samples were rinsed twice with DMEb/FCS containing cycloheximide and incubated in the same medium for different times in a waterbath at 31°C. Cells were then cooled on ice and processed for indirect immunofluorescence using a rabbit anti-vesicular stomatitis virus G protein (VSV-G) antibody (K. Simons, EMBL, Heidelberg) followed by incubation with a rhodamine-conjugated goat anti-rabbit IgG antibody (T. Kreis, EMBL). Quantitation of the amount of VSV-G at the cell surface was performed using a new fluoroimmunoassay (Davoust et al., 1987). The monolayer was reacted with a monoclonal antibody against G protein exoplasmic domain (17-2-21-4; K. Simons, EMBL) diluted to 0.5 μg/ml in MEMb for 30 min at 4°C. The cells were then washed 3 × 5 min with PBS containing 0.5% BSA, 1 mM $CaCl_2$, 0.5 mM $MgCl_2$, and treated for 1 h at 4°C with 2.5 ml PBS containing 0.2 μg affinity-purified sheep anti-mouse Fc antibody labeled with Eu (Hemmilä, 1984). The washing sequence was repeated and the monolayer was reacted with 0.5 ml Wallac enhancement solution (Wallac Oy, Turku, Finland) to release the bound Eu and quantitation of the amount of Eu was performed by measuring the delayed fluorescence of 0.2 ml aliquots of the enhancement solution in a Wallac/LKB time-resolved fluorimeter (LKB Instruments, Inc., Gaithersburg, MD).

In another set of experiments, monolayers of BHK cells were infected with VSV ts O45 as described for the PS120 and CCL39 cells. MEMb was substituted for DMEb in the different media and the cells were incubated for 105 min in MEMb/BSA containing 40 μg/ml of cycloheximide in a water bath at 19.5°C. At the end of the 19.5°C incubation, the cells were incubated for 0, 40, or 80 min in a water bath at 31°C either in MEMb/BSA at pH 7.4 or in MEMb/BSA containing 20 mM succinate pH 5.7. To test the reversibility of the treatment at low pH, the monolayers were returned in GME/FCS in the presence of 5% CO_2 at 31°C for 40 min. Quantitation of the amount of VSV-G at the cell surface in nontreated, acid-treated, or reversed cells was performed as for the PS120 and CCL39 cells.

Electron Microscopy and Stereology

Cells were prepared for epon embedding or cryosectioning and immunolabeling as previously described (Griffiths et al., 1983, 1984, 1985).

For the estimation of cell surface coated pits and coated vesicles, 36 random micrographs were taken of epon sections of acidified and control cells at a primary magnification of 28,000. These were enlarged on a projector system that enlarges by a linear factor ×4. The amount of membrane in coated pits (still in obvious continuity with the cell surface) was related to the total amount of plasma membrane by counting the ratio of intersections in both structures (Weibel, 1979). A double lattice grid (D164; Weibel, 1979) was used such that intersections of the total plasma membrane were counted with the large lattice and intersections with coated pits were counted with the small lattice.

Other Assays

The intracellular ATP levels were determined using the luciferin luciferase assay as already described (Davoust et al., 1987).

Results

We first established the conditions of acidification required to inhibit the receptor-mediated uptake of transferrin in mutant cells lacking the Na^+/H^+ antiport and the parent cells were used as a control. To acidify the cytoplasm of both cell lines, we used a pulse of 20 mM NH_4Cl followed by a chase in the absence of NH_4Cl. During the pulse, unprotonated NH_3 diffuses through the plasma membrane and protons generated by cell metabolism or attracted by the intracellular negative potential are captured in the form of NH_4^+. During the chase, the intracellular NH_4^+ dissociates into NH_3, which is permeable, and protons, which cannot cross the plasma membrane. In parent cells, the sodium concentration gradient drives the active extrusion of protons through the Na^+/H^+ antiport at the plasma membrane (L'Allemain et al., 1984), and intracellular pH was only transiently affected after the acidification (Fig. 1 *a*, *solid triangles*). In mutant cells lacking the functional Na^+/H^+ antiport which were derived from hamster lung fibroblasts (Pouysségur et al., 1984), the acidification of the cytosol reached a pH minimum of 6.2 within the first 2 min of the chase of NH_4Cl and the pH was maintained below pH 6.8 for ~20 min (Fig. 1 *a*, *solid squares*). This slow recovery of intracellular pH was probably due to a regulation of intracellular pH mediated by trace amounts of HCO_3^- in equilibrium with atmospheric CO_2 as described (L'Allemain et al., 1985). The intracellular ATP level was not affected by cytosolic acidification (data not shown). Cell viability, assayed by counting the cells 24 h after the acidification, was not altered in accordance with previous results (Pouysségur et al., 1984).

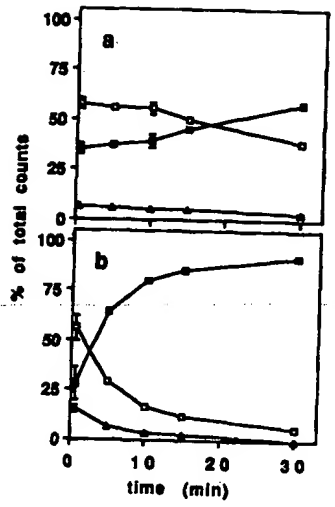

Figure 2. Effect of cytoplasmic acidification on recycling of ^{125}I-labeled transferrin. Mutant and parent cells (*a* and *b*, respectively) were preincubated for 30 min at 37°C with 20 mM NH_4Cl and 50 nM ^{125}I-labeled transferrin. The cells were then washed twice and chased in the absence of NH_4Cl and transferrin. At the indicated times of chase, the amount of ^{125}I-transferrin was determined in the cell medium (free counts; ■), at the cell surface (pronase-sensitive counts; ▲), and inside the cell (pronase-resistant counts; □). Each fraction was expressed as the percentage of total counts that varied from 100,000 to 120,000 cpm per dish. The experiments were performed in duplicate and the results expressed as the mean ± SD.

Cytosolic Acidification Inhibits Receptor-mediated Endocytosis and Recycling to the Cell Surface

We studied the effect of low intracellular pH on the endocytosis and the recycling of transferrin, since this is a well-characterized marker of receptor-mediated endocytosis (Hopkins and Trowbridge, 1983; Dautry-Varsat et al., 1983; Ciechanover et al., 1983; Klausner et al., 1983). The iron-loaded transferrin binds to the transferrin receptor and is internalized via clathrin-coated pits before being delivered to an acidic endocytic compartment. Fig. 1 shows the effect of cytoplasmic acidification on transferrin-mediated ^{55}Fe uptake. In the nonacidified mutant cells, ^{55}Fe accumulates linearly, up to 60 min (Fig. 1 *b*, *open squares*). The accumulation can be competed by an excess of 1 μM cold transferrin. When mutant cells were acidified at pH 6.2 a significant reduction (80%) in the rate of accumulation of ^{55}Fe was initially detected (Fig. 1 *b*, *solid squares*). After ~30 min endocytosis resumed at its normal rate. In the wild-type parent cells, ^{55}Fe accumulates at similar rates both with and without acidification (Fig. 1 *c*).

The whole cycle of transferrin internalization and recycling at the cell surface occurs with a half-time of ~7 min (Dautry-Varsat et al., 1983; Ciechanover et al., 1983; Klausner et al., 1983) and it was of interest to determine whether low cytoplasmic pH also had an effect on the recycling from the endosomes to the cell surface. For this purpose, mutant and parent cells were incubated with ^{125}I-transferrin during the 30-min pulse of NH_4Cl and we determined the amount of ^{125}I-transferrin present in the cell medium, inside the cell, or at the cell surface as a function of time during the chase. In the mutant cells acidified at pH 6.2, we observed an inhibition of the recycling to the cell surface of the internalized transferrin (Fig. 2 *a*). Recycling slowly resumed after 20 min, and after 90 min virtually all the internalized counts were released into the cell medium (data not shown). Experiments performed under the same conditions with the parent cells indicated a very rapid and complete exocytosis of ^{125}I-transferrin (Fig. 2 *b*). The same kinetics of transferrin recycling were found in the untreated parent or mutant cells (data not shown). The number of transferrin binding sites at the surface of the mutant cells was not markedly affected by the acidification protocol as quantitated with ^{125}I-transferrin. From 80 to 95% of the control amount of transferrin surface binding sites was detected at different times after the acidification. Furthermore, the proportion of plasma membrane surface area occupied by coated pits was similar in the mutant cells acidified for 10 min or not acidified, respectively, 2.8 ± 0.4% and 2.7 ± 0.5%.

Kinetics of Fluid Phase Endocytosis

To test whether the inhibition of endocytosis was restricted to receptor-mediated endocytosis via coated pits, we used two different fluid phase markers: LY, which can easily be detected by fluorescence microscopy (Swanson et al., 1985), and HRP, which can easily be quantitated (Steinman et al., 1974). In the nonacidified mutant cells, LY accumulated progressively into intracellular vesicles detectable after 10, 20, or 60 min (Fig. 3, *a*, *b*, and *c*). When the mutant cells were acidified at pH 6.2 no accumulation of the fluid phase marker was detected during the first 10 min (Fig. 3 *d*). Endocytosis resumed after 20 min (Fig. 3 *e*) as evidenced by the presence of fluorescent vesicles in the peripheral cytoplasm. After 60 min numerous intracellular vesicles loaded with LY were detected (Fig. 3 *f*). In the parent cells used as a control, there was no lag time in the formation of LY-positive endocytic vesicles. LY was clearly detectable in endocytic vesicles as bright fluorescent spots, but the quantitation of its uptake was not straightforward because it can slowly permeate the plasma membrane resulting in a weak and diffuse fluorescence in the cytoplasm of the acidified cells (Fig. 3 *d*). To obtain a quantitative estimate of the amount of fluid phase internalized, we used HRP. In the mutant cells without acidification, the accumulation of HRP was continuous for 60 min (Fig. 4 *a*, *open squares*). In the acidified mutant cells, the uptake of HRP was drastically reduced to 20% of the controls for the first 20 min, and from 30 min onwards endocytosis resumed at its normal rate (Fig. 4 *a*, *solid squares*). In the parent cells, the uptake of HRP was unaffected by the acidification (Fig. 4 *b*). When mutant cells were acidified and incubated in the presence of bicarbonate and 5% CO_2 to allow the cells to regulate their intracellular pH (L'Allemain et al., 1985), HRP endocytosis resumed within 5 min (data not shown).

We also compared the uptake of HRP with that of ^{125}I-transferrin presented during a 5-min pulse at different times of chase after acidification in the mutant cells (Fig. 5). The uptake of HRP and ^{125}I-transferrin was reduced to one-fifth of the control during the first 20 min of chase. After this time, internalization resumed with superimposable kinetics for both markers indicating that the reduction of intracellular pH below 6.8 had an identical effect on both the fluid phase uptake of HRP and the receptor-mediated endocytosis of transferrin.

Transport of VSV-G from the TGN to the Cell Surface

Since cytosolic acidification clearly interfered with the rate of membrane transport at various stages (internalization and

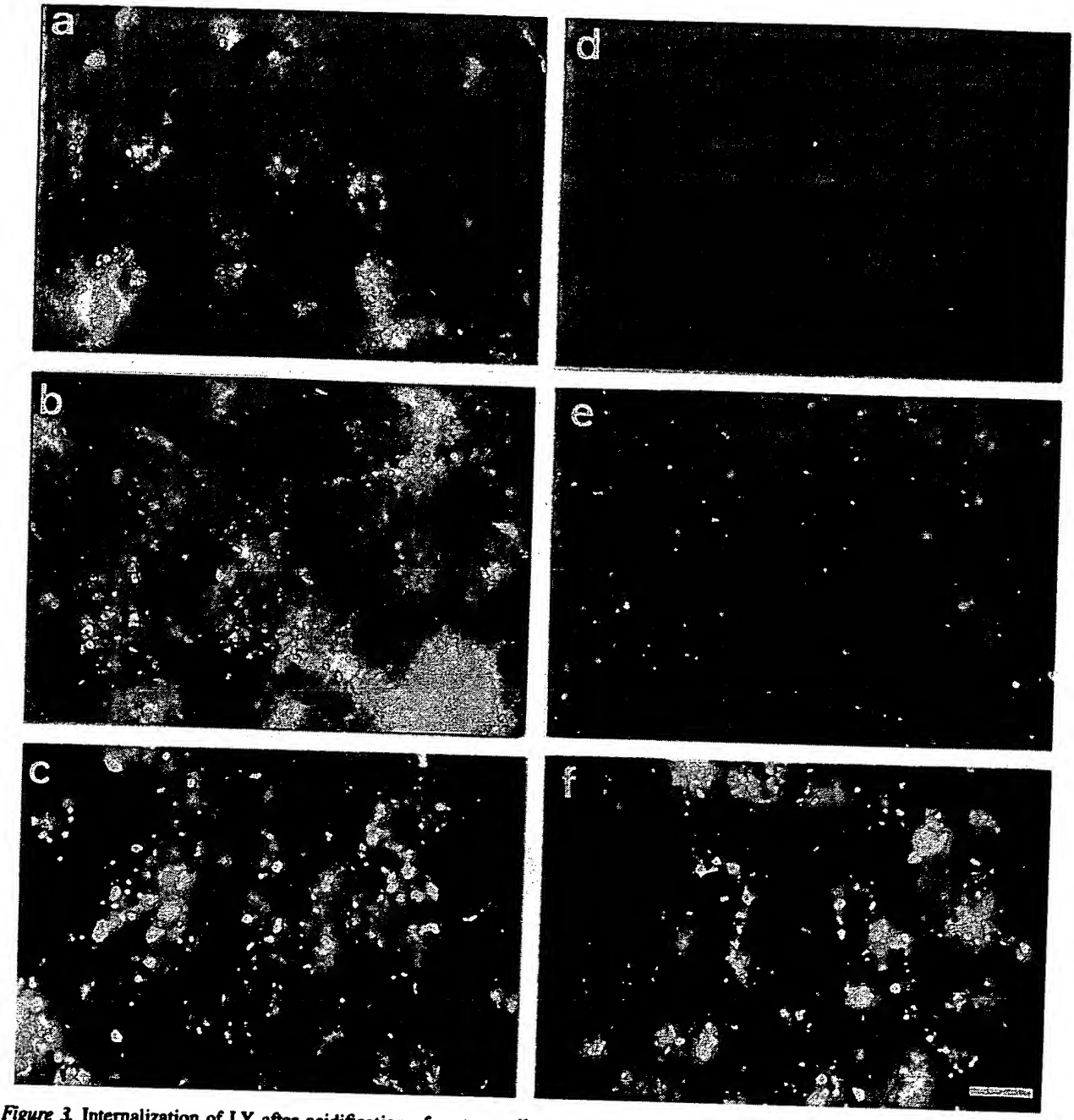

Figure 3. Internalization of LY after acidification of mutant cells. Mutant cells not acidified (*a*, *b*, and *c*) or acidified using a pulse of 20 mM NH_4Cl (*d*, *e*, and *f*) were incubated for different times in the presence of 1 mg/ml of LY. The cells were washed extensively at 4°C before photography using a fluorescence microscope equipped with a fluorescence filter set appropriate for LY and a 63× plan neofluar water immersion lens. Incubation time: 10 (*a* and *d*), 20 (*b* and *e*), and 60 (*c* and *f*) min. Bar, 20 μm.

recycling) in the endocytic pathway, it was conceivable that exocytic transport of proteins might also be affected in a similar way. We took advantage of the temperature-sensitive transport mutant ts O45 of VSV to test the effect of low cytoplasmic pH on the transport of VSV-G from the TGN to the cell surface. The cells were first incubated at the nonpermissive temperature (39°C) to accumulate VSV-G protein in the RER and VSV-G was then accumulated in the TGN for 105 min at 19.5°C in the presence of cycloheximide as previously described (Griffiths et al., 1985; de Curtis et al., 1988). The transport of VSV-G from the TGN to the cell surface was assayed in acidified or nonacidified mutant cells shifted to the permissive temperature of 31°C to allow normal transport of VSV-G protein to the plasma membrane. At 19.5°C, a concentration of 50 mM NH_4Cl (instead of 20 mM at 37°C) was necessary to induce the acidification of the cytoplasm to pH 6.2 when shifting the cells at 31°C. Under these conditions, the variations of intracellular pH with time were equivalent to those established at 37°C (see Fig. 1 *a*).

The transport of VSV-G was monitored either by immunofluorescence in permeabilized cells to reveal its intracellular distribution or by surface immunoassay to quantitate

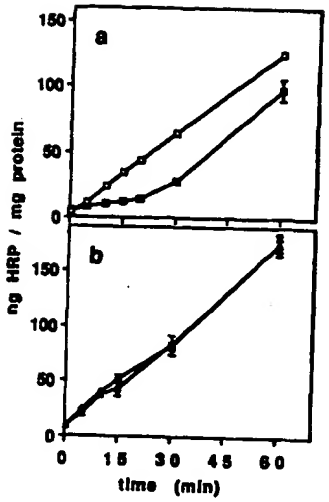

Figure 4. Effect of cytoplasmic acidification on fluid-phase uptake of HRP. Mutant and parent cells were incubated in the presence of 1 mg/ml HRP after acidification with a pulse of 20 mM NH_4Cl or without acidification. At the indicated times the cells were cooled on ice, washed, and the amount of internalized HRP was determined and normalized to the cellular proteins. (*a*) Mutant cells acidified (■) or not (□). (*b*) Parent cells acidified (▲) or not (△). The experiments were performed in duplicate and the results expressed as the mean ± SD.

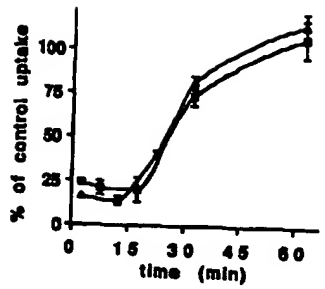

Figure 5. Comparison of fluid phase endocytosis and receptor-mediated endocytosis in acidified mutant cells. Mutant cells acidified with 20 mM NH_4Cl were incubated for different times in DMEb/BSA and then pulsed for 5 min with 1 mg/ml HRP or 50 nM ^{125}I-labeled transferrin. The cells were then cooled on ice, washed, and the internalized HRP (■) or transferrin (▲) were determined. The amounts of HRP or ^{125}I-transferrin uptake are expressed as a percentage of the control (nonacidified mutant cells). In the case of ^{125}I-transferrin, the nonspecific uptake (15% of total determined by an incubation in the presence of a 400-fold excess of unlabeled transferrin) was subtracted and the resulting specific uptake of ^{125}I-transferrin was normalized to the surface binding sites of ^{125}I-transferrin (determined at equivalent time points). The time points indicated on the graph correspond to the midpoint of the 5-min internalization pulses that were used to assay the uptake of HRP and ^{125}I-transferrin.

the rate of appearance of VSV-G at the cell surface. In the Na^+/H^+ mutant cells, VSV-G was localized in the RER at the nonpermissive temperature (Fig. 6 *a*) and then VSV-G moved to the Golgi region after a chase for 105 min at 19.5°C (Fig. 6 *b*). After an additional chase for 30 min at 31°C, most of the VSV-G was present at the surface of the nonacidified mutant cells (Fig. 6 *c*) whereas the VSV-G remained associated with the Golgi region in the acidified mutant cells (Fig. 6 *d*). After 60 min at 31°C, VSV-G was equally present at the cell surface of the nonacidified and acidified mutant cells (Fig. 6, *e* and *f*, respectively). No delay in the transport of VSV-G from TGN to surface was found in the control parent cells treated with a pulse of NH_4Cl (not shown). The time course of the cell surface appearance of VSV-G was determined in either acidified or nonacidified cells using a surface fluoroimmunoassay (Davoust et al., 1987). A half-time of 15 min was found for this process in the nonacidified mutant cells (Fig. 7, *open squares*). Upon cytoplasmic acidifica-

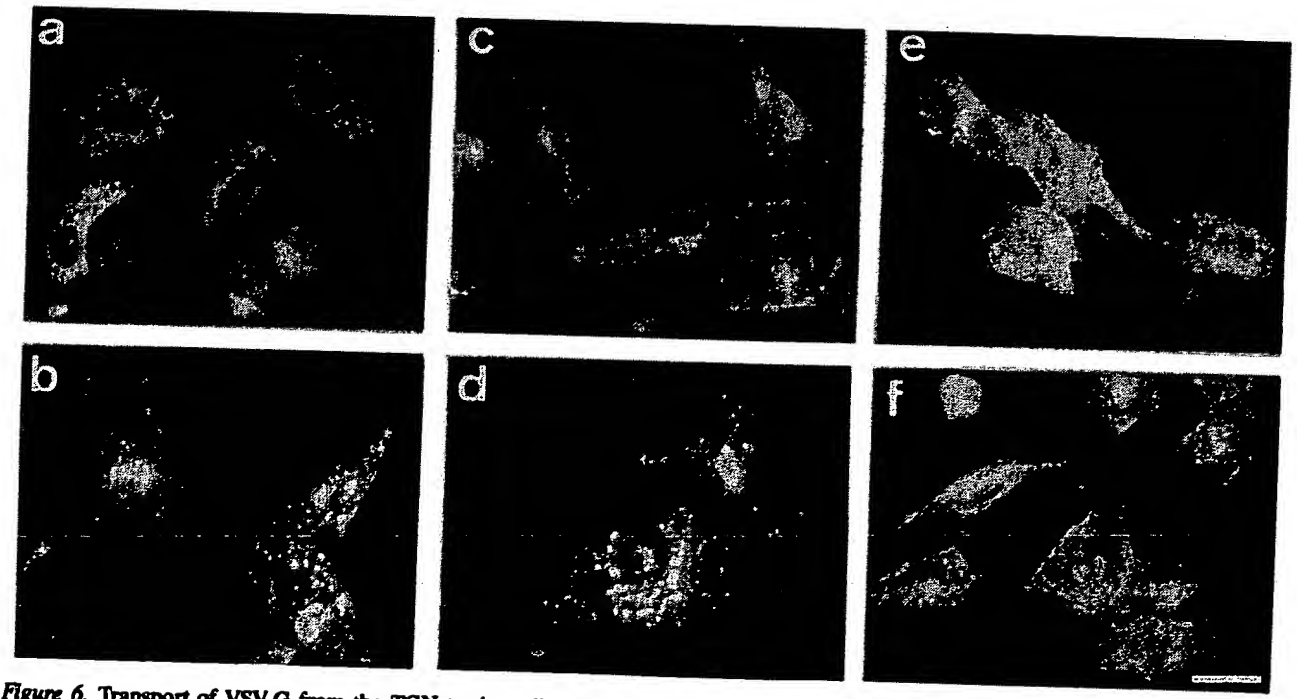

Figure 6. Transport of VSV-G from the TGN to the cell surface in infected mutant cells. Mutant cells were infected with VSV ts O45. VSV-G was accumulated first in the RER for 3.5 h at 39°C (*a*) and then chased to the TGN at 19.5°C in the presence of 40 μg/ml of cycloheximide either for 105 min in nonacidified cells (*b*, *c*, and *e*) or for 75 min followed by 30 min in the presence of 50 mM NH_4Cl for acidified cells (*d* and *f*). Cells were then rinsed twice and either fixed directly (*a* and *b*) or incubated at 31°C in the presence of 40 μg/ml cycloheximide for either 30 (*c* and *d*) or 90 min (*e* and *f*) before fixation. Cells were then processed for immunofluorescence using a rabbit anti-VSV-G antibody followed by a rhodamine-conjugated goat anti-rabbit antibody. Bar, 30 μm.

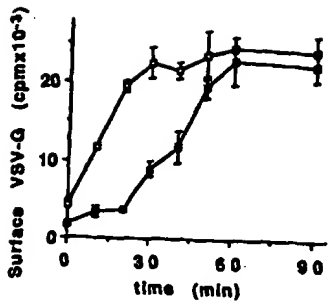

Figure 7. Surface appearance of VSV-G in infected mutant cells. The conditions of infection of mutant cells with VSV ts O45 and the conditions of accumulation of VSV-G in the TGN were identical to the ones of Fig. 6. After the indicated times of chase at 31°C, VSV-G present at the cell surface was quantitated using an anti-VSV-G monoclonal antibody. As a second antibody, we used an Eu-labeled anti-mouse antibody and we measured the delayed fluorescence emission of Eu, using a time-resolved spectrofluorimeter as described previously (Davoust et al., 1987). ■, acidified cells; □, nonacidified cells. Each point was performed in quadruplicate and the results are expressed as a number of photon counts per second ± SD.

tion of mutant cells, the half-time of VSV-G transport to the cell surface was increased to 35 min, but essentially the same amount of VSV-G was delivered to the cell surface after 60 and 90 min as compared to the controls, (Fig. 7, *solid squares*). In the parent cells, the pulse of NH_4Cl had no detectable effects on the rate of appearance of the VSV-G at the cell surface (not shown).

Electron microscopy was then performed either on cryosections labeled with antibodies against the VSV-G to study the intracellular distribution of the VSV-G or on epon sections to observe the morphology of the TGN loaded with VSV-G. On the cryosections obtained from the mutant cells acidified for 30 min (Fig. 8), the gold-labeled VSV-G was present in a membrane compartment indistinguishable from the TGN previously characterized in BHK cells (Griffiths et al., 1985). In agreement with our quantitation of the surface

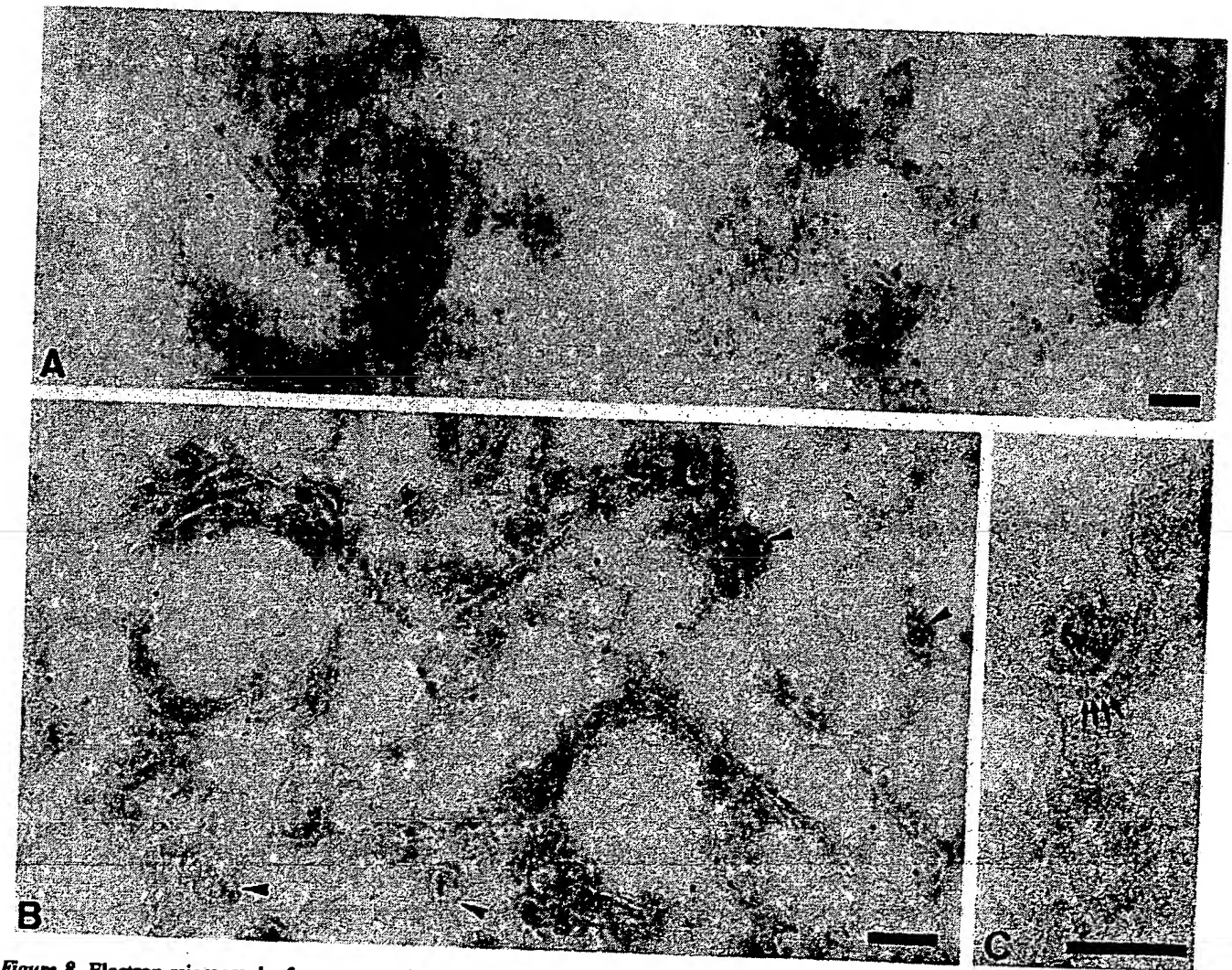

Figure 8. Electron micrographs from cryosections of VSV-infected mutant cells. The conditions of infection, of accumulation of VSV-G at 19.5°C in the TGN and acidification were equivalent to those of Fig. 6. After the pulse of 50 mM NH_4Cl at 19.5°C, the cells were incubated for 30 min without NH_4Cl at 31°C and fixed in 8% formaldehyde. Cells were then processed for cryosectioning and labeled (*A* and *B*) with an affinity-purified antibody against the luminal domain of G protein. Low magnification overview of the Golgi TGN region (*A*) and details of the labeling of the TGN (*B*), evidenced by the presence of numerous coated buds (*arrowheads*). In *C*, a region of the TGN is shown where the structure of the G protein spikes are evident on the luminal side of the membrane. Bars, 100 nm.

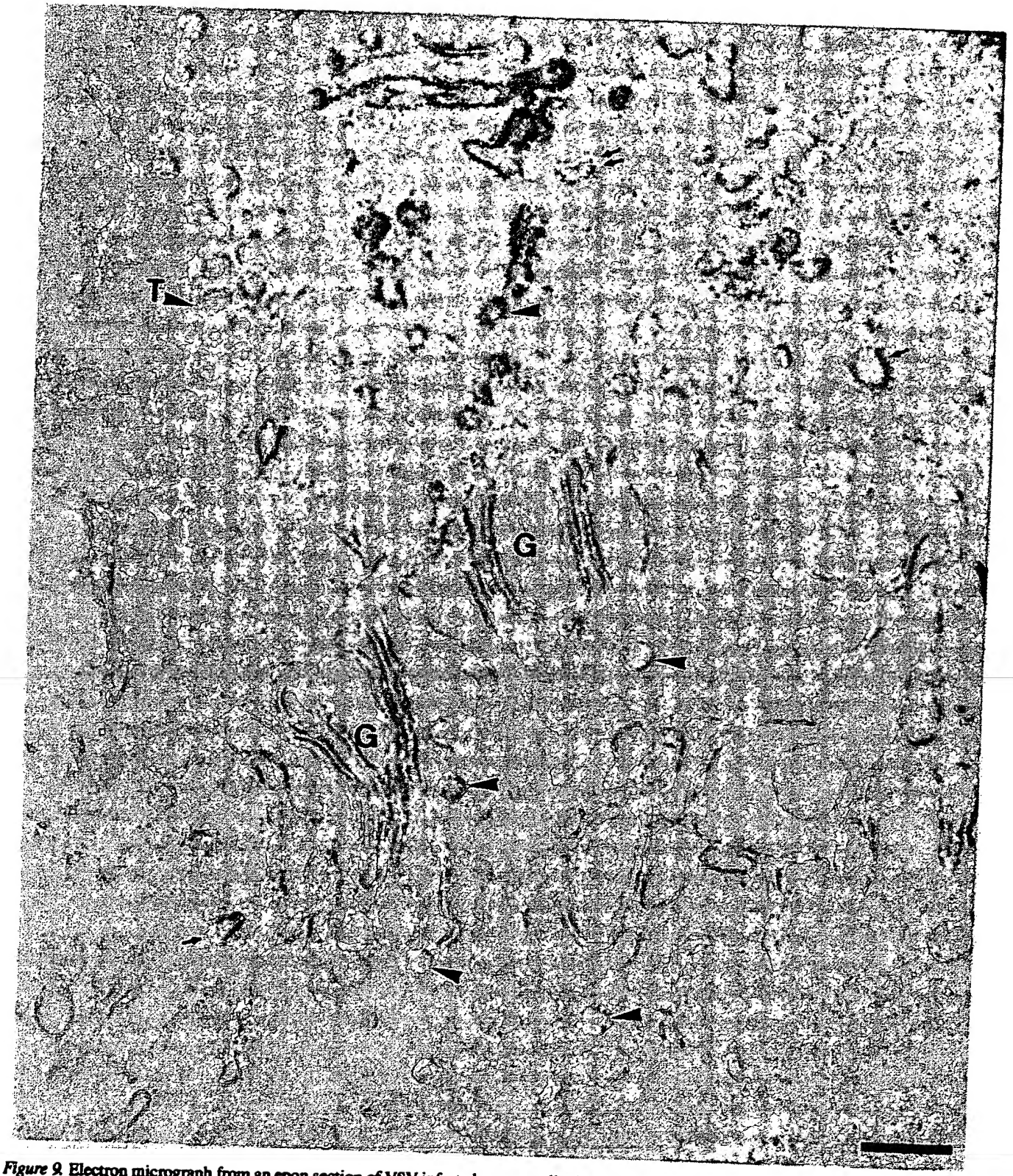

Figure 9. Electron micrograph from an epon section of VSV-infected mutant cells. Epon section of the same preparation as the cryosections in Fig. 8. Note the swollen Golgi stacks (*G*) and extensive TGN region (*T*) which has a distinct thick membrane when filled with VSV-G (see Griffiths et al., 1985). Both clathrin-coated (*arrows*) and nonclathrin-coated (*arrowhead*) vesicular profiles or buds can be seen. The double arrow indicates an oblique section through a clathrin vesicle where the hexagonal lattice is evident. Bar, 200 nm.

VSV-G, there were fewer gold particles at the cell surface as compared to the nonacidified cells (data not shown). On epon sections (Fig. 9), this post-Golgi compartment of accumulation of VSV-G was clearly distinguished from other membranes because of the very dense packing of VSV-G which tends to form invaginations characteristic of the TGN

Table I. Transport of VSV-G from the TGN to the Cell Surface in BHK Cells

Conditions of incubation at 31°C	Intracellular pH	Net amount* of VSV-G transported from the TGN to the cell surface
		counts/s × 10^{-3}
40 min in MEMb pH 5.7	6.2	37 ± 11
80 min in MEMb pH 5.7	6.2	61 ± 21
40 min in MEMb pH 5.7 followed by 40 min in GME‡ pH 7.4	6.2 followed by 7.2	186 ± 15
40 min in MEMb pH 7.4	7.2	148 ± 14
80 min in MEMb pH 7.4	7.2	145 ± 14
40 min in MEMb pH 7.4 followed by 40 min in GME‡ pH 7.4	7.2 followed by 7.2	196 ± 20

BHK cells were infected with VSV ts 045, and VSV-G was accumulated in TGN at 19.5°C under the same conditions as in Fig. 6. Cells were then rinsed twice and incubated at 31°C in the presence of 40 μg/ml cycloheximide as indicated. The amount of VSV-G present at the cell surface was measured with a fluoroimmunoassay as in Fig. 7.

* The background due to the VSV-G transported during the incubation at 19.5°C (32 ± 6 × 10^3 counts/s) was subtracted from the results to monitor only the net amount of VSV-G transported from the TGN to the cell surface during the 31°C incubation. The experiments were performed in triplicate and the results expressed as the mean ± SD.

‡ The BHK cells were incubated with GME/FCS containing bicarbonate in the presence of 5% CO_2 which is needed to reverse membrane transport in cells acidified by exposure to low pH.

loaded with VSV-G (Griffiths et al., 1985). The epon sections indicated also that two types of coated vesicles were still present in the acidified cells in the direct vicinity of the Golgi stacks and the TGN (Fig. 9). The vesicles having a thinner coat are probably equivalent to the nonclathrin-coated vesicles that were shown to contain VSV-G in purified Golgi fractions (Orci et al., 1986; Melançon et al., 1987) and some of them are associated with the rims of the Golgi stacks (see arrowheads in Fig. 9). The vesicles having the thicker coats were most likely clathrin coated (*thin arrows*) and in some cases tangential sections of these revealed the polygonal structure typical of clathrin-coated vesicles (double arrows in Fig. 9). Clathrin-coated and nonclathrin-coated vesicles were also found in the nonacidified cells in approximately equivalent amounts (not shown).

To test whether the inhibition of exocytic transport induced by the low cytosolic pH also occurred in other cell types, we checked the transport of VSV-G in BHK cells acidified by an incubation at an external pH of 5.7 as described (Davoust et al., 1987). Table I shows the quantitation of the VSV-G transported to the surface of BHK cells infected with VSV ts O45 and incubated at 19.5°C under the same conditions used for our parent and mutant cells. When the intracellular pH was dropped to 6.2 at 31°C, the transport of VSV-G from the TGN to the surface was reduced during the first 40 min of acidification to 25% of the control at pH 7.2, and only 41% of the total VSV-G reached the cell surface after 80 min. When the intracellular pH was first dropped to 6.2 for 40 min and then reversed to pH 7.2 in the presence of 5% CO_2, the transport of VSV-G to the surface resumed (126% relative of the control). In the cells incubated for 40 min in MEMb buffered at pH 7.4 and then for 40 min in GME/FCS in the presence of 5% CO_2, we also found a high amount of VSV-G at the cell surface (132% relative to the control).

Discussion

Metabolic inhibitors and reduction in temperature have been used extensively to arrest membrane transport at defined stages in the endocytic and exocytic pathways (reviewed in Mellman et al., 1986; Griffiths and Simons, 1986; Pfeffer and Rothman, 1987). In this study, we examined the effect of cytoplasmic acidification on endocytosis and exocytosis. The Na^+/H^+ antiport deficient cells can easily be acidified and used to study different steps of membrane transport. These cells differ from the parent cells by a point mutation. They are unable to regulate their intracellular pH in the absence of bicarbonate and their cytoplasmic pH can be dropped to pH 6.2 in <2 min using a pulse of 20 mM NH_4Cl followed by an incubation in NH_4Cl-free medium (Pouysségur et al., 1984). The parent cells are not acidified after the pulse of NH_4Cl, and they were used systematically as control cells. We examined in these two cell lines, the effect of cytosolic acidification on the endocytosis and the recycling of transferrin, on the endocytosis of two fluid phase markers, and on the export of a membrane glycoprotein from the TGN to the cell surface.

Influence of Low Intracellular pH on Endocytosis

We showed previously that two threshold values of low extracellular pH could block endocytosis of fluid phase and of plasma membrane proteins at two different stages in BHK cells, an effect that was probably due to the ensuing acidification of the cytosol (Davoust et al., 1987). Under these conditions of low intracellular pH, clathrin formed large intracellular aggregates. We proposed that in the acidified cells, plasma membrane proteins and molecules present in the fluid phase were not delivered to the endocytic compartment because of a strong stabilization of clathrin-coated pits. The same conclusion was reached in Vero or Hep-2 cells which were treated in Na^+ free medium to inhibit the Na^+/H^+ antiport and acidified by a pulse of 40 mM NH_4Cl followed by a chase of 10 min. This treatment lowered the cytoplasmic pH below pH 6.2 and blocked the uptake of HRP-labeled transferrin (Sandvig et al., 1987, 1988). However, when using a pulse of 25 mM NH_4Cl instead of 40 mM, followed by a chase of 30 min instead of 10 min, the endocytosis of LY in the fluid phase or that of ricin-gold conjugates, which binds to galactose-terminating membrane glycoproteins and glycolipids, was not affected by the acidification of the cytoplasm of Vero and Hep2 cells. This finding led to the proposal that nonclathrin-coated pits, also called "smooth" pits, might be responsible for the internalization of LY present in the fluid phase and of ricin bound to terminal galactose residues. Instead, we think that there was a difference in intracellular pH at the different time points considered to analyze the uptake of transferrin, LY, and ricin, and that endocytosis resumed at the longer time points of internalization.

In the Na^+/H^+ antiport deficient cells, we found that endocytosis can be inhibited to about one-fifth of the control by

lowering the cytosolic pH below pH 6.8 and that endocytosis resumes spontaneously after 20 min of acidification when the intracellular pH increases above pH 6.8. The rates of fluid phase endocytosis and of ^{125}I-transferrin endocytosis from the clathrin-coated pits were exactly superimposable at any time point after the initial acidification of the mutant cells (Fig. 4). Therefore, cytoplasmic acidification cannot be used to discriminate different pathways of internalization. Using fluorescent phospholipid analogues implanted at the cell surface in BHK cells, we noticed that the internalization of phospholipids was also reduced to ~20% (Davoust, J. and M. Kail, manuscript in preparation). The internalization of transferrin occurs at a slower rate between pH 6.2 and 6.8 indicating that clathrin-coated vesicles are able to pinch off at a slower rate from the cell surface. The residual internalization of other surface components or of markers present in the fluid phase probably occurs via the same coated vesicles in the acidified cell. In agreement with our interpretation, recent investigations have indicated that the endocytosis of fluid phase and viruses were inhibited to a similar extent in cells loaded with anti-clathrin antibodies (Doxsey et al., 1987). However, we cannot exclude a nonclathrin-coated pathway that would be inhibited at low pH or that would account for <20% of fluid phase uptake. The inhibition of the recycling of ^{125}I-transferrin present in early endosomes indicates that cytoplasmic acidification affects membrane transport at multiple stages in the pathway.

Influence of Low Intracellular pH on Transport from the TGN to the Cell Surface

In the exocytic pathway, several transport vesicles have been clearly identified in close association with the Golgi stacks and the TGN (Griffiths et al., 1985; Griffiths and Simons, 1986). Clathrin-coated vesicles are implicated in the exit of material out of this organel either to the secretory granules (Orci et al., 1984, 1985; Tooze and Tooze, 1986) or to the lysosomes (Lemansky et al., 1987). In addition to clathrin-coated vesicles, a new type of coated vesicle that appears not to contain clathrin has been recently identified in the Golgi complex (Orci et al., 1985; Griffiths et al., 1985). Using Golgi fractions purified from VSV-infected cells and primed with cytosol and ATP, these nonclathrin-coated vesicles were shown to contain VSV-G and it was proposed that these are the carrier vesicles responsible for the constitutive transport of membrane proteins through the Golgi stacks and possibly from the Golgi complex to the cell surface (Orci et al., 1986; Melançon et al., 1987). This finding prompted us to study the transport of VSV-G from the Golgi complex to the cell surface.

To monitor the transport of VSV-G out of the Golgi complex, the cells were infected with VSV ts O45; VSV-G was accumulated in the RER at the nonpermissive temperature of 39°C and then chased to the TGN at 19.5°C as previously described (Griffiths et al., 1985; de Curtis et al., 1988). When the cells were then shifted to the permissive temperature of 31°C, the surface appearance of VSV-G was clearly inhibited by cytosolic acidification for ~30–40 min and resumed afterwards as the cytoplasmic pH increased above pH 7.0. This most likely corresponds to an inhibition of the budding of the carrier vesicles from the TGN for ~20 min followed by a lag time of 10–20 min necessary for the transit of the VSV-G to the cell surface. In BHK cells acidified by exposure to low external pH, the transport of VSV-G from the TGN to the cell surface was also arrested at low cytoplasmic pH and resumed in the presence of a bicarbonate containing medium buffered at pH 7.4.

At the ultrastructural level, VSV-G labeled with immunogold particles on cryosections was clearly associated with a membranous network located in close apposition to Golgi stacks in the mutant cells acidified for 30 min. From its morphology, this intracellular compartment, which retains VSV-G in the acidified cells, is very likely to be the equivalent of the TGN, which has been characterized in details in other cell types (reviewed in Griffiths and Simons, 1986). Furthermore the epon sections revealed the presence of two distinct types of coated vesicles in the Golgi region of the cell. The vesicles having thick and irregular coats are most probably clathrin-coated vesicles whereas, the vesicles having a thinner and more regular coat are often found at the rim of Golgi stacks. This second type of coated vesicles is certainly the equivalent of the nonclathrin-coated vesicles that were recently shown to contain VSV-G in Golgi fractions primed for transport (Orci et al., 1986; Melançon et al., 1987). Since VSV-G was retained in Golgi membranes it is likely that the low cytosolic pH inhibits the formation of carrier vesicles involved in the transport of VSV-G from the TGN to the cell surface.

The VSV-G from the ts O45 mutant can also be used to monitor the transport from RER to Golgi complex by shifting the infected cells from 39 to 31°C. However, we were not able to acidify properly our mutant cells with the NH_4Cl technique during this shift from a bicarbonate-containing medium at 39°C to a bicarbonate-free medium at 31°C. In preliminary experiments, we used BHK cells exposed to an external pH of 5.7 at 31°C and we assayed the appearance of a high molecular weight form of the VSV-G due presumably to sialylation in the TGN (de Curtis et al., 1988). This shift in molecular weight of VSV-G was inhibited at low pH and resumed when returning the cells to neutral pH in a bicarbonate-containing medium as for the transport from the TGN to the cell surface. In all likelihood several processes of membrane budding and transport distributed in the endocytic and exocytic pathways are sensitive to cytoplasmic acidification. However, they might be sensitive to different threshold values of pH beyond the effective resolution of 0.2–0.4 pH unit achieved in our kinetic analysis of membrane transport in the Na^+/H^+ antiport deficient cells. Further experiments are needed to determine the extent of the inhibition of transport from RER to Golgi complex.

In summary the results obtained from the Na^+/H^+ antiport deficient cells indicate that cytosolic acidification below pH 6.8 can inhibit membrane transport in both the endocytic and exocytic directions. The intracellular pH is without doubt an important parameter for cellular functions and membrane traffic is sensitive to defined threshold values of low pH. This can provide new experimental conditions to arrest transiently the export of secretory protein without changing the temperature or the composition of the cell medium. Physiological variations of intracellular pH induced by externally applied growth factors (Pouysségur et al., 1982; Moolenar et al., 1983; Paris and Pouysségur, 1984) or neurotransmitters (Kaila and Voipo, 1987) could also modulate membrane traffic in specialized cells. For example, GABA can cause a drop in postsynaptic pH and it has been proposed that this

might play a role in the inhibition of postsynaptic functions (Kaila and Voipo, 1987). Our results suggest that cytoplasmic acidification could control the efficacy of synaptic transmission by arresting the formation or the release of synaptic vesicles. Future studies will need to focus on the mechanism by which cytoplasmic acidification affect the budding of the clathrin-coated and nonclathrin-coated vesicles involved in endocytic and exocytic processes.

We gratefully acknowledge Mark Kail for excellent technical assistance; Ruth Back for her help in electron microscopy; Ilkka Hemmilä for labeling the affinity-purified sheep anti-mouse Fc antibody with Eu; and Steve Fuller for a generous gift of ^{59}Fe-labeled transferrin. We also thank Jean Gruenberg, Thomas Kreis, and Kai Simons both for their helpful suggestions at various stages of the experiments and for reading drafts of the manuscript. We wish to thank Rachel Wainwright for typing this manuscript with patience and skill.

Received for publication 31 March 1988, and in revised form 7 September 1988.

References

Bradford, M. M. 1976. A rapid and sensitive method for the quantitation of microgram quantities of protein utilizing the principle of protein-dye binding. *Anal. Biochem.* 72:248–254.

Ciechanover, A., A. L. Schwartz, A. Dautry-Varsat, and H. F. Lodish. 1983. Kinetics of internalization and recycling of transferrin and the transferrin receptor in a human hepatoma cell line. Effect of lysosomotropic agents. *J. Biol. Chem.* 258:9681–9689.

de Curtis, I., K. Howell, and K. Simons. 1988. Isolation of a fraction enriched in the trans Golgi network from baby hamster kidney cells. *Exp. Cell Res.* 175:248–265.

Dautry-Varsat, A., A. Ciechanover, and H. F. Lodish. 1983. pH and the recycling of transferrin during receptor-mediated endocytosis. *Proc. Natl. Acad. Sci. USA.* 80:2258–2262.

Davoust, J., J. Gruenberg, and K. Howell. 1987. Two threshold values of low pH block endocytosis at different stages. *EMBO (Eur. Mol. Biol. Organ.) J.* 6:3601–3609.

Doxsey, S., F. M. Brodsky, G. S. Blank, and A. Helenius. 1987. Inhibition of endocytosis by anti-clathrin antibodies. *Cell.* 50:453–463.

Fuller, S. D., and K. Simons. 1986. Transferrin receptor polarity and recycling accuracy in "tight" and "leaky" strains of Madin-Darby canine kidney cells. *J. Cell Biol.* 103:1767–1779.

Griffiths, G., and K. Simons. 1986. The trans Golgi network: sorting at the exit site of the Golgi complex. *Science (Wash. DC).* 234:438–443.

Griffiths, G., K. Simons, G. Warren, and K. T. Tokuyasu. 1983. Immunoelectron microscopy using thin, frozen sections: application to studies of intracellular transport of Semliki forest virus spike glycoproteins. *Methods Enzymol.* 96:466–485.

Griffiths, G., A. McDowell, R. Back, and J. Dubochet. 1984. On the preparation of cryosections for immunocytochemistry. *J. Ultrastruct. Res.* 81:65–78.

Griffiths, G., S. Pfeiffer, K. Simons, and K. Matlin. 1985. Exit of newly synthesized membrane protein from the trans cisterna of the Golgi complex to the plasma membrane. *J. Cell Biol.* 101:949–964.

Hemmilä, I., S. Dakubu, V. M. Mukkala, H. Siitari, and T. Lövgren. 1984. Europium as a label in time-resolved immunofluorometric assays. *Anal. Biochem.* 137:335–343.

Hopkins, C. R., and I. Trowbridge. 1983. Internalization and processing of transferrin and transferrin receptor in human carcinoma A431 cells. *J. Cell Biol.* 97:508–521.

Kaila, K., and J. Voipo. 1987. Post synaptic fall in intracellular pH induced by GABA-activated bicarbonate conductance. *Nature (Lond.).* 330:163–165.

Klausner, C. R., G. Ashwell, J. van Renswoude, J. B. Hardford, and K. R. Bridge. 1983. Binding of apotransferrin to K562 cells: explanation of the transferrin cycle. *Proc. Natl. Acad. Sci. USA.* 80:2263–2266.

L'Allemain, G., S. Paris, and J. Pouysségur. 1984. Growth factor action and intracellular pH regulation in fibroblasts: evidence for a major role of the Na^+/H^+ antiport. *J. Biol. Chem.* 259:5809–5815.

L'Allemain, G., S. Paris, and J. Pouysségur. 1985. Role of a Na^+-dependent $Cl^-/HCO3^-$ exchange in regulation of intracellular pH in fibroblasts. *J. Biol. Chem.* 260:4877–4883.

Lemansky, P., A. Hasilik, K. von Figura, S. Helmy, J. Fishman, R. E. Finne, N. L. Kedersha, and L. Rhome. 1987. Lysosomal enzyme precursors in coated vesicles derived from the exocytic and endocytic pathways. *J. Cell Biol.* 104:1743–1748.

Melançon, P., B. S. Glick, V. Malhotra, P. J. Weidman, T. Serafini, M. L. Gleason, L. Orci, and J. E. Rothman. 1987. Involvement of GTP-binding "G" proteins in transport through the Golgi stack. *Cell.* 51:1053–1062.

Mellman, I., R. Fuchs, and A. Helenius. 1986. Acidification of the endocytic and exocytic pathways. *Annu. Rev. Biochem.* 55:663–700.

Moolenaar, W., R. Tsien, P. Van Der Saag, and S. De Laat. 1983. Na^+/H^+ exchange and cytoplasmic pH in the action of growth factors in human fibroblasts. *Nature (Lond.).* 304:645–648.

Orci, L., P. Halban, M. Amherdt, M. Ravazzola, J.-D. Vassalli, and A. Perrelet. 1984. A clathrin-coated, Golgi-related compartment of the insulin secreting cell accumulates proinsulin in the presence of monensin. *Cell.* 39:39–47.

Orci, L., M. Ravazzola, M. Amherdt, D. Louvard, and A. Perrelet. 1985. Clathrin-immunoreactive sites in the Golgi apparatus are concentrated at the trans pole in polypeptide hormone-secreting cells. *Proc. Natl. Acad. Sci. USA.* 82:5385–5389.

Orci, L., B. S. Glick, and J. E. Rothman. 1986. A new type of coated vesicular carrier that appears not to contain clathrin: its possible role in protein transport within the Golgi stack. *Cell.* 46:171–184.

Paris, S., and J. Pouysségur. 1984. Growth factors activate the Na^+/H^+ antiporter in quiescent fibroblasts by increasing its affinity for intracellular H^+. *J. Biol. Chem.* 259:10989–10994.

Pfeffer, S. R., and J. E. Rothman. 1987. Biosynthetic protein transport and sorting by the endoplasmic reticulum and Golgi. *Annu. Rev. Biochem.* 56:829–852.

Pouysségur, J., J. C. Chambard, A. Franchi, S. Paris, and E. van Obbergen-Schilling. 1982. Growth factor activation of an amiloride sensitive Na^+/H^+ exchange system in quiescent fibroblasts: coupling to ribosomal protein S6 phosphorylation. *Proc. Natl. Acad. Sci. USA.* 81:4833.

Pouysségur, J., C. Sardet, A. Franchi, G. L'Allemain, and S. Paris. 1984. A specific mutation abolishing Na^+/H^+ antiport activity in hamster fibroblasts precludes growth at neutral and acidic pH. *Proc. Natl. Acad. Sci. USA.* 81:4833–4837.

Ross, A., and W. F. Boron. 1981. Intracellular pH. *Physiol. Rev.* 61:296–434.

Rozengurt, E. 1986. Early signals in the mitogenic response. *Science (Wash. DC).* 234:161–166.

Sandvig, K., S. Olsnes, O. W. Petersen, and B. van Deurs. 1987. Acidification of the cytosol inhibits endocytosis from coated pits. *J. Cell Biol.* 105:679–689.

Sandvig, K., S. Olsnes, O. W. Petersen, and B. van Deurs. 1988. Inhibition of endocytosis from coated pits by acidification of the cytosol. *J. Cell Biochem.* 36:73–81.

Steinman, R. M., J. M. Silver, and Z. A. Cohn. 1974. Pinocytosis in fibroblasts. *J. Cell Biol.* 63:949–969.

Swanson, J. A., B. D. Yrinec, and S. C. Silverstein. 1985. Phorbol esters and horseradish peroxidase stimulate pinocytosis and redirect the flow of pinocytosed fluid in macrophages. *J. Cell Biol.* 100:851–859.

Tooze, J., and S. A. Tooze. 1986. Clathrin-coated vesicular transport of secretory proteins during the formation of ACTH-containing secretory granules. *J. Cell Biol.* 103:839–850.

van Adelsberg, J., and Q. Al-Awqati. 1986. Regulation of cell pH by Ca^{+2}-mediated exocytic insertion of H^+-ATPases. *J. Cell. Biol.* 102:1638–1645.

Weibel, E. R. 1979. Stereological methods. I. Practical methods for biological morphometry. Acad. Press Inc., New York. 318 pp.

REGULATION OF ORGANELLE ACIDITY

Introduction

Intracellular compartments are largely defined by their lumenal pH. Regulation of organelle acidity is a vital aspect of cellular homeostasis.

This lesson will show how to:

- Import predefined functions
- Import and fit experimental data

Additionally, we will explore in greater detail the mechanisms of ion transport.

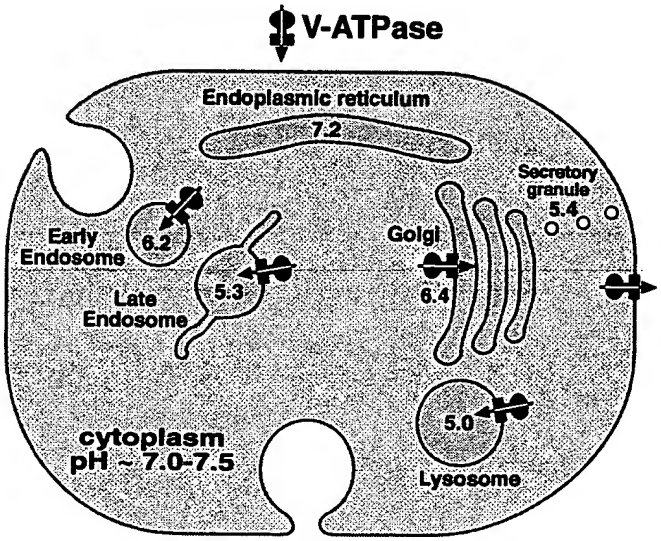

Figure 1. Typical organelle pH values.

A two compartment model

Biological Background

Acidity must be tightly regulated to sustain life. Blood pH is typically 7.4 pH units; when this value falls to just 7.2 severe acidosis ensues, and massive system failure follows and, if not treated , will result in death. Treatment involves the addition of buffer solutions to the blood. All cellular compartments maintain a distinctive pH that is essential to their function (see Figure 1); For example, lysosomes have pH ~ 5.0, in order to degrade harmful substances. The acidification of endosomes as they mature from early to late stages is required for the dissociation of receptors and ligands so that receptors can be recycled to the cell surface. A comprehensive understanding of how cellular organelles maintain their pH does not exist. As we will see, modeling can be a useful tool for interpreting experimental data.

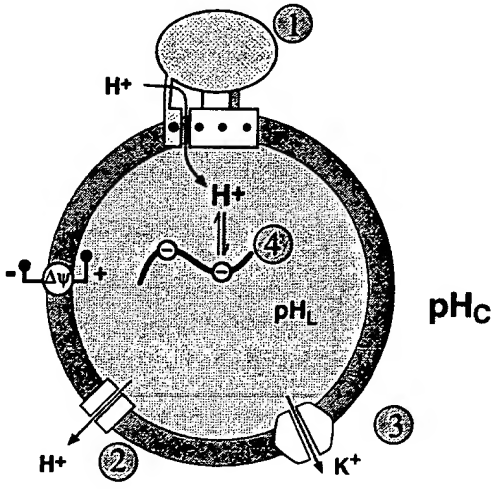

Figure 2. Key pH regulatory elements.
1 = V-ATPases, 2= proton leaks, 3 = K^+ leaks, 4 = lumenal buffering.

The principle components of organeller pH regulation are listed in Figure 2. It is believed that the competition between the proton pumping V-ATPase, (item #1), and channel mediated proton leaking, (item #2), determines the steady state pH of many organelles. In crudest terms, this is like trying to file up a swimming pool with a bunch of holes in it. The pool will fill until the input hose is overpowered by the leaks. The case of ion transport is complicated by other factors. The lumen of the organelle buffers many of the protons that are pumped from the cytoplasm,(item #4). Additionally, as positive protons move across the organelle membrane a membrane potential builds up. This membrane potential is offset by the counter-movement of ions like potassium, (item #3). All of these effects can be combined into a coherent model.

Mathematical Description

THE V-ATPASE PROTON PUMP ACIDIFIES ORGANELLES

The hydrolysis of ATP provides the energy for pumping protons against their concentration gradient. For our purposes, we require the average pumping rate of a single V-ATPase as a function of membrane potential and pH gradient, $J(\Delta pH, \Delta\Psi)$. This function is defined numerically in the file **VATPASE**; it has been computed from another more complicated model.

THE PASSIVE LEAK OF IONS DEPENDS UPON CONCENTRATION AND MEMBRANE POTENTIAL

Intact bilayers are somewhat permeable to protons, but impermeable to other ions. Ion-specific channels allow an organelle to equilibrate specific ions between the lumen and cytoplasm. Movement of these ions through the channel is driven by the transmembrane concentration difference and the membrane potential. The simplest model for the diffusion flux of ions in the presence of a membrane potential can be described by

$$J_{H\,leak} = P_H \cdot S \cdot \frac{U \cdot \left([H^+]_L - [H^+]_C \cdot e^{-U}\right)}{1 - e^{-U}}$$
$$J_{K\,leak} = P_K \cdot S \cdot \frac{U \cdot \left([K^+]_L - [K^+]_C \cdot e^{-U}\right)}{1 - e^{-U}} \qquad (1)$$

where P is the permeability of the membrane to each ion, S is the surface area of the compartment, C refers to cytoplasmic concentrations, L refers to lumenal concentrations, and U is the reduced membrane potential, $U = \Psi F/(RT)$. F is Faraday's constant, R is the gas constant, and T is absolute temperature. The value of F/(RT) at room temperature is given in Table 2.

PROTONS BECOME BUFFERED AFTER THEY CROSS THE MEMBRANE

Cellular spaces are sponges for protons and other ions. Proteins and molecules are constantly binding and releasing ions from solution. The buffering capacity, β (units: [mol/pH]), measures the ability of the lumenal matrix is to bind protons. When protons cross the lipid bilayer a certain fraction of them are immediately bound and do not contribute to the pH. The change in proton concentration of the lumen and the change in pH are given by:

$$\Delta[H^+] = -\beta \cdot \Delta pH \tag{2}$$

In general, spaces have different buffering capacities at different pH values, but we will assume that the buffering power is a fixed constant. For measured values see Table 1.

ACCUMULATED CHARGE AS A MODEL FOR MEMBRANE POTENTIAL

The membrane potential affects the flow of ions across lipid membranes and biases the distributions of those ions at steady state. Electroneutrality requires every small volume be electrically neutral. The membrane potential arises from the microscopic deviation from electroneutrality at a lipid boundary. We use an explicit form for the membrane potential *across the bilayer* in terms of the excess charge inside the organelle. This treatment is very similar to the treatment of the membrane potential in the axon models. We assume that the net charge localizes to the lumenal leaflet, so that we can treat the membrane as a parallel plate capacitor. The potential drop across the bilayer is then written as:

$$\Delta\psi = \frac{F}{C_0} \cdot \frac{V}{A} \cdot \left(\underbrace{[K^+]_L}_{1} + \underbrace{\beta \cdot (pH_C - pH_L)}_{2} - \underbrace{B}_{3} \right) \tag{3}$$

where A is the surface area of the membrane, C_0 is the capacitance per unit area of the membrane ($C_0 \cdot A$ is the total capacitance of the membrane), V is the volume of the organelle, and the numbered terms giving the concentrations of charged particles are:

1. Total concentration of potassium ions.
2. Total amount of buffered and free protons in the lumen. β is the buffering capacity. We assume that protons do not contribute to the membrane potential when the lumenal pH is equal to the cytoplasmic pH.
3. Molar concentration of all impermeant charges. This term primarily represents fixed negative protein charges trapped in the lumen.

Despite the complexity of this system, it is only a two-tank model. In the next section we will construct this model in Berkeley Madonna™.

Assembling the model

Pure proton and potassium leak

Using the equations window, we begin by writing down differential equations for H and K, the lumenal proton and potassium concentrations, respectively. At this point, only include the passive leak for each time dependent variable (see equation (1)). In general, reservoirs should represent numbers of things. Let H and K be moles/liter (molarity). (Always check the units of terms!) Specifically, we use liters and centimeters (1000 cm^3 = 1 liter). Use the function pH = -log10(H) to represent the pH.

TECHNICAL NOTE. Often we encounter equations such as y = x/x that we want to evaluate when the denominator is equal to zero. In this case, the answer is 1 but if we ask the computer to evaluate this it will return a divide by zero error. Computers do not take limits easily. Equation (1) exhibits this problem when the membrane potential is equal to zero. The easiest way to handle this problem is to rewrite the equation in an equivalent form at the troubled areas. For equation 1, we use the form:

$$J_{H\,leak} = \begin{cases} P_H \cdot S \cdot \dfrac{U \cdot \left([H^+]_L - [H^+]_C \cdot e^{-U}\right)}{1 - e^{-U}} & for\ -.01 > U > .01 \\ P_H \cdot S \cdot \dfrac{\left([H^+]_L - [H^+]_C \cdot e^{-U}\right)}{1 - \dfrac{U}{2} + \dfrac{U^2}{6}} & for\ -.01 < U < .01 \end{cases} \quad (4)$$

Use the **IF** statement in Berkeley Madonna™ to implement this form of the leak term for the protons and the potassium.

Use the numbers for the Golgi from Table 1 and let, Ψ (Psi), equal zero to answer the following questions.

1. Start off with the lumenal pH = 5.4 and watch the proton concentration decrease until it is the same as the cytoplasmic value. It might be easiest to determine this by actually looking at the pH's. What is the time constant for the proton movement (use the plot of concentration, not the pH)?
2. Start off with the lumenal K^+ concentration at 20 mM. What is the time constant for this movement? The ratio of time constants is related to the ratio of permeabilities. When the model

reaches steady state, if the lumenal and cytoplasmic quantities are not equal then the channels are not being treated properly.

Accounting for proton buffering

Use $\Delta pH = -1/\beta \cdot \Delta[H^+]$ to rewrite the differential equation for the proton concentration. Now make the proton concentration a function just as we made pH a function above.

3. Compare the time constants for the lumenal proton concentration when the buffering is 0.01, 0.02, and 0.04 M. Notice that the proton movement is extremely slow now. Additionally, the change in pH is proportional to the proton concentration not the pH. Therefore, the solution is not an exponential and the time constant depends upon the initial values.

Couple in the membrane potential

So far the leak terms should be well behaved. When we add in the membrane potential, which couples the ion flows, we might find that our equations are not quite right. Expect problems here. Represent the membrane potential as in equation (3). Let the Donnen particle concentration, B = 0.1 M. We must enforce electroneutrality at the start of the simulation. We do this with the initial potassium concentration. Set INIT K = $B-\beta \cdot (pH\_c-pH)$. Explore the model and once you are convinced that it is giving reasonable results continue.

Add in proton pumping

Select Data Sets and import the function VATPASE as a 2-D matrix. We can set the pump rate equal to this function by defining it like this:

$$J_{pump} = N\_pump * \# VATPASE(psi, pH) \tag{5}$$

This function returns the number of protons per second per pump. What factors must this function be multiplied by in order to be used in the differential equation for pH? Write the correct form of the equation into your model. You must define a new parameter, N_pumps = number of pumps on the organelle membrane. Once the entire model is complete move on to the case studies.

NOTE: Predefined numerical functions are only defined over a certain domain. If during a simulation your variables extend beyond this domain the predefined function will not give the correct results. VATPASE is defined for $4.0 < pH < 7.6$ and $-80\ mV < \Psi < 260\ mV$.

Case 1. Endosomal acidification

Endosomes have been extracted from cells and are bathing in a 7.4 pH solution with 140 mM K^+. The V-ATPase proton pumps are not working because the solution lacks ATP. The pH of the endosome is measured using pH sensitive dyes. At time=37 seconds, ATP is reintroduced to the bathing solution and the endosomes begins to acidify from pH 7.4. Load the file MVB_74 into your model (this is the acidification data).

4. Using the endosome (MVB) parameters from Table 1 determine the number of V-ATPase pumps and the proton permeability by fitting the model pH to the experimental data. Using the fact that the endosomal pH = 7.4 in the absence of any proton pumping, determine the concentration of donnan particles.

Case 2. Membrane leakiness

We want to determine the proton permeability of the Golgi and secretory granule. We have provided you with two data sets each containing five experiments:

Data Set #1 - [SG_1; SG_2; SG_3; SG_4; SG_5]

Data Set #2 - [Golgi_1; Golgi_2; Golgi_3; Golgi_4; Golgi_5]

Load this data into your program. In each of these experiments, intact cells have been loaded with pH fluorescent dyes that localize to specific organelles in the cell. The pH of the organelle can then be measured by recording the light emitted from the cell. At time zero, the cell was washed with a drug, bafilomycin, that inhibits the proton pump so that the organelles can no longer maintain their acidity, and they begin to alkalinize. This can be seen in the data sets.

5. For each experimental curve, begin with the initial pH near the pH of the first data point. Fit the model to the data using the curve fit procedure. Allow the program to adjust the proton permeability and the donnan particle concentration, B. Record the best-fit proton permeability. Remember that the proton pumps have been "turned off" experimentally. This means that N_pump=0 in your model. Repeat this for all the data sets and compute the mean and standard deviation for each organelle. Do these experiments show a noticeable difference in the bilayer leakiness between the Golgi and secretory granule?

NOTE: Remember to use the correct parameters from Table 1 when analyzing different organelles.

References

Grabe, M. and G. Oster (2001). Regulation of organelle acidity. J. Gen. Physiol.(In Press).

Rybak S, Lanni F, Murphy R. 1997. Theoretical Considerations on the Role of Membrane Potential in the Regulation of Endosomal pH. Biophys. J. 73(August 1997):674-687.

Tables

Parameter	Golgi	Secretory Granule	Endosome (MVB)
Surface Area [cm^2]	5.14×10^{-6}	1.26×10^{-9}	1.36×10^{-8}
Volume [L]	2.6×10^{-14}	4.2×10^{-18}	1.5×10^{-16}
Potassium permeability [cm/s]	1×10^{-5}	1×10^{-5}	1×10^{-5}
Buffering capacity [M/pH]	0.026	0.02	0.04

Table 1. Typical values for Golgi, secretory granules, and endosomes.

Parameter	Value
Cytoplasmic pH	7.4
Cytoplasmic potassium [M]	0.140
Membrane capacitance [kF/cm^2]	1×10^{-9}
Faraday's Constant [moles/Coulomb]	96,480
Avegadro's Number [molecules/mole]	6.02×10^{23}
F/(RT) [mV^{-1}]	$(25.69)^{-1}$

Table 2. Constants and typical variables.

EXHIBIT 6

Pure & Appl. Chem., Vol. 59, No. 11, pp. 1501–1508, 1987.
Printed in Great Britain.

Immobilized enzymes in preparative carbohydrate chemistry

Serge David* and Claudine Augé

Institut de Chimie Moléculaire d'Orsay, CNRS UA n° 462,
Université Paris-Sud, bt 420, 91405 Orsay, France

Abstract. The scope of a galactosylation procedure with five immobilized enzymes has been examined with oligosaccharides bearing terminal, non-reducing βGlcNAc residues. Tri-, penta- and hexasaccharides related to glycolipids or glycoproteins have been prepared. Cytidine monophosphate was converted to the triphosphate with phosphoenol pyruvate, ATP (catalytic) and two immobilized enzymes, and utilized in a synthesis of CMPNeu5Ac with an immobilized synthetase. Acylneuraminate pyruvate-lyase immobilized on agarose gave a gel which catalysed the synthesis of representative sialic acids from pyruvate and mannosamine derivatives.

INTRODUCTION

Glycosidation with glycosyl nucleotides and the highly specific glycosyltransferases is a very common biochemical practice, which has been applied to free oligosaccharides, glycoconjugates, and even whole cells, and would dispense the organic chemist from the tedious protection - deprotection strategy. However, its very low scale - from the nano- to the micromole - is a major drawback. Enzymes and glycosyl nucleotides are costly reagents, not easily recoverable. This may reflect only temporary economic conditions, but there is a more fundamental problem: the stoichiometric use of a glycosyl nucleotides accumulates in the medium the corresponding nucleotide, which may be inhibitory to the transferase at mM concentrations (Ref. 1). The now classical solution to these problems is to attach the enzyme to a suitable insoluble polymer which is used as an aqueous suspension. When the reaction is finished, the enzyme is separated from the products by filtration, and may be used again many times in favourable circumstances. Only catalytic quantities of glycosyl nucleotides are necessary, as they are constantly regenerated in the medium by the interplay of appropriate substrates with other enzymes, also present in the immobilized state.

The objection may be raised that many useful glycosyltransferases are poorly available, being found only in mammals, sometimes indeed only in human blood or milk. The presently rapidly developing cloning techniques may soon put an end to these shortages, so that it seems strongly advisable that organic chemists being at once to train themselves in the manipulation of these new reagents, which may be on the market in a not too distant future.

The transferase properties of the *Escherichia coli* β-galactosidase have been used for the synthesis of a disaccharide (Ref. 2). The immobilized β-galactosidase, acting on a mixture of lactose and N-acetylglucosamine, gave a mixture of products which contained 20% βGalp-(1→6)-GlcNAc. In view of the very low price of most simple sugars, the use of such glycosidases for disaccharide synthesis should be considered, especially for the preparation of starting material, whenever the product is not too difficult to separate from the reaction mixture on the 10-100 mmol scale. For later steps, the association of a specific transferase with the enzymes of glycosyl nucleotides regeneration appears more useful. We shall first describe the syntheses of oligosaccharides related to the Ii system of blood groups with the enzymes of the Leloir pathway, a method first used for a synthesis of lactosamine (Ref. 3).

We shall next discuss problems of sialylation : the syntheses of CTP and CMPNeu5Ac, and the high scale preparations of sialic acids.

GALACTOSYLATIONS WITH *N*-ACETYLGLUCOSAMINE β-(1 → 4)-GALACTOSYLTRANSFERASE

The galactosylation cycle is shown in Scheme 1. The transfer of β-D-galactopyranosyl unit from uridine diphosphate galactose to the 0-4 position of a terminal, non-reducing residue of β-N-acetylglucosamine, catalysed by transferase I, releases an equimolecular quantity of uridine diphosphate. This is enzymatically phosphorylated to uridine triphosphate by phosphoenolpyruvate in the presence of pyruvate kinase II. Another specific transferase, III, catalyses the synthesis of the glycosyl nucleotides, uridine diphosphate glucose, from uridine triphosphate and α-D-glucose 1-phosphate. This is a reversible reaction which must be displaced in the synthetic direction by the destruction of its other product, pyrophosphate, which is hydrolysed to inorganic phosphate with the help of pyrophosphatase IV. The last step is the conversion of uridine diphosphate glucose to uridine diphosphate galactose, catalysed by epimerase V. Broadly speaking, the system must be fed with α-D-glucose 1-phosphate and the "source of energy" (phosphoenolpyruvate) and releases inorganic phosphate and pyruvate as by-products.

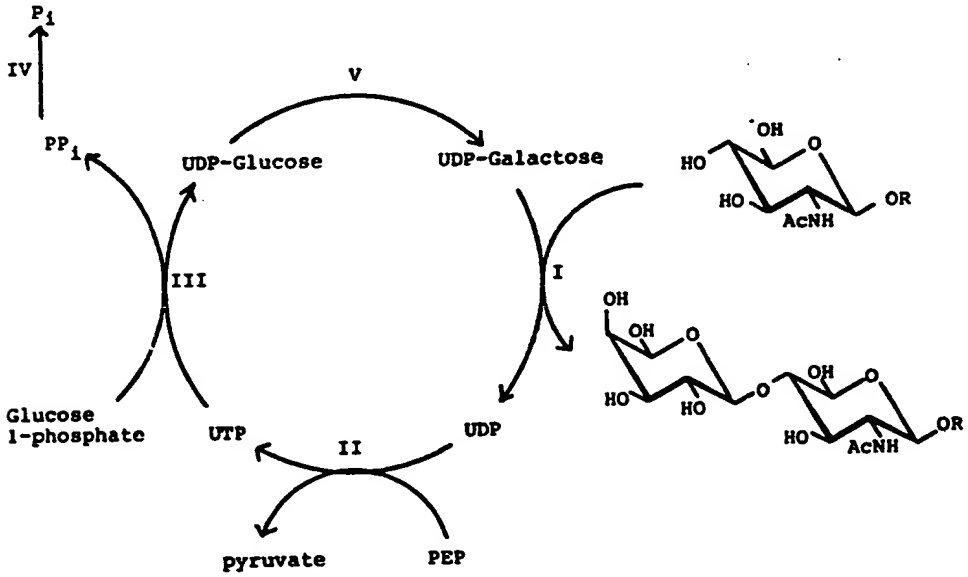

Scheme 1. The β-D-galactopyranosylation cycle.- Complete system (final concentrations, mM) : oligosaccharide substrate (6.7); α-D-glucose 1-phosphate (7); phosphoenolpyruvate, PEP (7); UDP-glucose (0.17); NAD^+ (1); $MnCl_2$ (2); $MgCl_2$ (4); KCl (70); dithiothreitol (10); NaN_3 (1.5). The pH is adjusted to 8, and the immobilized enzymes are added : I, β-D-galactosyltransferase (E.C. 2.4.1.22) (3.8 U); II, pyruvate kinase (E.C. 2.7.1.40 (34 U); III, UDP-glucose pyrophosphorylase (E.C.2.7.7.9) (5 U); IV, inorganic pyrophosphatase (E.C.3.6.1.1) (25 U); V, UDP-galactose 4-epimerase (E.C. 5.1.3.2) (3.7 U). Final volume 100 mL. Temperature : 30°C.

Enzymes I-V are commercially available; enzymes II, III and IV are relatively inexpensive. Nevertheless, we preferred to prepare galactosyltransferase in our laboratory. For this, the only necessary addition to the usual equipment of the organic chemistry laboratory was a refrigerated centrifuge. Our experience is that the carbohydrate chemist, trained to work with water-soluble substances, needs no extensive practical knowledge in enzymology to concentrate 180 U of this enzyme from 2 L of cow colostrum (Ref. 1). The five enzymes are immobilized separately as already described (Ref. 4 and 5). The nature of the support does not appear to be critical (see, for example, Ref. 3). The agarose gels are suspended in water, and the pH is maintained at its optimum value, 8.0, with pH-stat equipment. A 0.1 M Tris buffer, pH 8.0, may also be used for small scale preparations, when an excess of salts may be tolerated in the work up. The system is gently stirred at 30°C. The complete reaction requires a few days with 2 U of immobilized transferase per mmol of substrate. After it has stopped, the product is separated from the gels, which can generally be utilized again, either on the same substrate or another one. The oligosaccharide is recovered from its solution by ion-exchange de-ionization followed by freeze-drying. Starting material, if still present, is removed by silica gel column chromatography. The reaction may slow down at 70% completion. The reason is the accumulation of an ionic inhibitor, maybe phosphate. In such a case, the solution separated from the gel is deionized, and mixed again with the same gel, and, of course, a fresh batch of ionic cofactors.

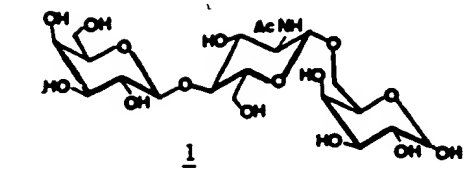

1

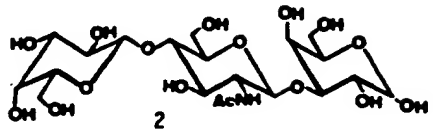

2

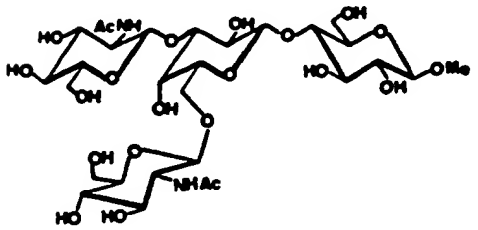

3

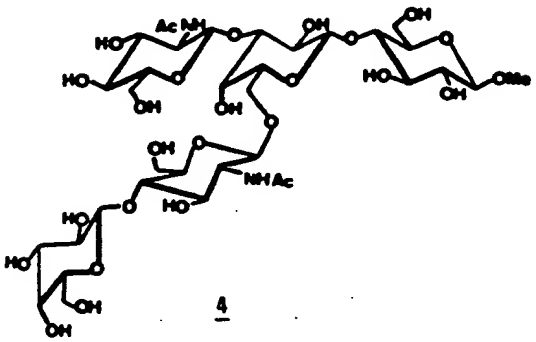

4

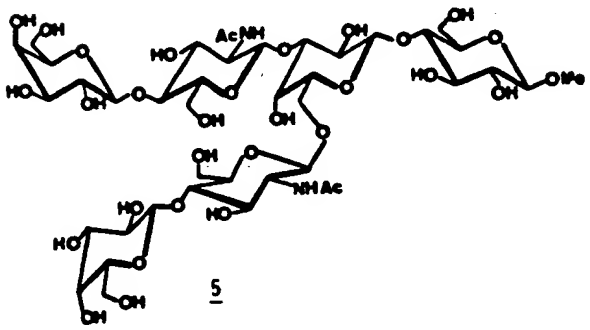

5

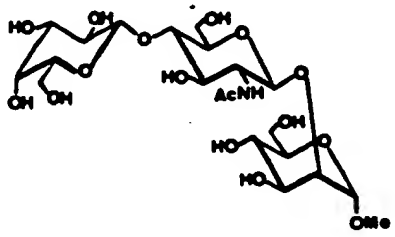

6

Oligosaccharides 1, 2, 4, 5 and 6 were prepared by mixed-type synthesis, enzymatic galactosylation being the last step in an otherwise traditional sequence (Ref. 6, 7, 8 and 9). The identification of 1, 2 and 5 rests on the comparison of their properties, especially the NMR spectra, with those of samples already prepared in our laboratory by classical means (Ref. 8 and 10). Trisaccharide 1 was first recognized as the epitope of one of the I-antigens in man, I(Ma); but it is likely that it has a more fundamental significance, the I(Ma) antigen being expressed on mouse embryos from the single cell stage until after the sixth day of development (Ref. 11). Trisaccharide 2 is a fragment of the main chain of glycolipids. The free hexasaccharide corresponding to glycoside 5 is a trace component of human milk (5 mg/L) (Ref. 12).

Galactosylation of the branched trisaccharide-glycoside 3 raised an interesting problem. In principle, there are two reactive positions, one on each terminal non-reducing β-N-acetylglucosamine residue. The residue linked to the primary position of galactose appears to be more reactive (but only marginally more) than the other one, as was shown in delicate kinetic experiments from the group of Van den Eijnden, with the soluble enzyme (Ref. 13). Moreover, the reaction of 3 (1 μmol) with excess uridine diphosphate galactose (4 μmol) and soluble transferase (0.1 U), afforded hexasaccharide 5 (Ref. 14). On the other hand, our immobilized enzyme system in the presence of one equivalent each of α-D-glucose 1-phosphate and phosphoenolpyruvate gave only traces of hexasaccharide 5, even after 6 days. The only product which was practically obtained was a pentasaccharide. The two-dimensional COSY ^{1}H NMR spectrum of the derived peracetate could be interpreted in a completely consistent manner. Assignment of chemical shifts to each of the 35 ring protons showed that, on the βGlcNAc residue linked to position 3 of galactose, proton H-4 was geminal to an acetoxy group, and in consequence, this residue was not galactosylated. This was confirmed by the comparison on the mppm scale of the chemical shifts of the anomeric protons of the pentasaccharide with those of tetrasaccharide 3 and hexasaccharide 5, already interpreted in our laboratory (Ref. 3). Thus, this pentasaccharide 4 was obtained with a selectivity probably unattainable by any current method of organic chemistry. Doubling the proportion of reagents changed nothing. Hexasaccharide 5 could only be prepared - in modest yield - with long reaction times and addition of fresh enzymes.

Trisaccharide 6 characterized by its 400 MHz ^{1}H-NMR spectrum in D_2O was prepared as a possible substrate for sialytransferase. The corresponding peracetate (Ref. 15) and free sugar (Ref. 16) were already known.

The 6-O-acetyl and 3-O-allyl derivatives of N-acetylglucosamine were not substrates. On the other hand, it seems that any unsubstituted, terminal, non-reducing β-N-acetylglucosamine residue can be galactosylated with our system. Long reaction times and renewal of immobilized enzymes may help in the case of sluggish reactions. Finally, the reactions may be scaled up as much as desired. Then, the problem is the introduction of the penultimate β-N-acetylglucosamine residue. The relevant transferases, although they are known (Ref. 17), are available only with difficulty for the time being. In this respect, we may mention a new chemical coupling procedure which has been developed in our laboratory and which utilizes the common 2-acetamido-3,4,6-tri-O-acetyl-2-deoxy-α-D-glucopyranosyl chloride with stannous triflate as promotor. Both products are stable and inexpensive. For example, this halogenose, "diacetone-galactose" (1 eq.), stannous triflate (1.5 eq.), and tetramethylurea (2 eq.) in dichloromethane solution at room temperature gave, after 4 h, a 77% yield of pure, protected disaccharide βGlcNAcp-(1-6)-Gal (94% based on recovered galactose - no α anomer detected). Yields are good to excellent with primary alcohols, and although less satisfactory at the 3-position, are nevertheless preparatively useful, since no exchange of acyl on nitrogen is necessary, as in phthalimido-based procedures.

PROBLEMS ASSOCIATED WITH SIALYLATION

This is obviously the field where the quest for high scale enzymatic techniques is most warranted, as the organic chemistry of sialic acids is fraught with problems. For instance the building of the sequence αNeup5Ac-(2-6)-βGalp-(1-4)-βGlcpNAc-(1-2)-Man, common in glycoproteins, is an arduous task (Ref. 19). Even more difficult is the sialylation at position 3 of galactose (Ref. 20). Moreover, in many cases - maybe in most cases - the sialic acid residue in the native antigen is present as a highly labile acetic or L-lactic ester (Ref. 21). The synthesis of such sialosides by the techniques of organic chemistry would involve a still uncertain adaptation of glycosidic coupling methods. Finally, we may forecast that in the near future, the problem will arise to sialylate glycoproteins without denaturation on a scale compatible with commercialization, and immobilized enzymes may help in this connection.

The sialyltransferases are a family to enzymes which catalyse the transfer of a sialic acid residue from the glycosyl nucleotides cytidine monophosphate-N-acetylneuraminic acid (7, CMPNeu5Ac) to a specific position in a specific sugar [reaction (2)]. Free, unphosphorylated N-acetylneuraminic acid is directly converted to its active derivative 7 by cytidine triphosphate (CTP) [reaction (1)] in the presence of a synthetase :

$$\text{CTP} + \text{Neu5Ac} \rightarrow \text{CMPNeu5Ac} + \text{PPi} \qquad (1)$$

$$\text{CMPNeu5Ac} + \text{ROH} \rightarrow \text{sialoside} + \text{CMP} \qquad (2)$$

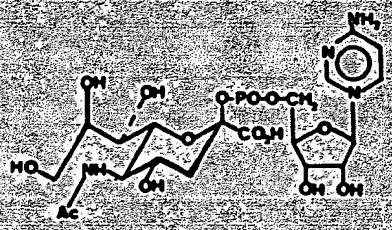

7

These two enzymes are neither commercially available nor easily prepared. Still, several enzymatic preparations of 7 on the 100 μmol scale have been reported by biochemists (Ref. 22 and literature cited there). This is already one order of magnitude higher than the final scale of some reported oligosaccharides syntheses in this field. We shall now describe a system of three immobilized enzymes for the preparation of CMPNeuAc (Scheme 2).

The not unduly expensive cytidine monophosphate (CMP) is phosphorylated to its diphosphate (CDP) in the presence of immobilized nucleoside monophosphate kinase, VI. The phosphate donor is ATP, which is regenerated as in Scheme 1 with phosphoenolpyruvate (PEP) and immobilized pyruvate kinase, V. Conversion of CDP to CTP must also be catalysed by the same system, that is, PEP and pyruvate kinase, and this creates a small problem for this enzyme.

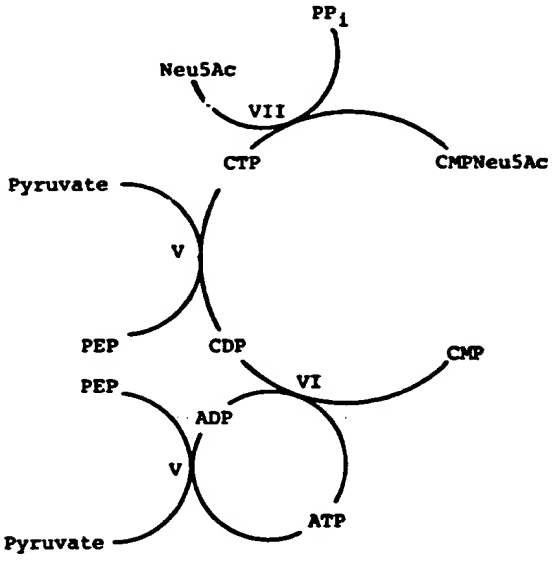

Scheme 2. Preparation of cytidine monophosphate N-acetylneuraminic acid from CMP and N-acetylneuraminic acid. Synthesis of CTP : to the immobilized enzymes, VI, nucleoside monophosphokinase (E.C.2.7.4.4) (0.3 U) and V, pyruvate kinase (10 U), suspended in Tris buffer (either 50 mM, pH 9, or 100 mM, pH 7) (15 mL) were added to the final concentrations given (mM), CMP (Na salt, 13.3); PEP (K salt, 27); ATP (Na salt, 1.3); $MgCl_2$ (4); KCl (50); thymol (1). Temperature 37°C. Synthesis of CMPNeuAc : to the immobilized CMPNeu5Ac synthetase (E.C.2.7.7.4.3) (0.6 U) in Tris buffer, pH 7.0 containing 3.75 mM mercaptoethanol were added, to the final concentrations given (mM), CTP (13); Neu5Ac (3.3); $MgCl_2$ (4); $MnCl_2$ (6.25); thymol (1). Temperature 37°C.

As the optimum pH of the synthetase is 9 in the presence of Mg^{++} ions, and that of sialyltransferase is in the vicinity of 7, any attempt to make them work together in the same vessel would be hopeless. Fortunately, Higa and Paulson, looking for suitable conditions to activate the alkali-labile acetates of N-acetylneuraminic acid, with the same enzyme in the soluble state, made the very pertinent observation that replacement of Mg^{++} ions lowers the optimum pH to 7, with only 30% loss of activity (Ref. 22). On the other hand, although there are no pH incompatibilities, enzyme V, VI and VII cannot work together because the synthetase is inhibited by CMP (K_i 20 mM). In any case, we desired to avoid conditions which might slow down reaction 2, as CMPNeu5Ac is reported not to be very stable in the medium (we have not noticed any degradation at pH 7 for 48 h). Thus the synthesis of CMPNeu5Ac is a two-step reaction, where every component is readily available except the synthetase. Higa and Paulson reported the extraction of 63 U from three calf brains, maybe in very favourable conditions. In principle, this would allow the preparation of 1.3 g of CMPNeuAc with our system, which could be utilized again.

In a very recent report (Ref. 25) describing the preparation of a collection of sialosides in the range of 10-20 µmol with soluble transferases, the authors stress the fact that the availability of CMPNeu5Ac might be a limiting factor in such approaches.

We are currently working on the immobilization of sialyltransferase from cow colostrum.

SYNTHESES OF SIALIC ACIDS

A list of natural sialic acids may be found in Schauer's review in 1982 (Ref. 21). Most are esters, primarily acetates, of the alcoholic functions at positions 4, 7, 8 and 9 of N-acetyl- or N-glycolylneuraminic acid. N-Acetylneuraminic acid itself, which has been obtained by synthesis (Ref. 26) or extraction from the urine of patients suffering from some rare diseases, is not a very accessible compound. All its congeners have been obtained by extraction from natural sources, for example, the submaxillary mucin of some domestic mammals (Ref. 22); they are even less easily available, but at least as important from the physiological point of view.

This state of affairs led us to examine the possibilities of enzymatic synthesis. A well-known, commercial aldolase, acylneuraminate pyruvate-lyase catalyses the reversible reaction (3) :

$$\text{Neu5Ac} \rightleftharpoons \text{ManNAc} + CH_3COCO_2^- \qquad (3)$$

The enzyme in water solution has already been used in the preparation of small amounts of labelled Neu5Ac (Ref. 27). The affinity of the bacterial enzyme from Clostridium perfringens for Neu5Ac (K_m 1.85 mM) is not very different from its affinity for the 9-O-acetyl derivative (K_m 2.00 mM) or the 7-O-acetyl derivative (K_m 4.55) (Ref. 28). Against the use of this enzyme, the objection may be raised at once that the difficulty is only shifted, because of the high price of N-acetylmannosamine itself. Actually, when we used this sugar as a starting material, we restricted ourselves to short reaction sequences with high yield: thus N-glycolylmannosamine was prepared by reaction of mannosamine with p-nitrophenyl 2-benzyloxyacetate followed by hydrogenolysis over palladium. The ester, 2-acetamido-6-O-acetyl-2-deoxy-D-mannose (13, R^1 = Me, R^2 = Ac), was obtained by selective acetolysis of the pertrimethylsilyl derivative of N-acetylmannosamine at positions 1 and 6, followed by hydrolytic removal of the remaining trimethylsilyl protecting groups. Finally the anomeric acetate was removed with concomitant conversion into the benzyl glycosylamine (Ref. 29). This method, elaborated by A. Veyrières, could also be used in an efficient synthesis of the D-gluco isomer (Ref. 30).

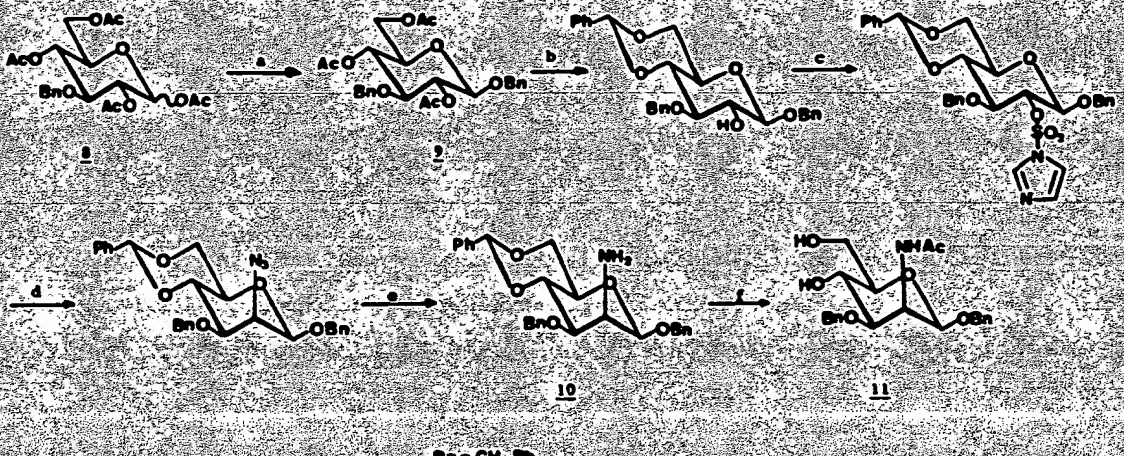

Scheme 3.
a) i: NH_3-MeCN; ii : CCl_3CN, K_2CO_3; iii : $PhCH_2OH$, BF_3-EtO;
b) i : MeONa-MeOH; ii : PhCHO, $ZnCl_2$;
c) i : NaH-DMF; ii : N,N'-sulfuryldiimidazole;
d) $Bu_4N^+N_3^-$, PhMe, 80°C, 2 h; e) $LiAlH_4$;
f) i : Ac_2O-pyridine; ii : AcOH-H_2O, 100°C, 0.5 h.

However, our general route to mannosamines substituted at positions other than 5 (Scheme 3) starts from the peracetate of 3-O-benzyl-D-glucose, 8, which can be prepared in 200 g batches. Selective anomeric de-acetylation according to a recent reported procedure (Ref. 31) allowed utilisation of the Schmidt procedure (Ref. 32) for the preparation of the benzyl glucoside 9. For azidation with inversion of configuration, we have used the new imidazolylsulfonyl leaving group discovered by Hanessian and Vatèle (Ref. 33). The reagent needed, N,N'-sulfuryldiimidazole, is very easily prepared and can be stored indefinitely without special precautions. Azidation of the sugar derivative is practically quantitative in mild conditions. Yields are excellent for all the reactions of Scheme 3. The highly crystalline protected mannosamine 10 precipitated directly on concentrating the ether solution after removal of inorganic material at the end of step e (Scheme 3). The function of this amine as a turn-table in our general route is illustrated by the preparation of the lactyl ester 12 (Scheme 4).

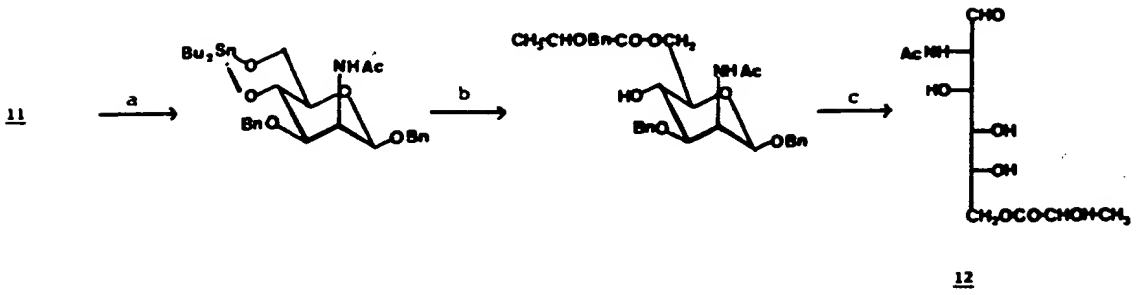

11 12

Scheme 4. a) Bu_2SnO-benzene; b) CH_3-CHOBn-COCl; c) Pd-H_2.

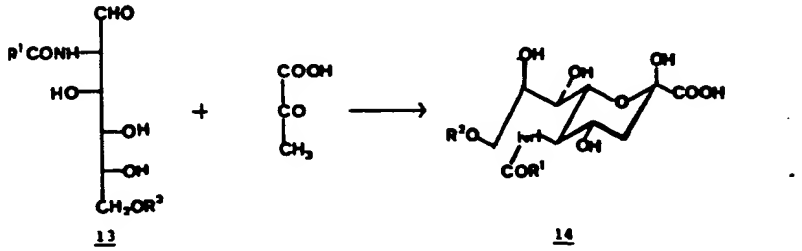

13 14

Scheme 5. Preparation of sialic acids.- Complete system : To the immobilized acylneuraminate-pyruvate lyase (E.C.4.1.3.3) (2.7 U) suspended in 50 mM phosphate buffer, pH 7.2 (36 mL), were added, to the final concentrations given (mM) : the N-acyl-mannosamine substrate (100); Na pyruvate (1000); dithiothreitol (1); NaN_3 (1.5). Temperature 37°C.

Commercial aldolase was immobilized on agarose, with a 51% yield of enzymatic activity, to give a gel with a specific activity of 1.25 U/mL. The conditions of the reactions are summarized in Scheme 5. We may note as a general comment that these synthetic pathways are completely unphysiological. The aldolase we use has only catabolic functions in cells. In nature, N-acetylneuraminic acid is built from phosphorylated precursors, and modifications only happen later on, by enzymatic oxidation of the N-acetyl to the N-glycolyl group, or enzymatic esterification.

N-Acetylneuraminic acid (14, R^1= CH_3, R^2=H).
With our enzymatic technique, it is not necessary to start from the costly pure N-acetylmannosamine. N-Acetylglucosamine is first epimerized in alkaline medium. Excess N-acetylglucosamine is then removed by one crystallization from the equilibrium mixture; and the enriched mother-liquor, with a 1:1 D-gluco/D-manno ratio, is directly treated with aldolase. Only the D-manno configuration is recognized by the enzyme, and the D-gluco epimer is not inhibitory. Furthermore, the carboxylic acid function of the product allows an easy separation from the unchanged neutral sugars in the medium. The yield is 1 mmol of N-acetylneuraminic acid per enzymatic unit (Ref. 34).

N-glycolylneuraminic acid (14, R' = CH_2OH, R" = H).
This acid, apparently absent in man, is very common in other mammals, up to 90% of the sialic acids fraction in some tissues. The mixture obtained by the alkaline epimerization of N-glycolylglucosamine may also be used in the enzymatic synthesis.

9-O-Acetyl-N-acetylneuraminic acid (14, R^1 = CH_3, R^2 = Ac).
This is an ester of common occurrence (Ref. 35). Interestingly, according to some recent reports, a N-acetyl-9-O-acetyl-neuraminic acid residue is present in the antigenic epitope of a ganglioside found in the developing rat embryonic neuroectoderm and in human melanoma cells recognized by a monoclonal antibody, Mab D1-1, prepared against the rat B49 cell lines (Ref. 36, 37).

9-O-Lactyl-N-acetylneuraminic acid (14, R^1 = CH_3, R^2 = $CH_3CHOHCO$).
The presence of the L-lactyl diastereoisomer in natural sources has been mentioned several times. The DL-lactic acid ester of N-acetylmannosamine 12 was found to be a substrate of the aldolase. However, the corresponding sialic acid was readily hydrolyzed at pH 7.2 during the enzymatic reaction, so that the product was contaminated with about 30% of N-acetylneuraminic acid. Partial resolution could be achieved with the reported chromatographic systems (Ref. 38). Its ready hydrolysis at pH 7.2 during the enzymatic reaction is a cause of low yield.

REFERENCES

1. R. Barker, K.W. Olsen, M. Shaper and R.L. Hill, J. Biol. Chem. 247, 7135-7147 (1972).
2. L. Hedbys, P.O. Larsson and K. Mosbach, Biochem. Biophys. Res. Commun. 123, 8-15 (1984).
3. C.H. Wong, S.L. Haynie and G.M. Whitesides, J. Org. Chem. 47, 5416-5418 (1982).
4. C. Augé, S. David, C. Mathieu and C. Gautheron, Tetrahedron Letters 25, 1467-1470 (1984).
5. C. Augé, C. Mathieu and C. Mérienne, Carbohydr. Res. 151, 147-156 (1986).
6. C. Augé and A. Veyrières, J. Chem. Soc. Perkin I, 1343-1345 (1977).
7. C. Augé and A. Veyrières, Carbohydr. Res. 54, 45-59 (1977).
8. A. Maranduba and A. Veyrières, Carbohydr. Res. 151, 105-119 (1986).
9. R. Kaifu, T. Osawa and R.W. Jeanloz, Carbohydr. Res. 40, 111-117 (1975).
10. C. Augé, S. David and A. Veyrières, Nouv. J. Chim. 3, 491-497 (1979).
11. T. Feizi, Blood Transf. Immunohaematol. 23, 563-577 (1980).
12. A. Kobata and V. Ginsburg, Arch. Biochem. Biophys. 150, 273-281 (1972).
13. W.M. Blanken, G.J.M. Hooghwinkel and D.H. Van den Eijnden, Eur. J. Biochem. 127, 547-552 (1982).
14. F. Piller, J.P. Cartron, A. Maranduba, A. Veyrières, Y. Leroyand B. Fournet, J. Biol. Chem. 259, 13385-13390 (1984).
15. H. Paulsen and R. Lebuhn, Carbohydr. Res. 125, 21-45 (1984).
16. R. Kaifu and T. Osawa, Carbohydr. Res. 52, 179-185 (1976); J. Arnap and J. Lönngren, J. Chem. Soc. Perkin I 2070-2074 (1981).
17. F. Pillar, J.P. Cartron, A. Maranduba, A. Veyrières, Y. Leroy and B. Fournet, J. Biol. Chem. 259, 13385-13390 (1984).
18. A. Lubineau and A. Malleron, Tetrahedron Letters 26, 1713-1714 (1985); A. Lubineau and A. Malleron, to be published.
19. T. Kitajima, M. Sugimoto, T. Nukada and T. Ogawa, Carbohydr. Res. 127, C1-C4 (1984); H. Paulsen and H. Tietz, Carbohydr. Res. 144, 205-229 (1985).
20. T. Ogawa and M. Sugimoto, Carbohydr. Res. 135, C5-C9 (1985); H. Paulsen and U. von Dessen, Carbohydr. Res. 146, 147-153 (1986).
21. R. Schauer, Adv. Carbohydr. Chem. Biochem. 40, 131-234 (1982).
22. H.H. Higa et J.C. Paulson, J. Biol. Chem. 260, 8838-8849 (1985).
23. A.P. Corfield, R. Schauer and M. Wemberg, Biochem. J. 177, 1-7 (1979).
24. D.H. van der Eijnden and W. van Dijk, Hoppe-Seyler's Z. Physiol. Chem. 353, 1817-1820 (1972).
25. S. Sabesan and J.C. Paulson, J. Am. Chem. Soc. 108, 2068-2080 (1986).
26. R. Kuhn and G. Baschang, Chem. Ber. 25, 2384-2385 (1962); A.M. Stephen and R. W. Jeanloz, Fed. Proc. 25, 409 (1966).
27. E. Kean and S. Roseman, Methods Enzymol., 8, 208-215 (1966).
28. R. Schauer, M. Wember, F. Wirtz-Peitzand C. Ferreira do Amaral, Hoppe-Seyler's Z. Physiol. Chem. 352, 1073-1080 (1971).
29. C. Augé, S. David, C. Gautheron and A. Veyrières, Tetrahedron Lett. 26, 2439-2440 (1985).
30. A. Veyrières, unpublished work.
31. J. Fiandor, M.T. Garcia-Lopez, F.G. de las Heras, P.P. Mendez-Castrillon, Synthesis 1121-1123 (1985).
32. R.R. Schmidt and J. Michel, Angew. Chem. Int. Ed. 19, 731-732 (1980).
33. S. Hanessian and J.M. Vatele, Tetrahedron Lett. 22, 3579-3582 (1981).
34. C. Augé, S. David and C. Gautheron, Tetrahedron Lett. 25, 4663-4664 (1984).
35. D.C. Gowda, G. Reuter, A.K. Shuklaand R. Schauer, Hoppe-Seyler's Z. Physiol. Chem. 365, 1247-1253 (1984).
36. D.A. Cheresh, A.P. Varki, N.M. Varki, W.B. Stallcup, J. Levine and R.A. Reisfeld, J. Biol. Chem. 259, 7453-7459 (1984).
37. J. Thurin, M. Herlyn, O. Hindsgau, N. Strömberg, K.A. Karlsson, D. Elder, Z. Steplewski and H. Koprowski, J. Biol. Chem. 260, 14556-14563 (1985).
38. R. Schauer, Methods Enzymol. 50, 64-89 (1978).

ADVANCES IN CARBOHYDRATE CHEMISTRY AND BIOCHEMISTRY, VOL. 49

EXHIBIT 7

pp 175-237.

ENZYMIC METHODS IN PREPARATIVE CARBOHYDRATE CHEMISTRY

BY SERGE DAVID, CLAUDINE AUGÉ, AND CHRISTINE GAUTHERON

Institut de Chimie Moléculaire d'Orsay, Université Paris-Sud, Bt 420, F-91405 Orsay cédex, France

I. Introduction 176
1. The Interest of Enzymic Methods 176
2. Difficulties in Defining the Scope of the Article 177
3. Definitions and Abbreviations 177
II. Immobilization 180
1. General 180
2. Agarose 181
3. Poly(acrylamide) Gels 186
4. Silica Gel–Glutaraldehyde 188
5. Dialysis Bags 188
III. Aldol Additions and Other C–C Bond-forming Reactions 189
1. General Considerations 189
2. Syntheses with the Glycolysis Aldolase 190
3. Syntheses with Sialyl Aldolase 194
4. Transketolase and Other Enzymes 204
IV. Phosphorylations 207
1. General Considerations 207
2. Sugar Phosphates 207
3. Nucleotides 210
4. "Nucleotide-Sugars" 213
V. Glycosylations with Transferases 218
1. General Considerations 218
2. Galactosylation 219
3. Sialylation 223
4. Glucosylation 231
VI. Transfer Reactions Catalyzed by Glycosidases 231
VII. Miscellaneous Syntheses in Aqueous Solution 234
VIII. Enzymes in Organic Solvents 235
IX. Addendum 236

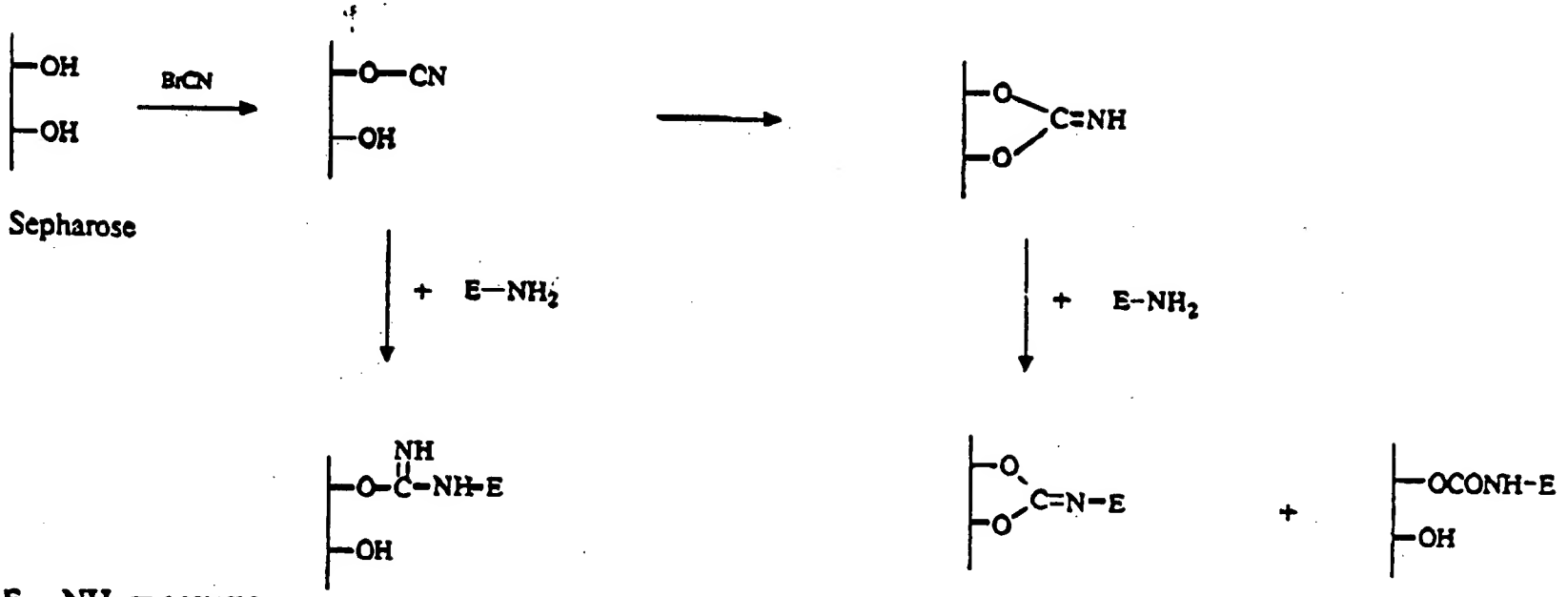

SCHEME 1.—Proposed Mechanism of Activation of Sepharose by CNBr and Subsequent Coupling of Enzyme.

derivatives having little or no activity. According to Kohn and Wilchek,[13] the constitution of agarose is not favorable to the building of imidocarbonates, and the linkages to enzyme may be mainly of the isourea type.

The enzyme–agarose conjugate, a gel, is stored as a suspension in the immobilization buffer. This gel is rather mechanically fragile. Magnetic stirrers should be avoided, and the contents of reaction vessels gently stirred on a rotary shaker. Attention is drawn to the poisonous nature of cyanogen bromide.

Agarose gels are excellent at the laboratory level, but their high cost precludes their use in Industry. The cheaper "Trisacryl," an all-synthetic polymer having similar properties, has gained wide acceptance for technical applications.[14]

To illustrate enzyme immobilization on agarose, we have purposely selected instances of enzymes prepared in an organic chemistry laboratory and not purified to homogeneity,[15] as in the preparation of immobilized cytidine-monophosphate-*N*-acetylneuraminic acid synthetase by Augé and coworkers.[15] Two calf brains (600 g, 40 U) were homogenized with 0.01 *M* sodium pyrophosphate (1 L) in a Waring Blendor. The homogenate was centrifuged, and the pellet was extracted twice with 0.4 *M* KCl (400 mL). After centrifugation at 30,000 *g* for 20 min, each supernatant liquor from the KCl extractions was separately precipitated with ammonium sulfate according to Higa and Paulson.[16] The precipitate was taken up in the buffer used for the immobilization step (0.1 *M* $NaHCO_3$, pH 8.8, containing 0.5 *M* NaCl). A quarter of the CMP-Neu5Ac synthetase (100 mL, 5 U) was stirred overnight at 4° under nitrogen with Ultrogel A4 (50 mL) freshly activated with BrCN (100 mg per mL of gel). The gel was successively washed with *M* NaCl, twice-distilled water, and 0.1 *M* Tris buffer, pH 9, containing 3 m*M* 2-mercaptoethanol, and then stored in suspension in this buffer (enzymic activity bound to agarose: 184 mU/mL of gel). The activity of immobilized CMP-Neu5Ac synthetase was determined by the thiobarbituric acid assay, using the standard procedure described for the soluble enzyme.[17] In this case, immobilization almost doubled the available activity.

Another example is the preparation of immobilized Gal*p*-β-(1→4)-Glc*p*NAc-α-(2→6)-sialyltransferase by Augé and coworkers.[15] Glassware was siliconized. Column fractions were collected in plastic tubes. Porcine liver (500 g) was homogenized with 25 m*M* Na cacodylate buffer containing 20 m*M* $MnCl_2$. The pellet was extracted twice with Triton X-100, and each

(13) J. Kohn and M. Wilchek, *Anal. Biochem.*, 115 (1981) 375–382.
(14) E. D. J. Brown and J. Touet, *J. Chem. Res.*, S (1979) 290–291.
(15) C. Augé, C. Gautheron, and R. Fernandez, *Carbohydr. Res.*, 200 (1990) 257–268.
(16) H. H. Higa and J. C. Paulson, *J. Biol. Chem.*, 260 (1985) 8838–8849.
(17) E. L. Kean and S. Roseman, *Methods Enzymol.*, 8 (1966) 208–215.

TABLE IV

Naturally Occurring Sialic Acids and Related Sugars[a]

Substrate	Acids	Scale mmol	Yield %	Units/ mmol	Ref.
N-Acetylglucosamine, *N*-acetylmannosamine, 1:1 mixture	*N*-acetylneuraminic acid	5	67	1	20,38,39
N-Glycolylglucosamine, *N*-glycolylmannosamine, 2:3 mixture	*N*-glycolylneuraminic acid	1	61	1	20,39
Derivatives of 2-amino-2-deoxy-D-mannose	Derivatives of neuraminic acid				
N-Acetyl-6-*O*-acetyl	*N*-acetyl-9-*O*-acetyl-	4	67	16	20,39,40
N-Acetyl-6-*O*-[(*S*)-(2-hydroxypropanoyl)]	*N*-acetyl-9-*O*-(L-lactyl)-	0.6	53	24	20
N-Acetyl-4-*O*-methyl	*N*-acetyl-7-*O*-methyl-	0.6	59	12	20
N-Acetyl-6-*O*-methyl	*N*-acetyl-9-*O*-methyl-	0.3	59	14	20
6-*O*-Acetyl-*N*-glycolyl	9-*O*-acetyl-*N*-glycolyl	1.3	63	6	20
N-(2-Acetoxyacetyl)	*N*-(2-acetoxyacetyl)-	0.25	50	12	20
Other compounds	Derivatives of 3-deoxyoctulosonic acid				
D-Arabinose	D-*manno*-(Kdo) and D-*gluco*-	1	35	12	41,42
D-Lyxose	D-*galacto*-	1	66	14	41,42
D-Xylose	D-*gulo*	1	18	20	41,42
D-Glucose	Derivatives of 3-deoxynonulosonic acid				
2-Deoxy-D-*arabino*-hexose	D-*glycero*-D-*gulo*-	1	28	16	41,42
4-Deoxy-D-*lyxo*-hexose	5-deoxy-D-*gluco*-	1	36	6	41,42
D-Mannose	7-deoxy-D-*galacto*-	1	67	12	41,42
2-Azido-2-deoxy-D-mannose	D-*glycero*-D-*galacto*-	1	84	15	41,42
2-Deoxy-2-*C*-phenyl-D-mannose	5-Azido-5-deoxy-D-*glycero*-D-*galacto*	1	78	12	43
	5-Deoxy-5-*C*-phenyl-D-*glycero*-D-*galacto*	1	76	8	44

[a] Condensations with pyruvate in the presence of *N*-acylneuraminate pyruvate lyase immobilized on agarose.

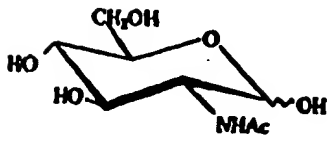

3

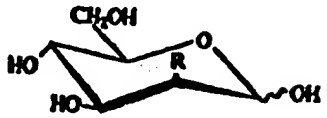

4 R = H
5 R = OH
6 R = $NHCOCH_2OH$
7 R = $NHCOCH_2OAc$
8 R = N_3
9 R = Ph

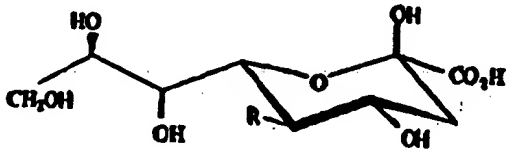

10 R = H
11 R = OH
12 R = $NHCOCH_2OH$
13 R = $NHCOCH_2OAc$
14 R = N_3
15 R = Ph

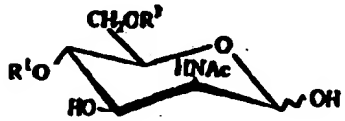

16 R^1 = H, R^2 = Ac
17 R^1 = H, R^2 = (*S*)MeCHOHCO
18 R^1 = Me, R^2 = H
19 R^1 = H, R^2 = Me

Mannose reduced at C-4 (24), or truncated to D-lyxose (giving 25), gave[41,42,44] nonulosonic acid 26 and octulosonic acid 27.

(38) C. Augé, S. David, and C. Gautheron, *Tetrahedron Lett.*, 25 (1984) 4663–4664.
(39) S. David and C. Augé, *Pure Appl. Chem.*, 59 (1987) 1501–1508.
(40) C. Augé, S. David, C. Gautheron, and A. Veyrières, *Tetrahedron Lett.*, 26 (1985) 2439–2440.
(41) C. Augé and C. Gautheron, *J. Chem. Soc., Chem. Commun.*, (1987) 859–860.
(42) C. Augé, B. Bouxom, B. Cavayé, and C. Gautheron, *Tetrahedron Lett.*, 30 (1989) 2217–2220.
(43) C. Augé, S. David, and A. Malleron, *Carbohydr. Res.*, 188 (1989) 201–205.
(44) C. Augé, C. Gautheron, S. David, A. Malleron, B. Bouxom, and B. Cavayé, *Tetrahedron*, 46 (1990) 201–214.

utilized (see Scheme 16). Acetyl phosphate is a chemical very easily prepared, either in ethyl acetate[64] or water[65] solution. Transfer of phosphate to ADP occurs in the presence of acetate kinase, found in *E. coli*. However, because of the relative instability of acetyl phosphate in water, it must be added gradually to the vessel in case of long incubation periods. It appears to have been abandoned in favor of enolpyruvate phosphate, which is more stable in water solution, despite a more-complex synthesis.[66] The enzyme associated with enolpyruvate phosphate is the widespread pyruvate kinase, which is one of the key glycolysis enzymes.

d. Preparation of Pentose Phosphates with Systems of More than Two Enzymes.—Scheme 16 indicates that phosphorylating systems are essentially two-enzyme systems, a substrate-specific kinase, and a kinase for ATP regeneration. However, other enzymes may be associated to the kinases in the same vessel, either for the *in situ* preparation of substrate, or the further processing of product. In the preparation of ribulose (D-*erythro*-pentulose) 1,5-diphosphate, the substrate of the phosphorylation enzyme, namely, ribulose 5-phosphate, is obtained by the oxidative decarboxylation of D-gluconic acid 6-phosphate with coenzyme NAD(P) as oxidant, and evolution of CO_2. The reduced coenzyme NADH(P) is oxidized back to NAD(P) with 2-ketoglutarate in the presence of NH_3, which is converted into glutamate, and is the final oxidant. The successful operation of this system demonstrated the possibility of preparing compounds on the mole scale with four immobilized enzymes.[67]

Alternatively, "ribulose" (D-*erythro*-pentulose) 5-phosphate may be isomerized to ribose 5-phosphate with pentose phosphate isomerase, but the same isomerase will convert D-ribose 5-phosphate into D-*erythro*-pentulose 5-phosphate, the equilibrium being displaced by phosphorylation to the diphosphate (involving three enzyme systems).

3. Nucleotides

Phosphorolysis of ribonucleic acid with polynucleotide phosphorylase gives a mixture of the diphosphates of the four common nucleosides, which are transformed into triphosphates with enolpyruvate phosphate and pyruvate kinase. This mixture may be used as such as a source of uridine triphosphate in the preparation of the nucleotide-sugar uridine 5′-(α-D-glucopyranosyl diphosphate) ("uridine-diphosphate-glucose," UDP-Glc), or as a

(64) D. C. Crans and G. M. Whitesides, *J. Org. Chem.*, 48 (1983) 3130–3132.
(65) R. J. Kazlauskas and G. M. Whitesides, *J. Org. Chem.*, 50 (1985) 1069–1076.
(66) B. L. Hirschbein, F. P. Mazenod, and G. M. Whitesides, *J. Org. Chem.*, 47 (1982) 3765–3766.
(67) C. H. Wong, S. D. McCurry, and G. M. Whitesides, *J. Am. Chem. Soc.*, 102 (1980) 7939–7940.

source of ATP in the preparation of glucose 6-phosphate.[63] In the same way, the enzymic hydrolysis of deoxyribonucleic acid gives deoxyadenosine monophosphate, which can be phosphorylated to deoxyadenosine triphosphate. In the latter synthesis, the double phosphorylation is catalyzed by pyruvate and adenylate kinase, the phosphate donor being enolpyruvate phosphate.[24] A three-enzyme system, namely, adenosine kinase, adenylate kinase, and acetokinase, converts the very common chemical adenosine into its most valuable triphosphate, ATP, with acetyl phosphate as the phosphate donor.[68]

Cytidine triphosphate is necessary to the activation of *N*-acetylneuraminic acid (see Section V,3). Its preparation[39,69] is given in Scheme 17. The not

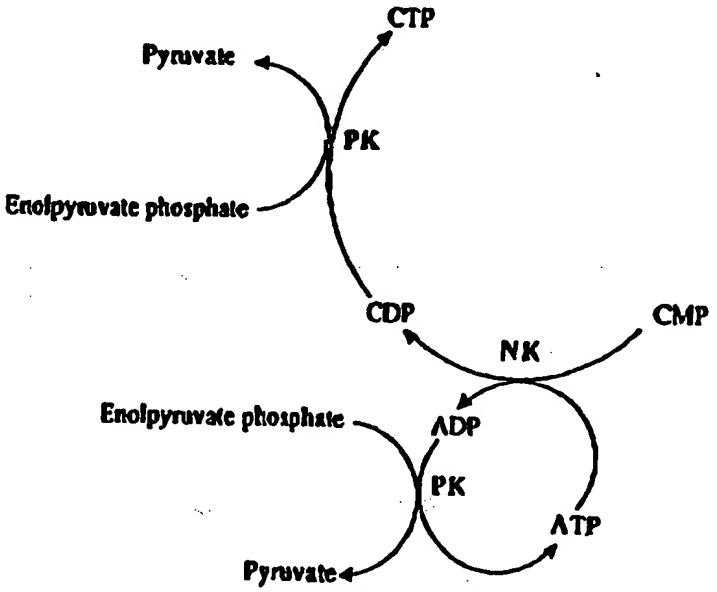

SCHEME 17.—Enzymic Preparation of CTP.

unduly expensive cytidine monophosphate (CMP) is phosphorylated to its diphosphate (CDP) in the presence of immobilized nucleoside-monophosphate kinase. The phosphate donor is ATP, which is regenerated with enolpyruvate phosphate and immobilized pyruvate kinase. Conversion of CDP into CTP must also be catalyzed by the same system, that is enolpyruvate phosphate and pyruvate kinase, and this creates a small problem, for this enzyme has much less affinity for CDP (K_m near 5 m*M*) than for ADP (K_m 0.1 m*M*), and so it must be added in excess. Stoichiometric amounts of CMP and enolpyruvate phosphate, together with catalytic amounts of ATP, gave a

(68) R. L. Baughn, O. Adalsteinsson, and G. M. Whitesides, *J. Am. Chem. Soc.*, 100 (1978) 304–306.

(69) C. Augé and C. Gautheron, *Tetrahedron Lett.*, 29 (1988) 789–790.

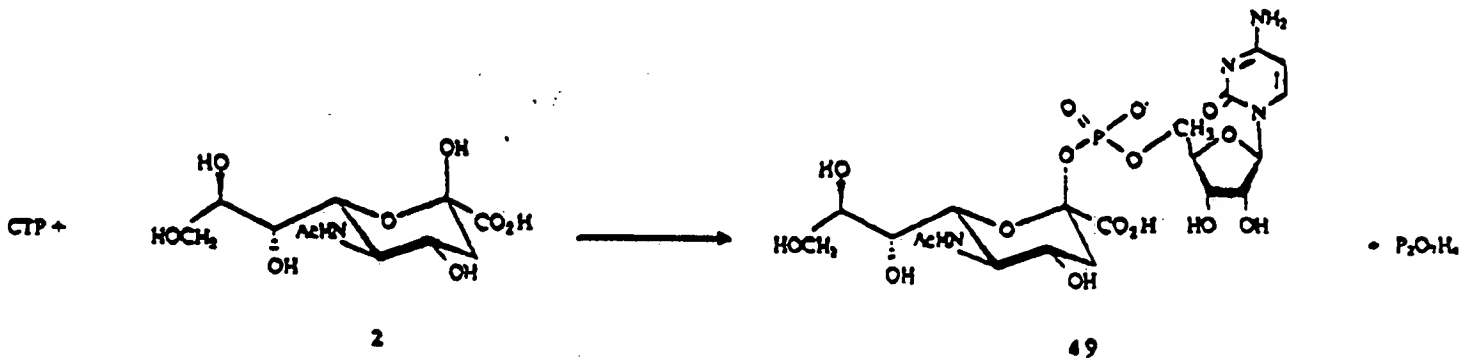

SCHEME 18.—The Reaction Catalyzed by Cytidine Monophosphate *N*-Acetylneuraminic Acid Synthetase.

V.2. This is not the case with cytidine monophosphate *N*-acetylneuraminic acid (49) (see Scheme 18), the activated form of *N*-acetylneuraminic acid for sialoside synthesis, as no sialylation cycle has so far been achieved, and thus this precursor must be added to the system in stoichiometric quantity. Thus, the availability of 49 is still the limiting factor in the large-scale synthesis of sialosides.

Free, unphosphorylated *N*-acetylneuraminic acid is directly converted into 49 by cytidine triphosphate in the presence of a synthetase (see Scheme 18). This enzyme is not commercially available for the time being, but calf brain is a good source,[73] and purification to homogeneity is not necessary. This synthetase accepts substrates other than *N*-acetylneuraminic acid, such as *N*-acetyl-9-*O*-acetylneuraminic acid (20), *N*-glycolylneuraminic acid (12), and, with less efficiency, "Kdn" (11). It is not possible to associate this synthetase to pyruvate kinase and nucleoside monophosphate kinase as a three-enzyme system in a single vessel, for CMP is degraded by this enzyme. This is not a severe problem: the crude solution of CTP obtained by the reactions of Scheme 17 is separated from the gel by filtration, and then, the sialic acid and the immobilized synthetase are added. Immobilized inorganic pyrophosphatase is also added in order to drive to the right the equilibrium in Scheme 18, by decomposition of the product pyrophosphate (see Scheme 19).[15,39,69]

The preparation of cytidine monophosphate *N*-acetylneuraminic acid (49) was described by Augé and coworkers.[15] Immobilized nucleoside monophosphokinase (0.6 U) and pyruvate kinase (10 U) were gently stirred at 37° under nitrogen with CMP (0.5 mmol), ATP (0.05 mmol), and enolpyruvate phosphate (1.5 mmol) in 0.1 *M* Tris buffer (pH 7.5) containing 35 m*M* KCl, 2 m*M* $MgCl_2$, 3 m*M* 2-mercaptoethanol, m*M* thymol, and 0.1 m*M* EDTA. The reaction was monitored by t.l.c. on PEI-cellulose with successive elutions with LiCl: 0.3 *M* (1 min), *M* (12 min), and 1.6 *M* (47 min). After 2 days, the gel was collected, and washed with 0.1 *M* Tris buffer (pH 7.5), and the filtrate and washings were used without further treatment for CMP-sialic acid synthesis. Immobilized CMP-sialic acid synthetase (3.7 U) and inorganic pyrophosphatase (6 U) were added to the crude preparation of CTP (0.5 mmol), together with *N*-acetylneuraminic acid (0.5 mmol). The substrate was adjusted to 2 m*M* by dilution with 0.1 *M* Tris buffer (pH 9). The pH was adjusted to 9 and the $MgCl_2$ concentration to 35 m*M*. 2-Mercaptoethanol and thymol were kept at 3 m*M* and 1 m*M*, respectively, and the mixture was gently stirred at 37° under nitrogen. The reaction was monitored by t.l.c. on PEI-cellulose as described for the synthesis of CTP, and on silica gel (7:3 1-propanol–water). After 10 h, the yield of 49 was 60% as

(73) D. H. van den Eijnden and W. van Dijk, *Hoppe-Seyler's Z. Physiol. Chem.*, 353 (1972) 1817.

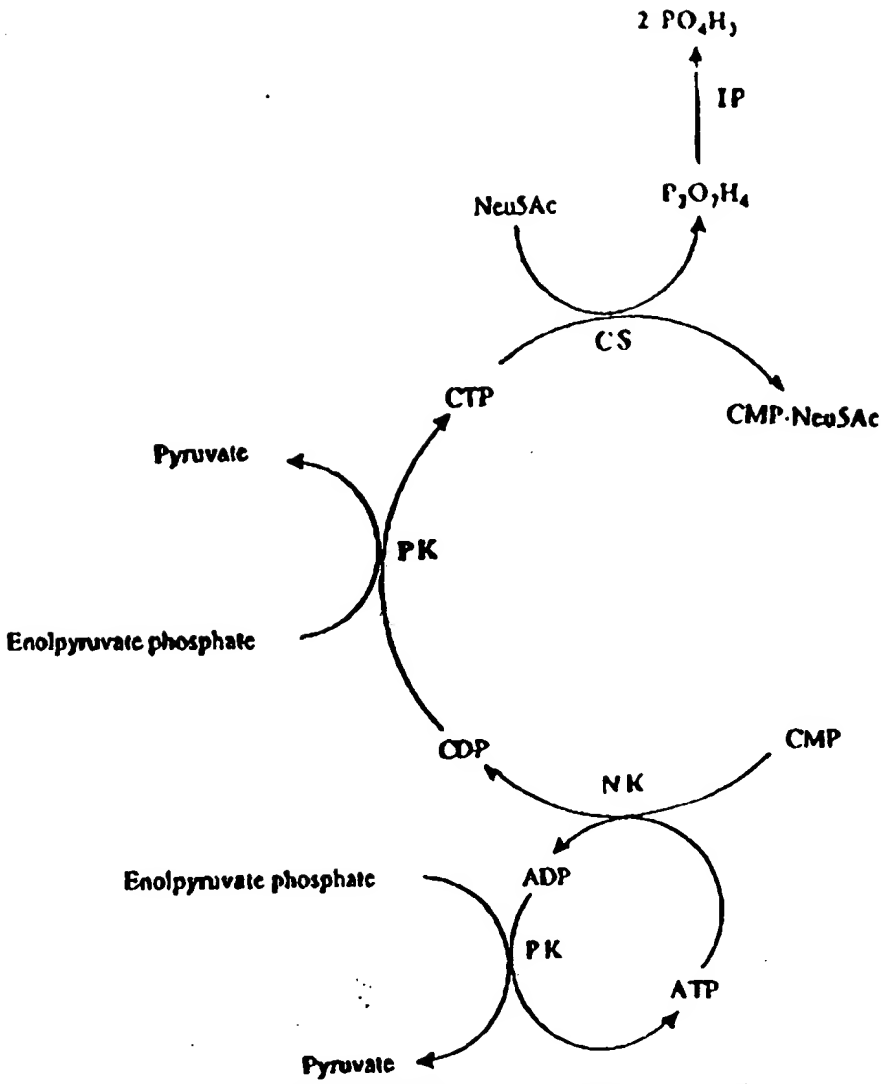

SCHEME 19.—Enzymic Synthesis of Cytidine Monophosphate *N*-Acetylneuraminic Acid Starting from CMP.

estimated by the thiobarbituric acid assay[17] and the reaction was stopped. The gel was collected, washed with 0.1*M* Tris buffer (pH 9), and the filtrate and washings were combined, and purified by chromatography on a refrigerated column (3 X 45cm) of DEAE-Sephadex A-25 (HCO_3^-). Elution with a gradient of 0 to 0.75*M* triethylammonium hydrogencarbonate (pH 7.8) gave 49 as its di(triethylammonium) salt (234 mg, 52%), R_F 0.53 (7:3 1-

(74) C. Augé and C. Gautheron, Colloque Int. Réactifs Supportés, Lyon, Juin 1982.
(75) J. Thiem and W. Treder, *Angew. Chem., Int. Ed. Engl.*, 25 (1986) 1096–1097.

TABLE VII

Nucleotide-Sugars[a]

Starting material	Nucleotide-Sugar	Scale (mmol)	Yield (%)	Units/mmol	References
UMP, D-glucosyl phosphate	"uridine-diphosphate-glucose"	1	92	AK: 2.5; UP: 1; IP: 4	74
ATP, GTP, CTP, UTP, D-glucosyl phosphate	"uridine-diphosphate-glucose"	6	97	UP[b]: 10; M[b]: 10; IP[b]: 10	63
CMP, *N*-acetylneuraminic acid	cytidine monophosphate-*N*-acetylneuraminic acid	0.5	60	PK: 20; NK: 1.2; CS: 7	39,69
CMP, *N*-glycolylneuraminic acid	cytidine monophosphate-*N*-glycolylneuraminic acid	0.1	80	PK: 20; NK: 1.2; CS: 6.5	69
CMP, *N*-acetyl-9-*O*-acetylneuraminic acid	cytidine monophosphate-*N*-acetyl-9-*O*-acetylneuraminic acid	0.5	52	PK: 20; NK: 1.2; CS: 12	69
CMP, 3-deoxy-D-*glycero*-D-*galacto*-nonulosonic acid	cytidine monophosphate-3-deoxy-D-*glycero*-D-*galacto*-nonulosonic acid	0.5	26	PK: 20; NK: 1.2; CS: 18	69
CTP, *N*-acetylneuraminic acid	cytidine monophosphate-*N*-acetylneuraminic acid	0.1	72	CS[c]	75

[a] Unless otherwise stated, enzymes were immobilized on agarose. [b] Immobilized in PAN gel. [c] Immobilized on silica gel–glutaraldehyde (a six-fold excess of CTP was utilized).

propanol–water); $[\alpha]_D^{20}$ −18° (*c* 1.9, water); ^{1}H-n.m.r data (D_2O): δ 1.65 (m, 1 H, H-3*a*), 2.05 (s, 3 H, NAc), 2.50 (dd, 1 H, $J_{3e,3a}$ 12.5, $J_{3a,4}$ 5 Hz, H-3*e*), 5.97 (d, 1 H, $J_{1,2}$ 4.5 Hz, H-1 of ribose), 6.10 (d, 1 H, $J_{5,6}$ 7.5 Hz, H-5 of cytosine), and 7.97 (d, 1 H, H-6 of cytosine).

The nucleotide-sialic acids **50**, **51**, and **52** could be prepared in the same way.[69]

Table VII gives a list of nucleotide-sugars prepared with immobilized enzymes.

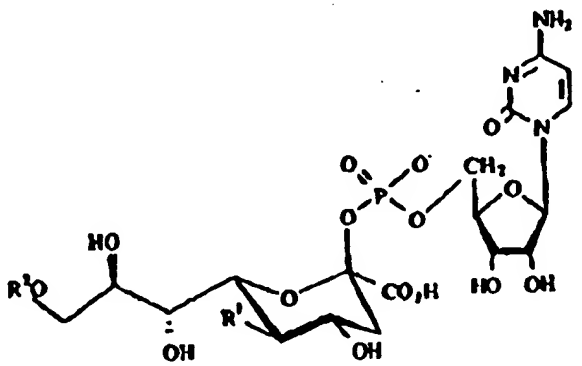

50 $R^1 = NHCOCH_3$, $R^2 = Ac$
51 $R^1 = NHCOCH_2OH$, $R^2 = H$
52 $R^1 = OH$, $R^2 = H$

V. Glycosylations with Transferases

1. General Considerations

Glycosylations occur in cells by the Leloir pathway, first demonstrated for galactosylation.[76] The glycosyl donor is a nucleotide-sugar, and the glycosylation step proper is catalyzed by a transferase. At the same time, a free nucleotide is released which may be used to regenerate the starting nucleotide-sugar in a few enzymic steps. Therefore, in principle, the role of nucleotides should only be catalytic. Only a limited number of nucleotide-sugars occur in cells, so that any one of them may be involved in different types of coupling. On the other hand, the transferase is highly specific, with respect to the glycosyl donor, the sugar acceptor, and the position and anomeric orientation of the coupling. Variations may be tolerated in the sugar units of the

(76) L. F. Leloir, *Science*, 172 (1971) 1299–1303.

oligosaccharide acceptor not directly involved, but this part of the acceptor is by no means totally indifferent.

Relatively early reports (1980 – 1982) from Barker and his group described galactosylation[77] and fucosylation[78] with soluble transferases.

2. Galactosylation

Scheme 20 shows the corresponding cycle, first reported for the synthesis of *N*-acetyllactosamine on the 10-g scale (R = H),[23] and later utilized in the

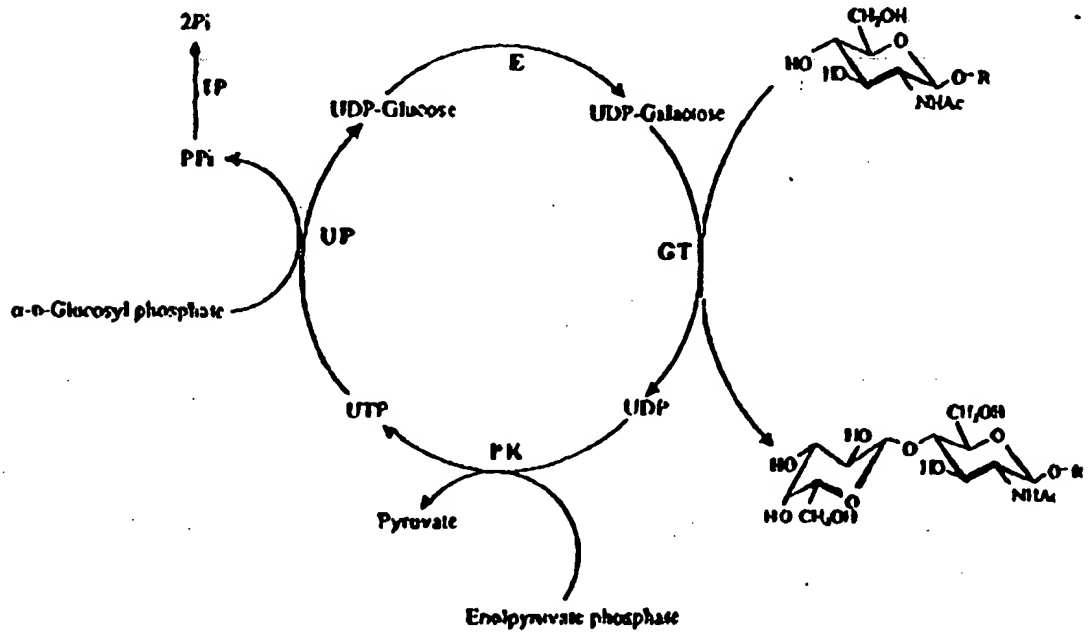

SCHEME 20.—The Multi-enzyme System which Regenerates UDP-Galactose *in situ* for Enzymic D-Galactosylation.

synthesis of many complex oligosaccharides (R = oligosaccharide residue).[15,19,79,80] The transfer of a β-D-galactopyranosyl group from "uridine-diphosphate-galactose" to O-4 of a terminal, nonreducing residue of *N*-acetyl-β-D-glucosamine, catalyzed by galactosyl transferase (GT) releases an equimolecular quantity of uridine diphosphate. This is enzymically phosphorylated to uridine triphosphate by enolpyruvate phosphate in the presence of pyruvate kinase. Another transferase, UDP-pyrophosphorylase

(77) H. A. Nunez and R. Barker, *Biochemistry*, 19 (1980) 489–495.
(78) P. R. Rosevear, H. A. Nunez, and R. Barker, *Biochemistry*, 21 (1982) 1421–1431.
(79) C. Augé, S. David, C. Mathieu, and C. Gautheron, *Tetrahedron Lett.*, 25 (1984) 1467–1470.
(80) C. Augé, C. Gautheron, and H. Pora, *Carbohydr. Res.*, 193 (1989) 288–293.